

ENTROPY, COCYCLES, AND THEIR DIAGRAMMATICS

MEE SEONG IM AND MIKHAIL KHOVANOV

ABSTRACT. The first part of the paper explains how to encode a one-cocycle and a two-cocycle on a group G with values in its representation by networks of planar trivalent graphs with edges labelled by elements of G , elements of the representation floating in the regions, and suitable rules for manipulation of these diagrams. When the group is a semidirect product, there is a similar presentation via overlapping networks for the two subgroups involved.

M. Kontsevich and J.-L. Cathelineau have shown how to interpret the entropy of a finite random variable and infinitesimal dilogarithms, including their four-term functional relations, via 2-cocycles on the group of affine symmetries of a line.

We convert their construction into a diagrammatical calculus evaluating planar networks that describe morphisms in suitable monoidal categories. In particular, the four-term relations become equalities of networks analogous to associativity equations. The resulting monoidal categories complement existing categorical and operadic approaches to entropy.

CONTENTS

1. Introduction	2
2. Planar networks of group-valued flows	4
2.1. Diagrammatics of G -flows and a monoidal category for a group G	4
2.2. A monoidal category from a G -module U	13
2.3. Twisting by a one-cocycle	17
2.4. Diagrammatics for a two-cocycle	25
3. Diagrammatics for two types of lines	36
3.1. Crossed products of groups and overlapping networks of two kinds	36
3.2. Two examples: crossed modules and nonabelian one-cocycles	38
4. Entropy and infinitesimal dilogarithms	42
4.1. Entropy of a finite random variable and its cohomological interpretation	42
4.2. Cathelineau's infinitesimal dilogarithm	45
5. Diagrammatics of infinitesimal dilogarithms	50
5.1. Motivation for the diagrammatics	50
5.2. Monoidal categories for the infinitesimal dilogarithm	53
5.3. Monoidal category \mathcal{C}_k°	63
6. Diagrammatics of entropy	64
6.1. A monoidal category for entropy	64

Date: October 8, 2024.

2020 Mathematics Subject Classification. Primary 94A17, 20J06, 18M10, 18M30; Secondary 18B40, 37A20, 18G45.

Key words and phrases. Entropy, infinitesimal dilogarithm, cocycles, planar networks, diagrammatics, group representations, affine group, Cathelineau-Kontsevich cocycle.

6.2. More entropy and cocycle remarks	72
References	77

1. INTRODUCTION

The concept of entropy has fascinated mathematicians over the past decades [Gro13, Zor11, CC09, Rio21, Lei21a, Bae24]. The remark “no one knows what entropy really is”, attributed to von Neumann [Rio21], apparently still holds in the minds of at least some of us, about eighty years later. Categorical interpretations of entropy and of the foundations of probability theory are explored in [BFL11, Bae22, Bra21, Voe04, Voe08, Spi23, BB15, Vig20, Vig19].

Defect networks with facets labelled by elements of a group G appear throughout mathematical physics, see [Tac20, BBFT⁺24, BB20, TKBB23] and many other references. Labeling domain walls in a topological quantum field theory (TQFT) by elements of a finite group G and introducing 2-cocycles in relation to codimension two submanifolds (seams) where domain walls for g and h merge into a gh -wall is now common in condensed matter and TQFT theories. Surface G -networks appear as Poincaré duals of Moore–Segal encodings of G -equivariant 2D TQFTs [MS06] and they are implicit in Turaev’s homotopy QFTs [Tur10]. Finite extensions of fields give other examples of 2D TQFTs with G -networks [IK21]. There is a large amount of literature on defects in TQFTs, see [FMT24] and references therein.

In the present work we explain how to interpret the entropy of a finite random variable via a suitable monoidal category where morphisms can be represented by pairs of overlapping planar defect networks. Our approach builds on the explicit cohomological interpretation of entropy by M. Kontsevich [Kon02] and J.-L. Cathelineau [Cat88, Cat90, Cat96, Cat07, Cat11] in terms of a suitable 2-cocycle on the group of affine symmetries of the real line.

Entropy and its diagrammatical calculus have additive properties, as opposed to multiplicative properties of the TQFT invariants. G -cocycles that appear in physics typically take values in the multiplicative group \mathbb{R}^* or \mathbb{C}^* of the ground field, while the present paper discusses diagrammatical calculi for *additive* 1-cocycles and 2-cocycles. (Exponential of the entropy, but as an element of the tropical semiring, appears in [CC09, MT14].)

Let us now briefly survey the contents of the paper. In Section 2 we describe several variations on a diagrammatical calculus of planar networks where lines are labelled by elements of a group G and in a vertex three lines can meet as long as the appropriate product of their labels or their inverses is $1 \in G$.

- Section 2.1 defines G -flows and corresponding monoidal categories \mathcal{C}_G^I and \mathcal{C}_G (these two categories are isomorphic).
- In Section 2.2 to a G -module U there is assigned a monoidal category \mathcal{C}_U , where morphisms are represented by diagrams of G -networks with boundary and elements of U can float in the regions of these networks.
- In Section 2.3 to a U -valued one-cocycle $f : G \rightarrow U$ we assign a monoidal category \mathcal{C}_f .
- In Section 2.4 to a U -valued normalized two-cocycle $c : G \times G \rightarrow U$ we assign a monoidal category \mathcal{C}_c .

The twisting from a 2-cocycle c can be encoded by a boundary line that absorbs and emits morphisms in \mathcal{C}_c , and likewise for a 1-cocycle f . It is shown as the blue horizontal line in the figures in Section 2.4.

In Section 3.1 we introduce diagrammatics for a cross-product group, using two types of lines to label the elements of the two subgroups and their interactions. In Section 3.2 we sketch related diagrammatics for crossed modules and for non-abelian cocycles and list several examples of the latter.

Section 4 reviews cohomological interpretation of entropy of a finite random variable due to Kontsevich and Cathelineau and Cathelineau’s theory of infinitesimal dilogarithms. This interpretation uses a 2-cocycle on the group $\text{Aff}_1(\mathbb{R})$ of affine symmetries of the real line (for entropy), and on the group $\text{Aff}_1(\mathbf{k})$ of affine transformations over a field \mathbf{k} for the infinitesimal dilogarithm.

Homological interpretation of Shannon’s entropy was pointed out by Cathelineau in [Cat96] based on his earlier work [Cat88] and by Kontsevich [Kon02]. Entropy and its functional equation (4.7) can be interpreted and generalized via the infinitesimal dilogarithms of Cathelineau [Cat88, Cat96, Cat11] and Bloch–Esnault [BE03]. Those papers consider the analogue of the entropy functional equation over any field. Furthermore, detailed relations between the infinitesimal dilogarithms for a field \mathbf{k} and one- and two-cocycles on various groups associated to \mathbf{k} are worked out in [Cat11], see also [Kon02, Gar09, Ü21, Par07] and follow-up papers for related developments.

The main goal of the present paper is to reinterpret some of Cathelineau’s and Kontsevich’s work via diagrammatics for suitable monoidal categories. Affine symmetry group $\text{Aff}_1(\mathbf{k})$ is a cross-product of the additive \mathbf{k} and the multiplicative \mathbf{k}^\times groups of the field \mathbf{k} , so we utilize overlapping networks for these two groups to build monoidal categories $\mathcal{C}_{\mathbf{k}}$ and $\mathcal{C}_{\mathbf{k}}^\circ$ which are then used for an interpretation of entropy (when $\mathbf{k} = \mathbb{R}$) and of the infinitesimal dilogarithm. Diagrammatics of 2-cocycles from Section 2.4 is used as well.

Our approach is developed in Section 5. We first describe diagrammatics for Cathelineau’s infinitesimal dilogarithm over any field \mathbf{k} . Then, in Section 6, we specialize to the ground field \mathbb{R} and the entropy functional and corresponding categories \mathcal{C}_H and \mathcal{C}_H° . A subcategory of \mathcal{C}_H is equivalent to the Baez–Fritz–Leinster category of finite random variables [BFL11]. One can pose a rather speculative question whether the bigger categories $\mathcal{C}_H, \mathcal{C}_H^\circ$ may give some hints about the nature of probability beyond its familiar classical and quantum interpretations.

A busy reader may want to start with Sections 4 and 5, devoted to entropy, infinitesimal dilogarithms and their diagrammatics, and flip back to earlier sections as needed.

Acknowledgments: The authors are grateful to Sri Tata for pointing out papers [TKBB23, BB20] and an interesting discussion. The authors are also thankful to Danny Calegari, Andrew Dudzik, Slava Krushkal, Lev Rozansky, and Joshua Sussan for insightful conversations. M.S. Im would like to acknowledge research members at the Naval Research Laboratory in Washington, DC for interesting discussions. The authors thank Yale University, Dublin Institute for Advanced Studies, Mathematisches Forschungsinstitut Oberwolfach, Hausdorff Research Institute for Mathematics, Okinawa Institute of Science and Technology Graduate University, the Simons Foundation, and Rényi Institute for providing a productive work environment. M.S. Im acknowledges partial support from the Naval Research Laboratory.

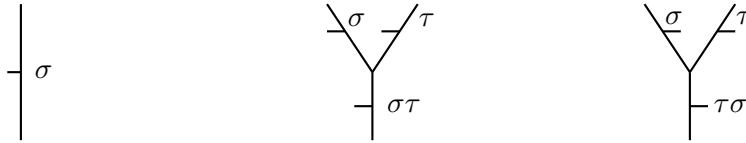


FIGURE 2.1.1. Left: a σ -labelled edge with a co-orientation. Middle and right: two possible diagrams of co-orientations at a vertex, with edges carrying G -labels $\sigma, \tau \in G$, and either $\sigma\tau$ or $\tau\sigma$. Vertices with such co-orientations are called *type I vertices*.

M.K. would like to acknowledge partial support from NSF grant DMS-2204033 and Simons Collaboration Award 994328.

2. PLANAR NETWORKS OF GROUP-VALUED FLOWS

2.1. Diagrammatics of G -flows and a monoidal category for a group G .

Fix a group G and consider trivalent graph networks in the plane \mathbb{R}^2 where edges of graphs are co-oriented in the plane, each edge is labelled by an element of the group G and at each trivalent vertex there is a flow condition shown in Figure 2.1.1.

Co-orientation is an orientation of the normal bundle to a submanifold. Figure 2.1.1 shows, on the left, an individual edge with a co-orientation and a G -label σ , and in the middle and on the right – two possible vertices with co-orientations and labels of adjacent edges. One can think of each vertex as merging two compatibly co-oriented lines σ and τ into the line $\sigma\tau$ or $\tau\sigma$, depending on where co-orientations point. Orientation of the ambient \mathbb{R}^2 is fixed. Circles, equipped with co-orientation and labels, are allowed in the networks.

We call these *type I G -flow networks* or just *type I G -networks*. These networks are *closed*, that is, have no boundary points. Denote the set of closed type I G -networks by Net_G^I .

If smooth structure is important, one can make σ and τ lines tangent at a vertex in Figure 2.1.1, to emphasize that they are merging into a single line (or that a single line splits into two), making all three tangency rays at a vertex belong to a single tangent line, see a later Figure 2.1.9, for instance.

Given a G -network $\mathcal{N} \in \text{Net}_G^I$ in the plane and point p in the complement $\mathbb{R}^2 \setminus \mathcal{N}$, define *the winding number* $\omega(p, \mathcal{N})$ of \mathcal{N} around p or *the index of p relative to \mathcal{N}* as follows, see Figure 2.1.2. Pick a ray going off from p to infinity in the plane that intersects \mathcal{N} transversally in several points (none of which are vertices and flip points; see the paragraph before Remark 2.1 for the definition of a flip point). Multiply the G -labels of edges at the intersection points to

$$(2.1) \quad \omega(p, \mathcal{N}) := \sigma_1^{\varepsilon_1} \sigma_2^{\varepsilon_2} \cdots \sigma_n^{\varepsilon_n} \in G,$$

where $\sigma_1, \dots, \sigma_n$ are the G -labels of edges along the ray, reading from the infinite point towards p and $\varepsilon_i = 1$ if at the i -th intersection point the co-orientation is towards the infinite point of the ray and $\varepsilon_i = -1$ if the co-orientation is towards p .

It is clear that $\omega(p, \mathcal{N})$ does not depend on the choice of a generic ray out of p and is an invariant of p and of the region of $\mathbb{R}^2 \setminus \mathcal{N}$ where p is located. A *region* of a network is a connected component of $\mathbb{R}^2 \setminus \mathcal{N}$. Denote by $r(\mathcal{N})$ the set of regions of \mathcal{N} . The G -winding number can be viewed as a function

$$(2.2) \quad \omega : r(\mathcal{N}) \longrightarrow G.$$

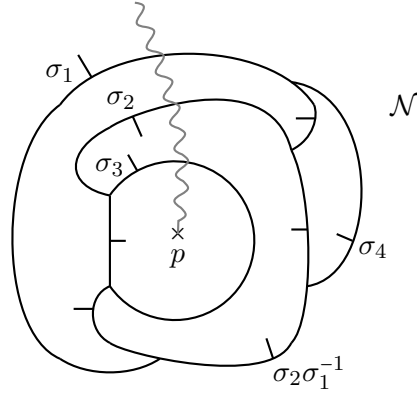


FIGURE 2.1.2. The G -winding number $w(p, \mathcal{N}) = \sigma_1 \sigma_2^{-1} \sigma_3$ of a point p relative to network \mathcal{N} . For this particular G -network labels of the remaining edges can be uniquely reconstructed from the labels $\sigma_1, \dots, \sigma_4$ that are shown.

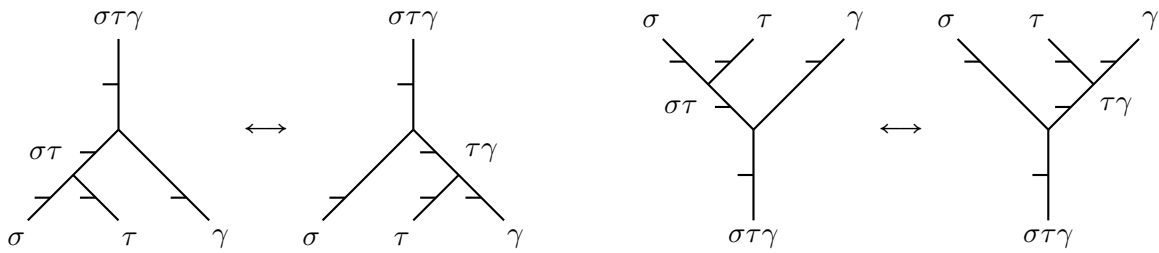


FIGURE 2.1.3. Associativity transformation for a merge (or a split) of σ, τ and γ .

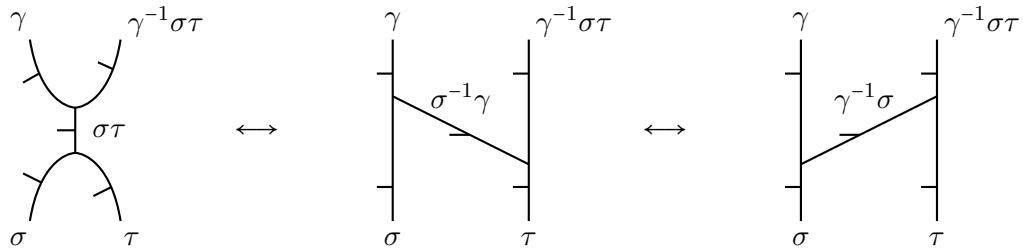


FIGURE 2.1.4. These transformations are essentially versions of the Figure 2.1.3 for other co-orientations. The second transformation comes from reversing the coorientation and label of the central edge.

For points p outside \mathcal{N} , that is, when a ray out of p to infinity disjoint from \mathcal{N} exists, $w(p, \mathcal{N}) = 1 \in G$. The corresponding region is called *the outside* or *outer region*.

Consider transformations of networks shown in Figures 2.1.3, 2.1.4 and 2.1.5. In Figure 2.1.3 there is bijection between the regions or the networks on the left and right, and this bijection preserves winding numbers of the regions. Likewise, there are bijections between the regions of the three networks in Figure 2.1.4, preserving winding numbers of regions. Figure 2.1.5

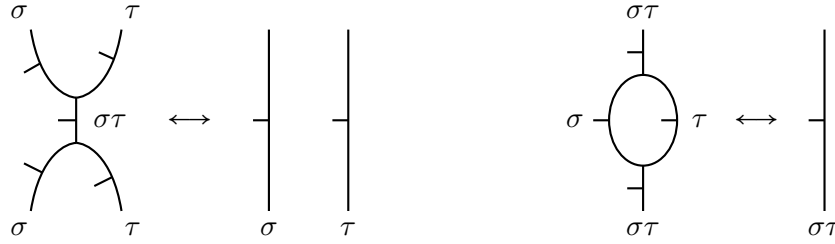


FIGURE 2.1.5. Composition of a merge and a split of σ and τ lines with compatible co-orientations.

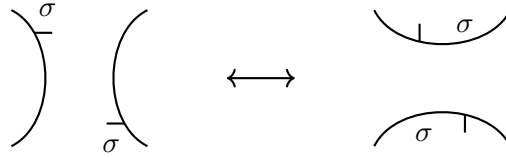


FIGURE 2.1.6. A *flip move* for compatibly oriented σ -lines.

transformations change the number of regions (or, in the first case, can change topology of one of the regions). We also consider Figure 2.1.6 move.

We are interested in having various equivalence relations on these networks, including the ones for identifying networks in Figures 2.1.3–2.1.6 as well as an equivalence for Figures 2.1.3–2.1.5 only, without the relation in Figure 2.1.6 holding, see Section 2.3. A convenient framework for that is the *universal construction of topological theories* [CFW10, Kho20, IKO23, IK24b, GIK⁺23a, IK22, IK23, GIK23b, IZ22]. In our situation the networks are planar and one should use the universal construction for monoidal categories which are not necessarily symmetric. This setup is considered in [KL21, IKO23].

We apply the universal construction to closed G -networks and, for now, do the simplest case. Pick a one-element set, say $\{0\}$, and declare that any closed G -network evaluates to the element of that set (to 0). Denote this evaluation

$$(2.3) \quad \alpha_0 : \mathbf{Net}_G^I \longrightarrow \{0\}.$$

To build a category \mathcal{C}_G^I from G -networks and α_0 , consider a generic cross-section of a network \mathcal{N} by a horizontal line. The line intersects \mathcal{N} in a number of points, which inherit labels in G and co-orientations from \mathcal{N} . We can denote a point with label $\sigma \in G$ and co-oriented pointing to the left of \mathbb{R} by X_σ^+ and a σ -labelled point co-oriented to the right by X_σ^- .

Then X_σ^+, X_σ^- are the generating objects of \mathcal{C}_G^I . Given a sequence $\underline{\sigma} = (\underline{\sigma}_1, \dots, \underline{\sigma}_n)$ of pairs (element of G , sign), that is, $\underline{\sigma}_i = (\sigma_i, \varepsilon_i)$, $\sigma_i \in G$, $\varepsilon_i \in \{+, -\}$, define the object

$$(2.4) \quad X_{\underline{\sigma}} := X_{\sigma_1}^{\varepsilon_1} \otimes X_{\sigma_2}^{\varepsilon_2} \otimes \dots \otimes X_{\sigma_n}^{\varepsilon_n}.$$

Define the *weight* of the sequence $\underline{\sigma}$ by

$$(2.5) \quad \langle \underline{\sigma} \rangle := \sigma_1^{\varepsilon_1} \sigma_2^{\varepsilon_2} \dots \sigma_n^{\varepsilon_n} \in G.$$

(Diagrammatically, we merge the sequence $\underline{\sigma}$ into a single left-pointed dot (object), see Figure 2.1.7.)

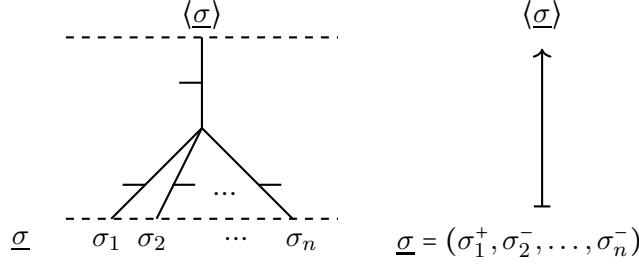


FIGURE 2.1.7. Merging a sequence of group elements and signs into a single element. Weight of the sequence $\underline{\sigma} = (\sigma_1^+, \sigma_2^-, \dots, \sigma_n^-)$ is denoted by $\langle \underline{\sigma} \rangle$.

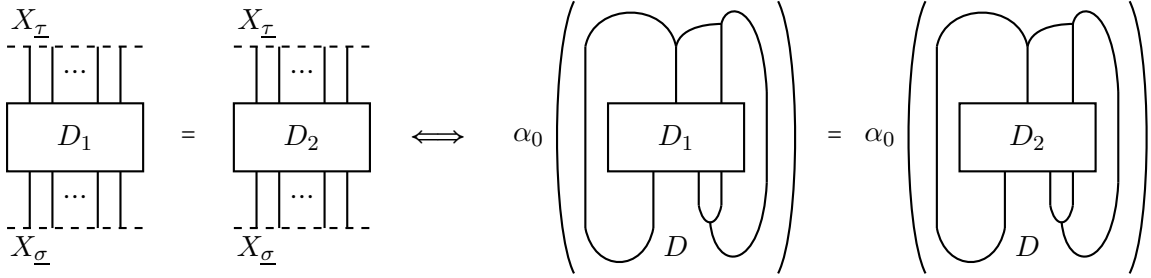


FIGURE 2.1.8. Diagrams D_1, D_2 define equal morphisms in \mathcal{C}'_G if and only if any closure using an outside diagram D results in equal evaluations, $\alpha_0(DD_1) = \alpha_0(DD_2)$. Since α_0 is constant, $D_1 = D_2$ in \mathcal{C}'_G if they have the same source object $X_{\underline{\sigma}}$ and the same target object $X_{\underline{\tau}}$.

Morphisms from $X_{\underline{\sigma}}$ to $X_{\underline{\tau}}$ are given by all networks D with boundary, $\partial_0 D = X_{\underline{\sigma}}$, $\partial_1 D = X_{\underline{\tau}}$, modulo universal relations: two networks D_1, D_2 are equal if and only if no matter how they are closed on the outside into closed networks $\mathcal{N}_1, \mathcal{N}_2$, the evaluations are equal, $\alpha_0(\mathcal{N}_1) = \alpha_0(\mathcal{N}_2)$, see Figure 2.1.8.

Evaluation α_0 is constant on all closed diagrams, so the above condition is vacuous. We obtain that diagrams D_1, D_2 with the same bottom sequence $\underline{\sigma}$ and same top sequence $\underline{\tau}$ (diagrams from $\underline{\sigma}$ to $\underline{\tau}$) give equal morphisms in \mathcal{C}'_G , and any two morphisms from $X_{\underline{\sigma}}$ to $X_{\underline{\tau}}$ are equal.

Merges and splits in Figure 2.1.1 and their reflections about the x -axis give isomorphisms

$$(2.6) \quad X_{\sigma}^+ X_{\tau}^+ \cong X_{\sigma\tau}^+, \quad X_{\sigma}^- X_{\tau}^- \cong X_{\tau\sigma}^-.$$

A possible isomorphism $X_{\sigma}^+ \cong X_{\sigma^{-1}}^-$ is shown in Figure 2.1.9 on the right. It is convenient to encode it by a special diagram with a marked point on a line where σ -line is turned into a σ^{-1} -line and the co-orientation is reversed. We call this reversal mark a *flip point*.

Remark 2.1. In general, one needs to be careful with flip points. There are four ways to define a flip point by inserting a 1-labelled *lollipop* of a line and a circle, both labelled $1 \in G$, see Figure 2.1.10.

The circle edge can merge with the 1-labelled edge into itself in two possible ways and the lollipop of 1-edges can be inserted on the opposite side. These four choices can be reduced to

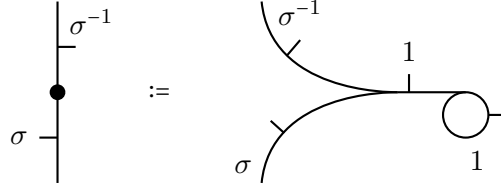


FIGURE 2.1.9. Left: a flip point reverses co-orientation and label along an edge. It can be defined, as shown on the right, using a “lollipop” G -flow network.

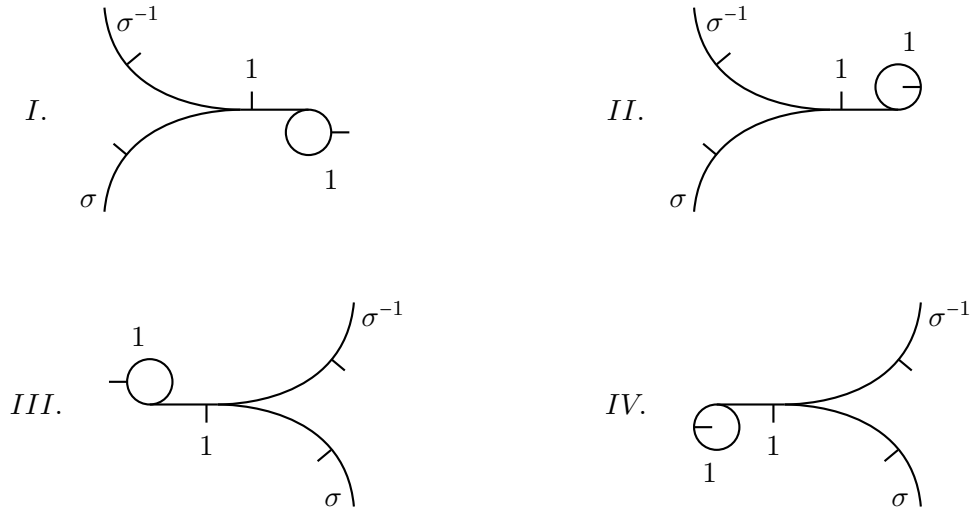


FIGURE 2.1.10. Four ways to define a flip point via a lollipop diagram. Notice that the isotopy that rotates the flip point by π exchanges I and III , II and IV , simultaneously with replacing σ by σ^{-1} .

two choices using the orientation of \mathbb{R}^2 , but one needs to either pick between the two or check that the resulting morphism does not depend on the choice. For our present construction it is the latter case (since the evaluation does not depend on the diagram). In the former case, a co-orientation can be added to the flip point to indicate which diagram is selected for the definition. Equality of morphisms is determined by the universal construction, so one needs to examine whether various choices of a lollipop result in the same evaluation of the diagram. Evaluation α_0 in (2.3) takes values in the one-element set, so any two morphisms with the same source object and the same target object are equal in the quotient category. In particular, choice of a lollipop for this evaluation does not matter.

Two consecutive flip points along an edge can be cancelled, see Figure 2.1.11 on the right, which is immediate from the degeneracy of α_0 .

We sometimes write X_σ in place of X_σ^+ , for convenience. From the discussion above we see that any object $X \in \text{Ob}(\mathcal{C}_G^I)$ is isomorphic to X_σ , for a unique $\sigma \in G$. The object $X_{\underline{\sigma}}$ in (2.4) is isomorphic to X_σ for $\sigma = \sigma_1^{\varepsilon_1} \cdots \sigma_n^{\varepsilon_n}$, where σ_i^- stands for σ_i^{-1} and σ_i^+ for σ_i , by merging the n strands into one and adding flip points when needed to match co-orientations. Homs are

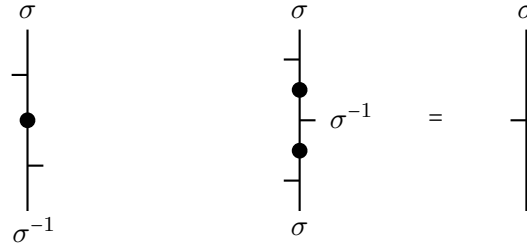


FIGURE 2.1.11. Left: a flip point along an edge that reverses coorientation and the G -label. Right: cancellation of two adjacent flip points.

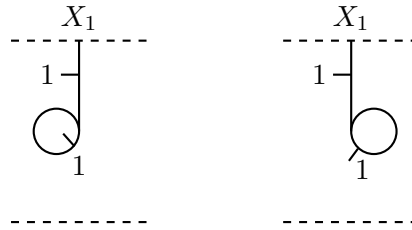


FIGURE 2.1.12. Two ways to define the morphism from identity to X_1 via a lollipop. For concreteness, we use the one on the left.

given by

$$\mathrm{Hom}_{\mathcal{C}_G^I}(X_\sigma, X_\tau) = \begin{cases} \{\mathrm{id}_{X_\sigma}\} & \text{if } \sigma = \tau, \\ \emptyset & \text{otherwise.} \end{cases}$$

That is, the identity morphism is the only endomorphism of X_σ , and there are no morphisms between X_σ and X_τ if $\sigma \neq \tau$.

The category \mathcal{C}_G^I is monoidal, with the tensor product given by placing diagrams next to each other. In our diagrammatics the unit object $\mathbf{1}$ is not represented by a dot on a line and instead can be inserted anywhere on the line. The isomorphism $\mathbf{1} \cong X_1$ and its inverse can be given by a lollipop morphism, see Figure 2.1.12 (for \mathcal{C}_G^I , the choice of lollipop convention does not matter).

Category \mathcal{C}_G^I is pivotal [Sel11], with the dual $(X_\sigma^+)^* := X_\sigma^-$ and duality morphisms given by cups and caps, see Figure 2.1.13. Alternatively, one can set $X_\sigma^* := X_{\sigma^{-1}}$, with the rigidity (U-turns) morphisms for the pivotal structure given by lollipop diagrams, see Figure 2.1.14. For the category \mathcal{C}_G^I , due to the triviality of the evaluation function, the choice of duality morphisms once the formula $X_\sigma^* := X_{\sigma^{-1}}$ is fixed is unique, and the four maps in Figure 2.1.14 define the same morphism in \mathcal{C}_G .

We summarize our observations on the category \mathcal{C}_G^I .

Proposition 2.2. *Category \mathcal{C}_G^I is a pivotal monoidal category with isomorphism classes of objects parameterized by elements of G , and hom sets between isomorphic (respectively, non-isomorphic) objects being one-element sets (respectively, the empty set).*

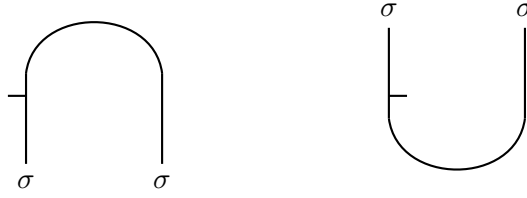


FIGURE 2.1.13. Two of the four duality morphisms, for $X_\sigma^* = X_\sigma^-$.

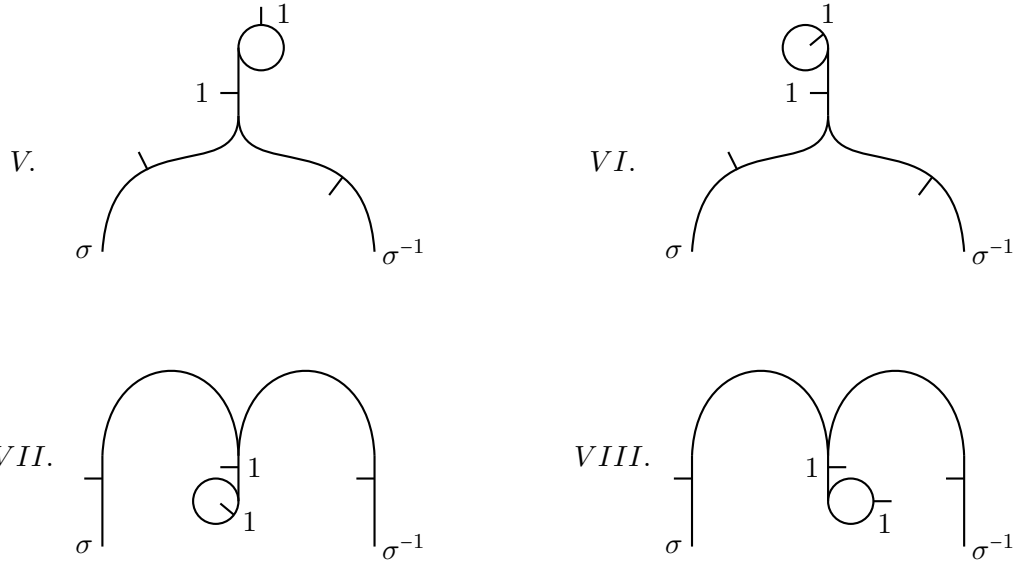


FIGURE 2.1.14. Defining duality morphisms for the pivotal structure via lollipops.

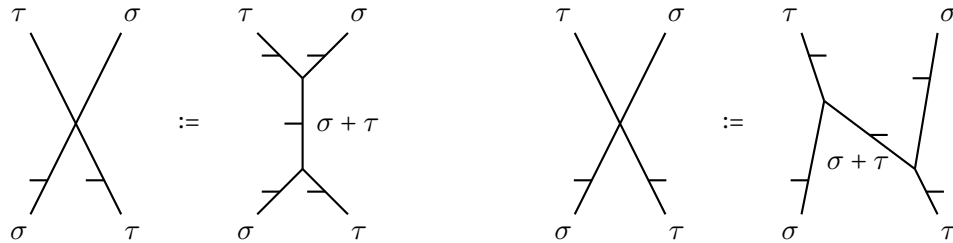


FIGURE 2.1.15. Symmetric tensor structure morphisms for an abelian G , with the group operation written as $+$ to emphasize commutativity.

Remark 2.3. Objects $X_\sigma^+ X_\tau^+$ and $X_\tau^+ X_\sigma^+$ are isomorphic if and only if σ and τ commute. Category \mathcal{C}_G^I is symmetric if and only if G is abelian, and the symmetric structure can be described as shown in Figure 2.1.15.

Next, we use flips to define trivalent vertices where the three co-orientations all go clockwise or all go counter-clockwise around a vertex, see Figure 2.1.16. We call these *type II* vertices, and the ones with co-orientations as in Figure 2.1.1 *type I* vertices. One needs to check

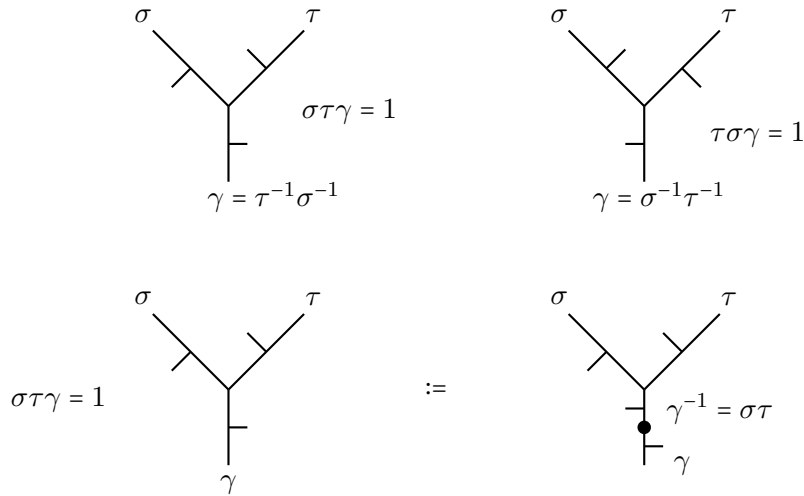


FIGURE 2.1.16. Top row: *type II* vertices with all three co-orientations counterclockwise or clockwise around the vertex. The product of the three labels, in suitable order, is $1 \in G$. In top left, the labels are read clockwise, giving the relation $\sigma\tau\gamma = 1$. In top right, the labels are read counterclockwise, resulting in $\tau\sigma\gamma = 1$. Bottom row: defining these vertices via one of Figure 2.1.1 vertices and a flip point.

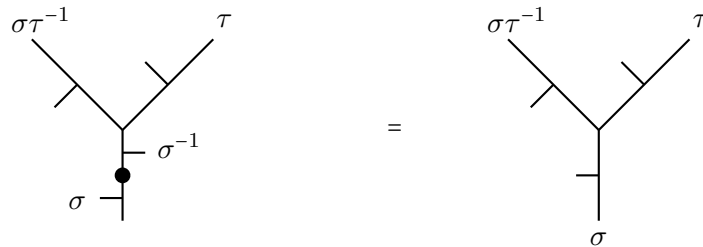


FIGURE 2.1.17. Creating or removing a flip point along an edge near a vertex. Flip point creation or annihilation can happen independently at each of the three edges adjacent to the vertex.

independence of this definition from the choice of an edge where to put a flip. In the present case, it is immediate, since the evaluation function for the universal construction is constant, but in more complicated cases independence requires verification.

With this definition, there is no restriction on possible triples of co-orientations at vertices. Consequently, at a trivalent vertex, one or more edge co-orientations may be reversed, by adding a flip point on the edge and replacing label σ by σ^{-1} near the vertex, see Figure 2.1.17 for a particular choice of co-orientations. As a special case of these transformations, a flip point can slide across a vertex, as shown in Figure 2.1.18.

Figure 2.1.11 (on the right) and Figure 2.1.17 transformations allow to remove flip points completely from an edge and from a circle. Adding a flip point near one endpoint of an edge and then removing it via the opposite endpoint allows to convert an edge without flip points

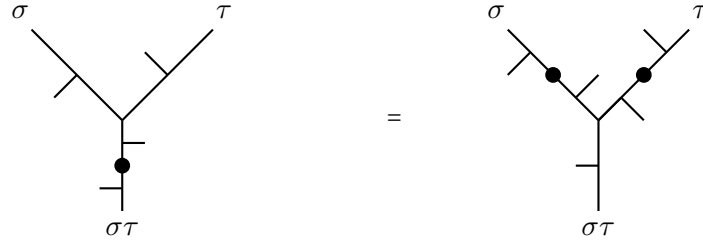


FIGURE 2.1.18. A relation to move a flip point through a vertex.

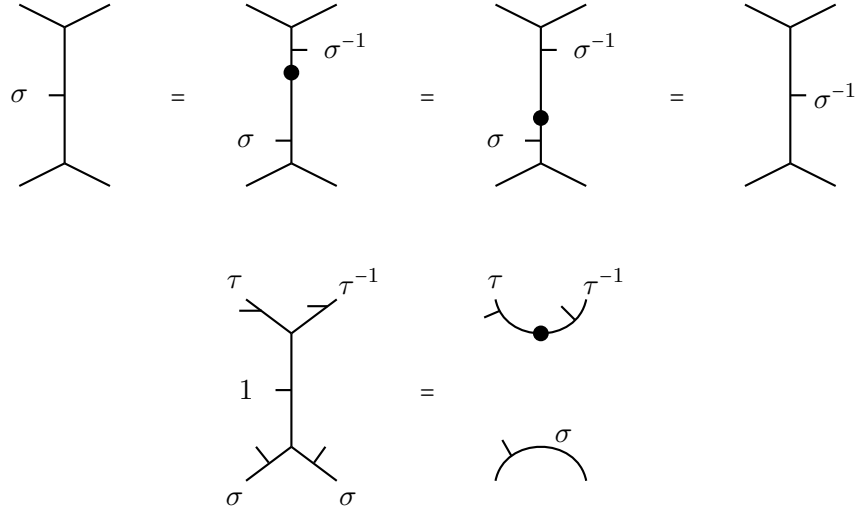


FIGURE 2.1.19. Top row: converting an edge to the oppositely co-oriented and labelled edge. Bottom row: removing a 1 edge.

to an oppositely co-oriented edge, with the label replaced by its inverse, see Figure 2.1.19. An edge labelled $1 \in G$ can be removed, possibly adding flip points at one of both of its endpoints, see Figure 2.1.19. Co-orientation and the label of the circle can be reversed, see Figure 2.2.4 bottom row.

Define *type II G -networks* by allowing *flip points* and vertices of arbitrary type as have just been discussed. The evaluation function α_0 on these more general networks is still defined to be constant. Denote the monoidal category for the universal construction via α_0 for type II networks by \mathcal{C}_G . This category is equivalent (even isomorphic) to \mathcal{C}_G^I as a pivotal monoidal category. In particular, sets of objects of the two categories are identical: finite sequences of pairs (element of G , sign).

Denote the set of G -networks of type II by Net_G^{II} or just by Net_G . Any type I network is also a type II network.

Allowing the possibility of a different evaluation of closed networks, one can consider planar networks of either type (I or II) built from the above elementary diagrams (trivalent vertices, flip points, edges with labels and co-orientations) modulo isotopies but no other relations. The relations would then be defined given an evaluation.

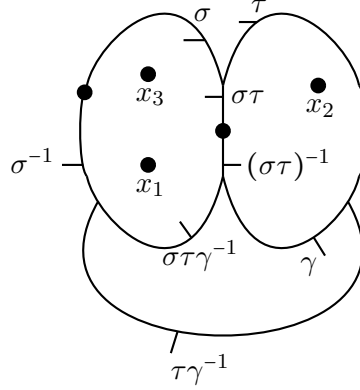


FIGURE 2.2.1. Example of a planar network $\tilde{\mathcal{N}}$ of G -labelled lines with co-orientations and U -labelled dots floating in the regions. At each vertex the flow condition on the labels and co-orientations of the three edges holds. The network contains two flip points. Here $\sigma, \tau, \gamma \in G$ and $x_1, x_2, x_3 \in U$. The evaluation of this network is $\alpha(\tilde{\mathcal{N}}) = \sigma^{-1}(x_1) + \sigma^{-1}(x_3) + \tau(x_2)$.

Remark 2.4. Category \mathcal{C}_G is equivalent to a set-theoretic version of the monoidal category in [EGNO15, Example 2.3.6]. The set-theoretic version has objects δ_g , over elements $g \in G$, tensor product $\delta_g \otimes \delta_h = \delta_{gh}$ and $\text{Hom}(\delta_g, \delta_h) = \delta_{g,h}$ (where $\delta_{g,h}$ is a one-element set if $g = h$ and the empty set otherwise). In our case there are more objects, but isomorphism classes of objects are parametrized by G .

2.2. A monoidal category from a G -module U .

Suppose U is a left $\mathbb{Z}[G]$ -module. Consider G -flow networks as above, either type I or type II, and additionally allow elements of U , shown as dots with labels from U , to float in the regions of the plane. Denote the network \mathcal{N} together with floating dots in the regions by $\tilde{\mathcal{N}}$, see Figure 2.2.1 for an example. We call $\tilde{\mathcal{N}}$ a U -network or a (G, U) -network. Denote by \mathcal{N} the underlying G -network, given by removing floating points and their labels.

A floating point or dot p with a label $x \in U$ has the G -winding number $\omega(p, \mathcal{N}) \in G$ relative to the network \mathcal{N} , see (2.1). Define

$$(2.7) \quad \alpha_U(p, \mathcal{N}) := \omega(p, \mathcal{N}) x \in U,$$

that is, we apply the group element $\omega(p, \mathcal{N})$, the G -winding number of p , to element x in U . Element $\alpha(p, \mathcal{N})$ depends only on the region where p floats and on its label x . We may also write α in place of α_U if U is fixed.

For a U -network $\tilde{\mathcal{N}}$ define the evaluation

$$(2.8) \quad \alpha_U(\tilde{\mathcal{N}}) := \sum_{p \in P(\tilde{\mathcal{N}})} \alpha_U(p, \mathcal{N}) = \sum_{p \in P(\tilde{\mathcal{N}})} \omega(p, \mathcal{N}) x_p \in U,$$

where $P(\tilde{\mathcal{N}})$ is the set of floating dots of $\tilde{\mathcal{N}}$. The evaluation is given by summing over all floating dots p their contributions, which are labels x_p twisted by G -winding numbers of the points. An example of an evaluation can be found in the caption for Figure 2.2.1. The

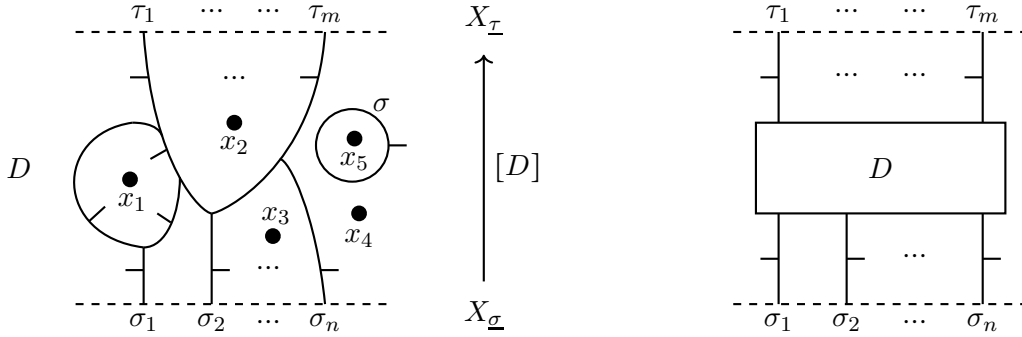


FIGURE 2.2.2. Left: example of a diagram D with top boundary $\underline{\tau}$ and bottom boundary $\underline{\sigma}$. Right: box notation for a diagram.

evaluation α_U is additive, $\alpha_U(\tilde{\mathcal{N}}_1 \sqcup \tilde{\mathcal{N}}_2) = \alpha_U(\tilde{\mathcal{N}}_1) + \alpha_U(\tilde{\mathcal{N}}_2)$, where \sqcup denotes placing two diagrams next to each other.

We now use evaluation α_U to define a monoidal category $\mathcal{C}_U = \mathcal{C}_{G,U}$ as usual in the universal construction. We use type II networks (using type I networks results in an isomorphic category).

Objects of \mathcal{C}_U are generic cross-sections of the network above, thus they are in a bijection with objects of \mathcal{C}_G , which are parameterized by sequences $\underline{\sigma}$, see formula (2.4). We define objects X_σ and $X_{\underline{\sigma}}$ of \mathcal{C}_U in the same way as for \mathcal{C}_G .

Networks $\mathcal{N} \in \text{Net}_G$ of G -flows without dots are a special case of networks $\text{Net}_U = \text{Net}_{G,U}$ of G -flows with U -labelled dots. The inclusion of sets $\text{Net}_G \subset \text{Net}_U$ is compatible with evaluations, since both α_0 and α_U evaluate networks in Net_G to $0 \in U$, where we choose the obvious inclusion $\{0\} \subset U$ to relate the two evaluations:

$$\begin{array}{ccc} \text{Net}_U & \xrightarrow{\alpha_U} & U \\ \cup & & \cup \\ \text{Net}_G & \xrightarrow{\alpha_0} & \{0\} \end{array}$$

To define morphisms in \mathcal{C}_U , consider diagrams D of G -flow networks with U -labelled dots with boundary $\partial_0 D = \underline{\sigma}, \partial_1 D = \underline{\tau}$ for some sequences $\underline{\sigma}, \underline{\tau}$. Denote corresponding objects of \mathcal{C}_U by $X = X_{\underline{\sigma}}, Y = X_{\underline{\tau}}$, see Figure 2.2.2 for an example. Denote the set of such diagrams by $\text{Net}_U(X, Y)$.

Each diagram $D \in \text{Net}_U(X, Y)$ defines a morphism, denoted $[D]$ (alternatively, denoted $\alpha_U(D)$) from X to Y in \mathcal{C}_U . Two diagrams D_1, D_2 with the same boundary (X, Y) define the same morphism, $[D_1] = [D_2]$, if for any way to close them up via some diagram D' the two evaluations are equal, $\alpha_U(D_1 D') = \alpha_U(D_2 D')$, also see Figure 2.1.8, picture on the right, with α_U replacing α_0 .

Category \mathcal{C}_U has at least the following relations. Relations in Figures 2.1.3, 2.1.4 and 2.1.5 hold in \mathcal{C}_U (replace arrows by equalities). Flip points and trivalent vertices of new types are defined as earlier, see Figures 2.1.9 and 2.1.16 and relations in Figures 2.1.17, 2.1.18, and 2.1.19 hold.

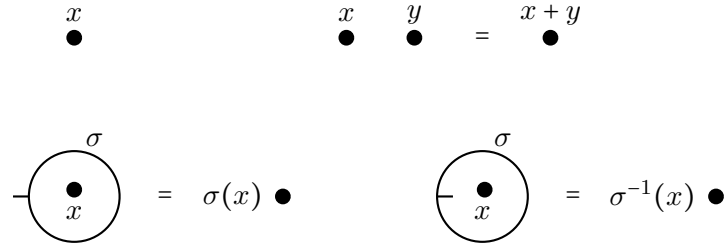


FIGURE 2.2.3. Top left: a dot labelled $x \in U$. Top right: Merging dots x, y floating in the same region into a single dot $x + y$. Bottom left: out-pointed σ -circle around x simplifies to $\sigma(x)$. Bottom right: in-pointed (or in-cooriented) σ -circle reduces to $\sigma^{-1}(x)$.

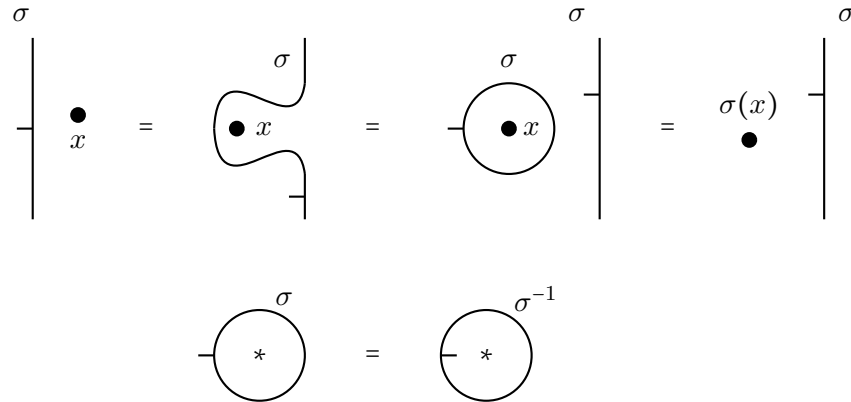


FIGURE 2.2.4. Top row: dot x crossing an edge is twisted to $\sigma(x)$. For the opposite co-orientation of the edge, the result would be $\sigma^{-1}(x)$. Bottom row: a circle labelled σ around a network can be converted to the oppositely oriented circle labelled σ^{-1} .

Two dots floating in a region can be merged into a single dot, see Figure 2.2.3 top right. A σ -circle around a dot x can be converted to the dot $\sigma^{\pm 1}(x)$ depending on co-orientation of the circle, see Figure 2.2.3 bottom row.

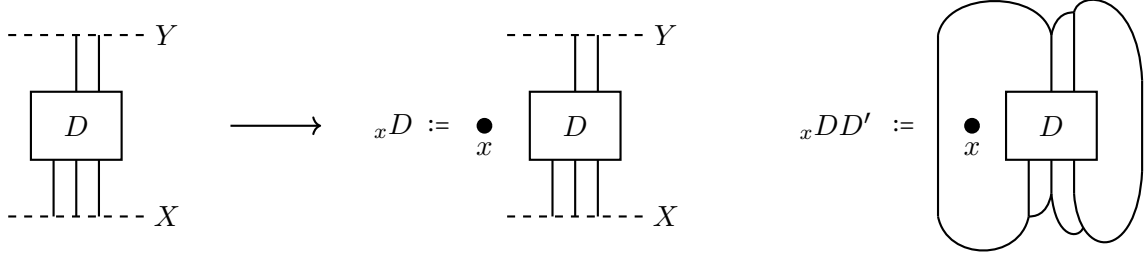
Dot labelled x can move through a σ -line, being twisted by $\sigma^{\pm 1}$, depending on co-orientation of the line, see Figure 2.2.4.

Proposition 2.5. *Category \mathcal{C}_U is a pivotal monoidal category. Any object of \mathcal{C}_U is isomorphic to X_σ , for a unique $\sigma \in G$. The hom spaces between these objects are*

$$(2.9) \quad \text{Hom}_{\mathcal{C}_U}(X_\sigma, X_\tau) = \begin{cases} U & \text{if } \sigma = \tau, \\ \emptyset & \text{otherwise.} \end{cases}$$

For two isomorphic objects $X, Y \in \text{Ob}(\mathcal{C}_U)$ (we can also write $X = X_{\underline{\sigma}}, Y = X_{\underline{\tau}}$ with $\langle \underline{\sigma} \rangle = \langle \underline{\tau} \rangle$) the hom set $\text{Hom}_{\mathcal{C}_U}(X, Y)$ is naturally a U -torsor, that is, (abelian) group U acts on it with one orbit and trivial stabilizers.

The group U acts on the hom set by taking a diagram D representing an element $[D] = \alpha_U(D) \in \text{Hom}_{\mathcal{C}_U}(X, Y)$ and placing $x \in U$ in the leftmost region of D to get a diagram ${}_x D$. As

FIGURE 2.2.5. Twisting a diagram D by $x \in U$.

one runs over all $x \in U$, elements ${}_x D$ are in a bijection with elements of $\text{Hom}_{\mathcal{C}_U}(X, Y)$. Picking any outside diagram D' that closes inward onto the pair (X, Y) of isomorphic objects, closing and evaluating $\alpha_U({}_x DD')$ gives a bijection $U \rightarrow U$, $x \mapsto \alpha_U({}_x DD')$. See Figure 2.2.5. This bijection depends on the choice of D and D' , but bijections differ by shift by elements of U .

Likewise, for two diagrams D_1, D_2 representing elements in $\text{Hom}_{\mathcal{C}_U}(X, Y)$, the difference

$$\alpha_U(D_1 D') - \alpha_U(D_2 D') \in U$$

does not depend on the choice of outside diagram D' if it closes around D_1, D_2 on the right (with no lines in D' to the left of D_1, D_2) and can be denoted $[D_1 - D_2] \in U$. Furthermore, if D_1, D_2 differ only by placement of dots, the difference can be computed by moving all dots in D_1, D_2 to the leftmost region, via Figure 2.2.4 top row move, merging (adding) the dots once they are in that region, and taking the difference of the labels of the two dots.

Alternatively, one can choose a parametrization of $\text{Hom}_{\mathcal{C}_U}(X, Y)$ by fixing a diagram D and placing the dots $x \in U$ in the rightmost region. The two parametrizations differ by action of σ on U , where $X_\sigma \cong X \cong Y$, since diagrams ${}_{\sigma(x)} D$ and D_x are equivalent, that is, $\alpha_U({}_{\sigma(x)} DD') = \alpha_U(D_x D')$ for any closure diagram D' .

Remark 2.6. We do not consider formal sums of diagrams. For instance, formally taking $D + D$ and pairing with D' results in evaluation $2\alpha_U(DD')$, which is usually not of the form $\alpha_U(D_1 D')$ for any diagram D_1 , varying over all D . It is possible to enlarge the space of morphisms and consider a larger category where morphisms are \mathbb{Z} -linear combinations of diagrams modulo skein relation derived via the evaluation α .

Endomorphisms $\text{End}_{\mathcal{C}_U}(X) \cong U$ as abelian monoids, for any $X \in \text{Ob}(\mathcal{C}_U)$, by identifying $x \in U$ with the diagram given by placing x in the leftmost region of the identity diagram id_X . The latter diagram consists of vertical lines, one for each term in X .

Remark 2.7. There is an isomorphism of rigid monoidal categories $\mathcal{C}_{G,0} \cong \mathcal{C}_G$, where 0 stands for the zero $\mathbb{Z}[G]$ -module.

If G acts trivially on U , dots move through diagram without twisting by elements of G , and there are natural isomorphisms of abelian groups $\text{Hom}_{\mathcal{C}_U}(X_{\underline{\sigma}}, X_{\underline{\tau}}) \cong U$, not just of U -torsors, when $\langle \underline{\sigma} \rangle = \langle \underline{\tau} \rangle$, that is, when the objects are isomorphic.

A homomorphism $\phi : U \rightarrow U'$ of $\mathbb{Z}[G]$ -modules induces a pivotal monoidal functor $\mathcal{F}_\phi : \mathcal{C}_U \rightarrow \mathcal{C}_{U'}$ which is the identity on objects and takes a diagram D describing a hom in \mathcal{C}_U to the diagram $\mathcal{F}_\phi(D)$ where labels $x \in U$ of floating dots are replaced by $\phi(x) \in U'$.

The homomorphism $0 \rightarrow U$ from the trivial G -module to U induces a faithful monoidal functor $\mathcal{C}_G \rightarrow \mathcal{C}_U$ for any G -module U .

Remark 2.8. Category \mathcal{C}_U is equivalent to the category in [EGNO15, Example 2.3.7]. Note that the category in that example has objects corresponding to elements of G , while for us objects are sequences of elements of G with signs.

2.3. Twisting by a one-cocycle.

Given a group G and a left G -module U , a one-cocycle $f \in Z^1(G, U)$ is a function $f : G \rightarrow U$ subject to the condition

$$(2.10) \quad f(\sigma\tau) = f(\sigma) + \sigma f(\tau), \quad \sigma, \tau \in G.$$

In particular $f(1) = f(1 \cdot 1) = f(1) + 1f(1) = 2f(1)$, so that $f(1) = 0$ and $0 = f(1) = f(\sigma\sigma^{-1}) = f(\sigma) + \sigma f(\sigma^{-1})$. Thus,

$$(2.11) \quad f(1) = 0, \quad f(\sigma) = -\sigma f(\sigma^{-1}).$$

A one-cocycle f is *null-homologous* (we write $f \in B^1(G, U)$) if

$$f(\sigma) = \sigma u - u$$

for some $u \in U$. The first cohomology group of G with coefficients in U is the quotient

$$(2.12) \quad H^1(G, U) := Z^1(G, U)/B^1(G, U).$$

We fix a one-cocycle $f : G \rightarrow U$ and construct a category $\mathcal{C}_f = \mathcal{C}_{G, U, f}$ as follows. First, consider diagrams in Net_U^I of G -flows of type I with U -labelled dots floating in the region. Any such diagram has evaluation α_U given by summing twisted labels $\omega(\mathcal{N}, p)(x_p) \in U$ over the dots p in $\tilde{\mathcal{N}}$. We shift the evaluation via cocycle f . Position the network \mathcal{N} so that all vertices are as in Figure 2.1.1 and the projection onto the y -axis is generic. Each local maximum and minimum point for this projection carries co-orientation of the line at the point (either upward or downward) and the label σ of the line. For a local extremum point m pick a point $p = p(m)$ in $\mathbb{R}^2 \setminus \mathcal{N}$ slightly above m . This point has index $\omega(p, \mathcal{N})$, the winding number of \mathcal{N} around p .

For an upward-cooriented local maximum or minimum point m define its local contribution

$$(2.13) \quad \alpha_f(m) := \pm \omega(p(m), \mathcal{N}) \cdot f(\sigma) \in U,$$

where $+$ is chosen for maximum points and $-$ for minimum points. The contribution is given by applying the winding number $\omega(p, \mathcal{N}) \in G$ to $f(\sigma) \in U$.

Downward-cooriented local extrema contribute 0, so for them $\alpha_f(m) = 0$. It is convenient to add vertices to the list of local diagrams and have them contribute 0 as well. The contributions are summarized in the table in Figure 2.3.1. Define the evaluation

$$(2.14) \quad \alpha_f(\tilde{\mathcal{N}}) := \sum_m \alpha_f(m) + \alpha_U(\tilde{\mathcal{N}}).$$

Thus, α_f is given by summing local contributions over all upward-cooriented local extrema of \mathcal{N} and contributions from dots of $\tilde{\mathcal{N}}$, see (2.8).

Proposition 2.9. *Evaluation $\alpha_f(\tilde{\mathcal{N}})$ is an isotopy invariant of $\tilde{\mathcal{N}}$.*

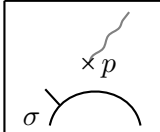
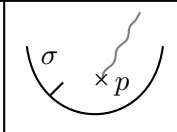
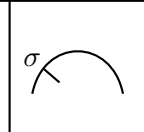
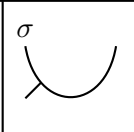
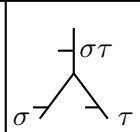
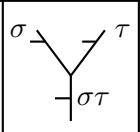
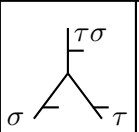
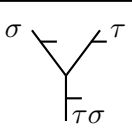
							
$\omega(p)f(\sigma)$	$-\omega(p)f(\sigma)$	0	0	0	0	0	0

FIGURE 2.3.1. Contributions of local maxima and minima are determined by $\omega(p)$, the G -winding number of the point p placed directly above the maximum or minimum, and the value of one-cocycle f on the label of the arc. The contributions are nonzero only if the co-orientation points up at the extremum point. A wavy line at p is a reminder to compute the winding number.

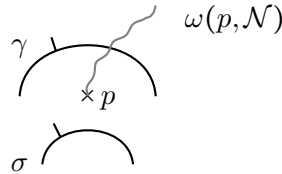


FIGURE 2.3.2. Contribution of a local maximum along an upward-oriented strand to the evaluation in Figure 2.3.1 table is given by $\omega(p)f(\sigma) \in U$, where p is a point slightly above the maximum. The G -winding number $\omega(p) = \omega(p, \mathcal{N})$ is given by moving p to infinity, along the wavy line and taking the product $\gamma^{\pm 1}$ over the intersections of the line with arcs labelled $\gamma \in G$.

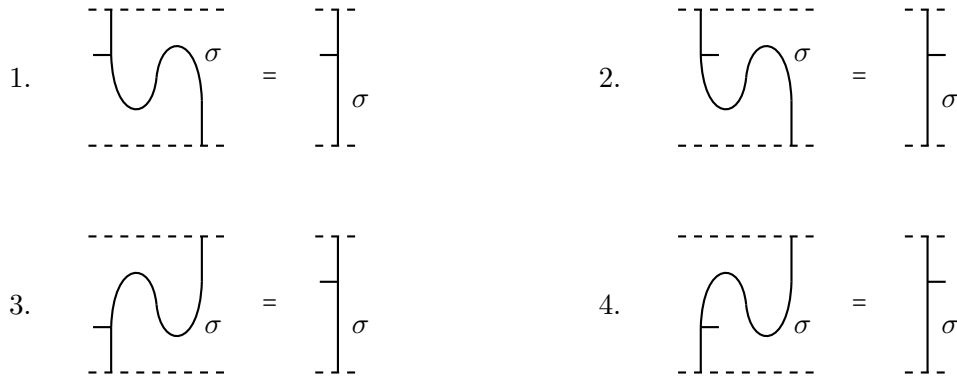


FIGURE 2.3.3. Line isotopies.

Proof. One checks that for a set of generating isotopies $\{D_1 \sim D_2\}$ the contributions of D_1, D_2 to α_f in each isotopy are equal. For instance, for line isotopies in Figure 2.3.3, diagrams D_1, D_2 both contribute 0 in cases 1, 4. In case 2, the local maximum and minimum have associated dots p_1, p_2 above them in the same region, so that $\omega(p_1, \mathcal{N}) = \omega(p_2, \mathcal{N})$ and the contributions from the two extrema add up to 0 due to the minus sign, see the first two entries of Figure 2.3.1 table. The same computation takes care of case 3.

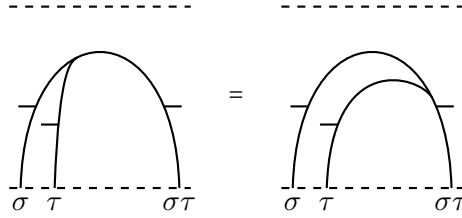


FIGURE 2.3.4. An isotopy of a vertex across a local maximum with upward arc co-orientations.

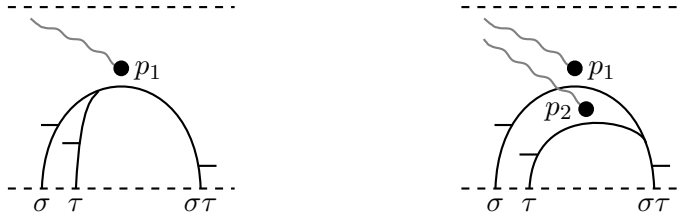


FIGURE 2.3.5. Isotopy of a vertex through a local maximum. Wavy lines show that for G -winding numbers the relation $\omega(p_1, \mathcal{N}) = \omega(p_2, \mathcal{N})\sigma^{-1}$ holds.

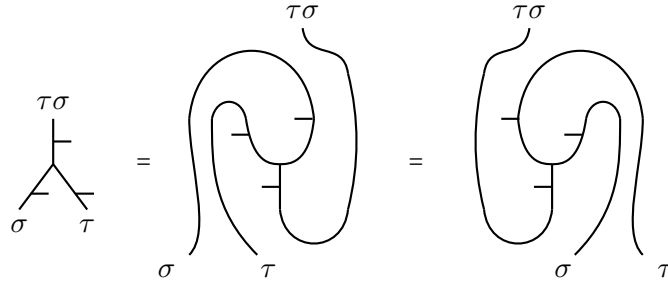


FIGURE 2.3.6. Variations on the isotopy in Figure 2.3.4.

For the diagrams in Figure 2.3.4, D_1 has a single maximum contributing $\omega(p_1, \mathcal{N}) \cdot f(\sigma\tau)$, see Figure 2.3.5. Diagram D_2 has two local maxima, with the corresponding points p_1, p_2 contributing

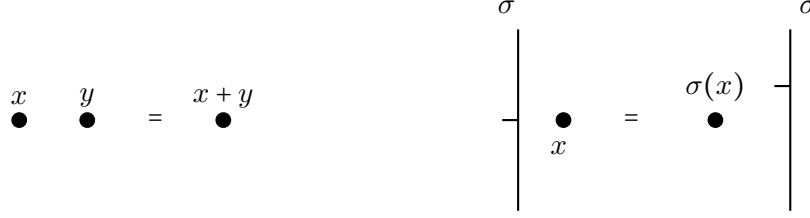
$$\omega(p_1, \mathcal{N}) \cdot f(\sigma) + \omega(p_2, \mathcal{N}) \cdot f(\tau),$$

and $\omega(p_3, \mathcal{N}) = \omega(p_1, \mathcal{N})\sigma$. Consequently, the contribution of D_2 equals

$$\omega(p_1, \mathcal{N}) \cdot f(\sigma) + \omega(p_1, \mathcal{N})\sigma \cdot f(\tau) = \omega(p_1, \mathcal{N}) (f(\sigma) + \sigma f(\tau)) = \omega(p_1, \mathcal{N}) \cdot f(\sigma\tau),$$

where the last equality is exactly the one-cocycle condition on f . We see that D_1, D_2 contribute the same amount to α_f .

For Figure 2.3.4 with the opposite co-orientations of strands, both D_1 and D_2 contribute 0 to α_f , since in that case co-orientations point downward, see entries 3 and 4 in Figure 2.3.1. Similar considerations take care of moving a vertex through a local minimum with either co-orientation. These computations also imply that the three diagrams in Figure 2.3.6 each contribute 0 to α_f , allowing the corresponding isotopies.

FIGURE 2.3.7. Dot relations in \mathcal{C}_f .

□

We can now define category \mathcal{C}_f via the universal construction for evaluation

$$\alpha_f : \text{Net}_U^I \longrightarrow U.$$

For now, we are using G -flow networks of type I , without flip points or more general vertices. This category has the same objects $X_{\underline{\sigma}}$ as categories \mathcal{C}_G and \mathcal{C}_U , over all finite sequences $\underline{\sigma}$, see earlier. It shares many features with \mathcal{C}_U , c.f. Proposition 2.5.

Proposition 2.10. *Given a one-cocycle $f : G \longrightarrow U$, category \mathcal{C}_f is a pivotal monoidal category. Any object of \mathcal{C}_f is isomorphic to X_σ , for a unique $\sigma \in G$. The hom spaces between these objects are*

$$(2.15) \quad \text{Hom}_{\mathcal{C}_U}(X_\sigma, X_\tau) = \begin{cases} U & \text{if } \sigma = \tau, \\ \emptyset & \text{otherwise.} \end{cases}$$

For a general sequence $\underline{\sigma}$ there is an isomorphism $X_{\underline{\sigma}} \cong X_{\langle \underline{\sigma} \rangle}$. Homs between two objects $\text{Hom}_{\mathcal{C}_f}(X_{\underline{\sigma}}, X_{\underline{\tau}})$ either constitute a U -torsor, if $\langle \underline{\sigma} \rangle = \langle \underline{\tau} \rangle$, or the empty set, if $\langle \underline{\sigma} \rangle \neq \langle \underline{\tau} \rangle$. Discussion following Proposition 2.5 up until Remark 2.6 applies to \mathcal{C}_f as well without any changes.

Proposition 2.11. *The following relations hold in \mathcal{C}_f :*

- (1) *Isotopy relations on diagrams.*
- (2) *Associativity of merge and split relations in Figures 2.1.3 and 2.1.4 and the merge-split invertibility relations in Figure 2.1.5.*
- (3) *Dot relations shown in Figure 2.3.7 (the same relations hold in \mathcal{C}_U).*
- (4) *Circle evaluation relations in Figure 2.3.8. Innermost outward-cooriented circle evaluates to a dot labelled $f(\sigma)$. Innermost inward-cooriented circle evaluates to the dot $f(\sigma^{-1})$.*

Note that the relation in Figure 2.1.6 does not hold for this evaluation.

The 1-cocycle relation can now be interpreted via an evaluation of nested circles in Figure 2.3.9.

Remark 2.12. A closed dotless diagram evaluates to an element of U which is usually not zero. For instance, the σ -circle diagram with outward co-orientation evaluates to $f(\sigma) \in U$, see Figure 2.3.8, and a net of three circles in Figure 2.3.10 to $f(\gamma\sigma) + \gamma f(\tau)$. To get the most freedom for that evaluation we can form the module U on generators $[\sigma]$, $\sigma \in G$, with defining relations given by the one-cocycle equations $[\sigma\tau] = [\sigma] + \sigma[\tau]$, $\sigma, \tau \in G$.

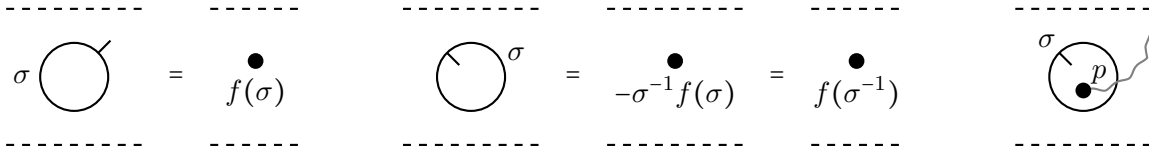


FIGURE 2.3.8. Left: evaluation of an innermost outward-cooriented circle. Middle: evaluation of an innermost inward-cooriented circle. Right: local minimum contributes to the evaluation, and the G -winding number of p relative to the outer region is σ^{-1} , which explains the computation. For the other terms in $-\sigma^{-1}f(\sigma)$ see the 2nd column in Figure 2.3.1.

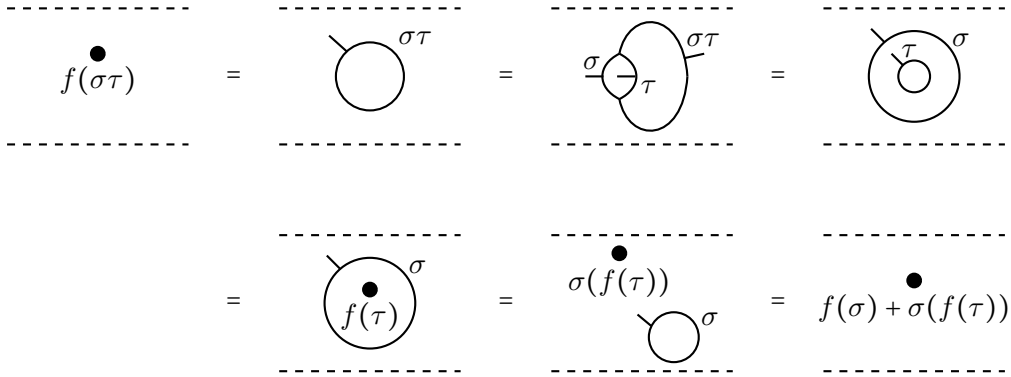


FIGURE 2.3.9. Another way to derive the cocycle relation $f(\sigma\tau) = f(\sigma) + \sigma f(\tau)$ from the evaluation, by splitting $\sigma\tau$ -circle into concentric σ - and τ -circles.

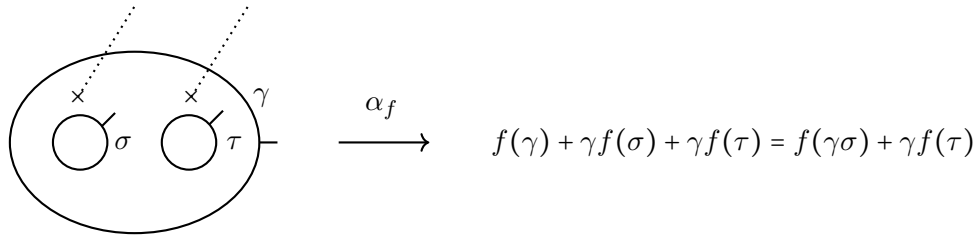


FIGURE 2.3.10. A net of three circles evaluates to $f(\gamma\sigma) + \gamma f(\tau)$.

We now extend the evaluation α_f and the diagrammatics to type II diagrams (with flip points and vertices of type II). Flip points in Figure 2.3.11 on the left (two possibilities, depending on co-orientation) are positioned vertically, and to define them as morphisms in \mathcal{C}_f we bend the upper arc down to the side where the co-orientation of the lower arc points and add a lollipop, see Figure 2.3.11.

The evaluation α_f of a flip point is computed from this reduction of a flip point to a type I diagram. Notice that the top arc bends either to the left or to the right in Figure 2.3.11, depending on co-orientations. The contribution to α_f of flip points is shown in the first two columns in Figure 2.3.12.

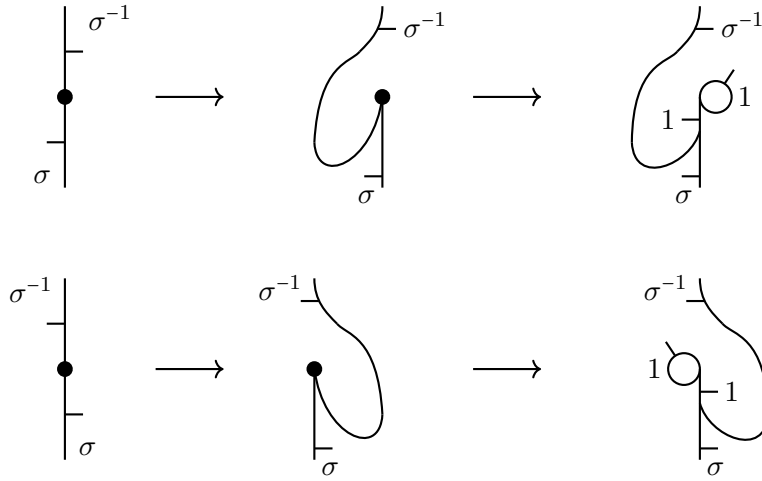


FIGURE 2.3.11. Definition of a vertically positioned flip point.

$-\omega(p)f(\sigma)$	$-\omega(p)f(\sigma)$	$-\omega(p)f(\sigma\tau)$	$-\omega(p)f(\gamma)$	$-\omega(p)f(\tau\sigma)$	$-\omega(p)f(\gamma)$

FIGURE 2.3.12. Local contributions from flip points and type II vertices.

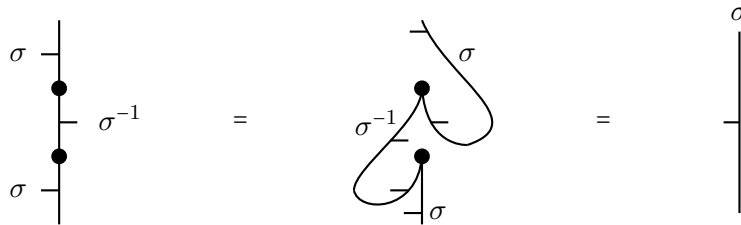


FIGURE 2.3.13. To motivate the above definition of a flip point, take a pair of them on a vertical line. Bending the two arcs in the opposite direction results in a diagram with two upward-oriented minima contributing to the evaluation (lollipops are omitted for simplicity and they don't contribute, since $f(1) = 0$). Contributions from the minima cancel out due to property (2.11) of the cocycle, and the two adjacent flip points can be removed from a vertical line.

This normalization of flip points is chosen to have the cancellation property for two flip points on a vertical line, see Figure 2.1.11 on the right and Figure 2.3.13. This is the normalization used in the paper. However, sliding flip points through local maxima and minima requires additional terms as shown in Figure 2.3.14.

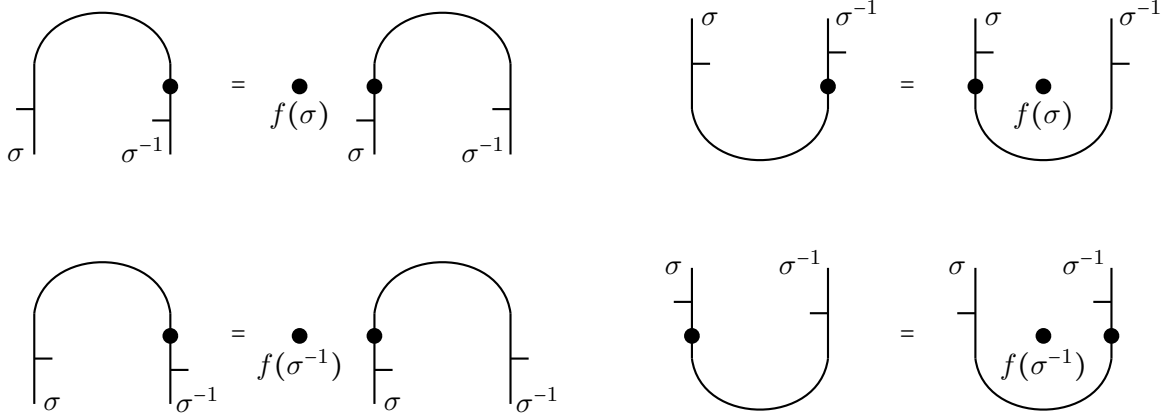


FIGURE 2.3.14. Moving a flip point across a local maximum or minimum.

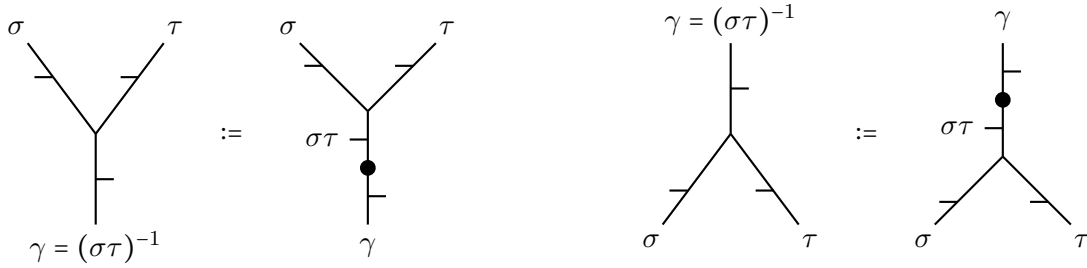


FIGURE 2.3.15. Type II vertex is defined via a composition of a type I vertex and a flip point.

Next, consider type II vertices, where co-orientations are compatible, all pointing clockwise or anticlockwise around the vertex, see Figure 2.1.16, top row. We use the convention that type II vertices must be positioned so that two or one edge at the vertex point up and the other one of two edges point down. In this way the three edges at a vertex are split into two groups: two edges and one edge. It is then natural to reduce type II vertices to type I vertices by adding a flip point to the edge which is by itself. Figure 2.3.15 shows examples of this convention.

One can take a leg (or ray) at a vertex that is among the two that point together and isotop it to be next to the other one. This move has evaluation invariance only in half of the possible cases and otherwise requires an extra term, see Figure 2.3.16.

Proposition 2.13. *For any one-cocycle $f \in Z^1(G, U)$, categories \mathcal{C}_f and \mathcal{C}_U are isomorphic as monoidal categories, and an isomorphism can be made the identity on objects.*

Proof. Define the functor $\mathcal{F}_f : \mathcal{C}_f \rightarrow \mathcal{C}_U$ to be the identity on objects and given as shown in Figure 2.3.17 on morphisms. Also, the endomorphism $m_x \in \text{End}(\mathbf{1})$ of multiplication by $x \in U$ is sent to itself by \mathcal{F}_f .

It is straightforward to see that \mathcal{F}_f is an isomorphism of monoidal categories. □

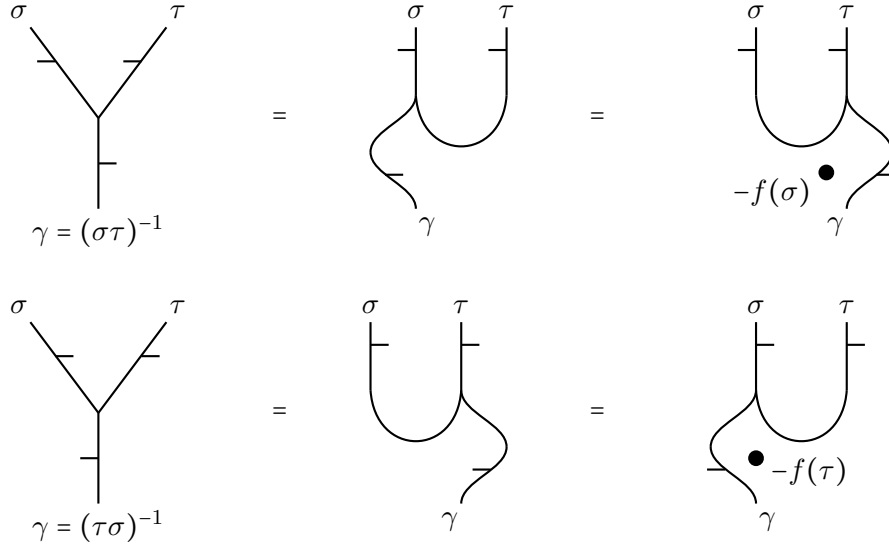


FIGURE 2.3.16. Type II vertex rotation relations.

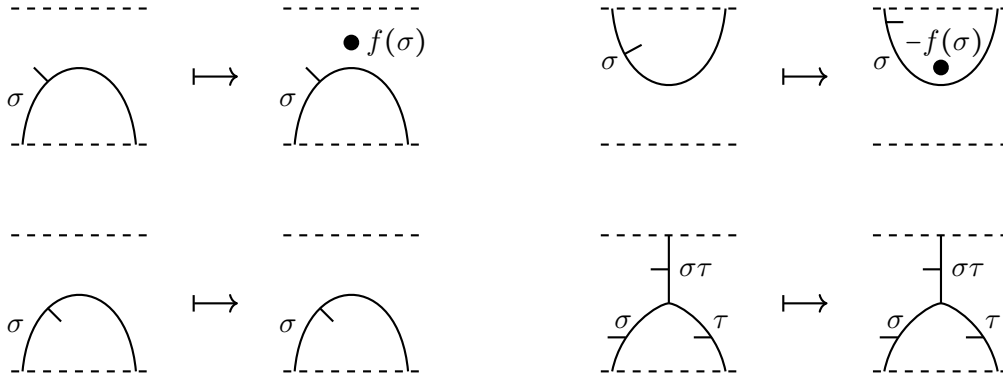


FIGURE 2.3.17. Isomorphism between categories \mathcal{C}_f and \mathcal{C}_U . The map twists generating morphisms as encoded in Figure 2.3.1. Entry 0 in that table signifies that a morphism is sent to itself (for two out of six such morphism, this is shown in the second row of the figure).

Note that we are using cups and caps to capture 1-cocycle contributions. The significance of the twist by a cocycle f is that it *changes the pivotal structure of the category*, and \mathcal{C}_f and \mathcal{C}_U are not isomorphic as pivotal monoidal categories, in general. The pivotal structure of the category is essential for incorporating this 1-cocycle twist to the evaluation.

Remark 2.14. A cocycle f is null-homologous if $f(\sigma) = \sigma u - u$ for some $u \in U$. For a null-homologous cocycle maps in Figure 2.3.17 can be rewritten to not depend on the label σ of an arc, as shown in Figure 2.3.18. More generally, if $f_1 - f_2$ is null-homologous, for cocycles f_1, f_2 , the isomorphism between categories \mathcal{C}_{f_1} and \mathcal{C}_{f_2} can be defined on generators to not depend on the labels of the arcs.



FIGURE 2.3.18. Isomorphism maps if a one-cocycle is null-homologous.

In this section 1-cocycles of G took values in an abelian group U . We briefly discuss diagrammatics for 1-cocycles valued in arbitrary groups in Section 3.2, which requires replacing floating U -labelled dots by U -labelled planar networks interacting with those for G .

2.4. Diagrammatics for a two-cocycle.

Two-cocycles. Let U be a $\mathbb{Z}[G]$ -module, as before, and assume given a 2-cocycle $c : G \times G \rightarrow U$, so that

$$(2.16) \quad \sigma(c(\tau, \gamma)) = c(\sigma, \tau) + c(\sigma\tau, \gamma) - c(\sigma, \tau\gamma), \quad \sigma, \tau, \gamma \in G.$$

We can further assume the cocycle to be normalized, so that

$$(2.17) \quad c(\sigma, 1) = c(1, \sigma) = 0, \quad \sigma \in G.$$

Denote the abelian group of normalized cocycles by $Z_0^2(G, U)$.

Specializing (2.16) to $\tau = \sigma^{-1}, \gamma = \sigma$ results in the relation

$$(2.18) \quad c(\sigma, \sigma^{-1}) = \sigma(c(\sigma^{-1}, \sigma)), \quad \sigma \in G,$$

where cocycle c is normalized.

A 2-cocycle c is called *null-homologous* if

$$c(\sigma, \tau) = b(\sigma) + \sigma(b(\tau)) - b(\sigma\tau)$$

for some function $b : G \rightarrow U$. We say that a function b is *normalized* if $b(1) = 0$. Denote by $Z_0^2(G, U)$ the set of 2-cocycles associated to normalized functions $b : G \rightarrow U$. These are normalized null-homologous cocycles.

Subtracting from c the null-homologous 2-cocycle for the constant function $b(\sigma) = c(1, 1)$ results in a normalized 2-cocycle. We assume from now on that our 2-cocycles are normalized.

The second cohomology group of G with coefficients in U can be defined as the quotient

$$(2.19) \quad H^2(G, U) = Z_0^2(G, U) / B_0^2(G, U).$$

Consider an extension T of a group G by an abelian group U , which can be written as

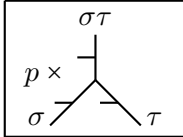
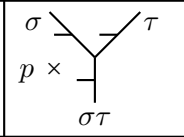
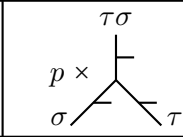
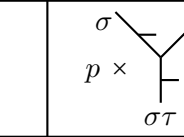
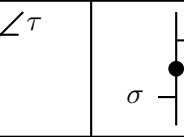
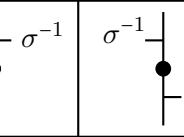
$$(2.20) \quad 1 \rightarrow U \xrightarrow{\iota} T \rightarrow G \rightarrow 1.$$

Pick a section $s : G \rightarrow T$, a map of sets, allowing to write $T \cong U \times G$ (isomorphism of sets) representing $t \in T$ as $us(\sigma)$, parameterized by (u, σ) , for unique $u \in U, \sigma \in G$. Assume that $s(1) = 1$ (normalization). Note that we write group operation in U additively and multiplicatively in T and G , so that $\iota(u_1 + u_2) = \iota(u_1)\iota(u_2)$ and $\iota(0) = 1$. Then

$$s(\sigma)s(\tau) = c(\sigma, \tau)s(\sigma\tau),$$

for a unique function $c : G \times G \rightarrow U$, and $c(\sigma, \tau)$ satisfies the additive cocycle condition (2.16) and normalization (2.17). This central extension has multiplication

$$(u_1, \sigma_1)(u_2, \sigma_2) = (u_1 + \sigma_1(u_2) + c(\sigma_1, \sigma_2), \sigma_1\sigma_2).$$

					
$\omega(p)c(\sigma, \tau)$	$-\omega(p)c(\sigma, \tau)$	$\omega(p)c(\sigma^{-1}, \tau^{-1})$	$-\omega(p)c(\sigma^{-1}, \tau^{-1})$	0	0

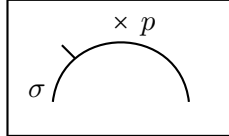
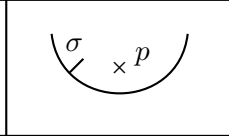
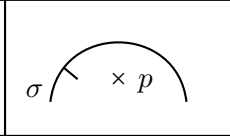
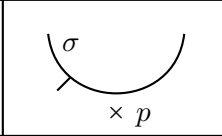
			
$\omega(p)c(\sigma, \sigma^{-1})$	$-\omega(p)c(\sigma, \sigma^{-1})$	$\omega(p)c(\sigma, \sigma^{-1})$	$-\omega(p)c(\sigma, \sigma^{-1})$

FIGURE 2.4.1. Local contributions from a two-cocycle c .

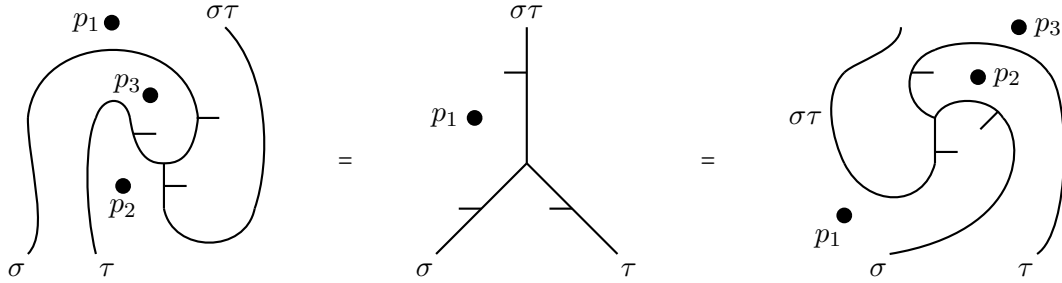


FIGURE 2.4.2. Left: isotopy at a vertex with clockwise rotation. Right: isotopy at a vertex with counterclockwise rotation.

Denote by T_c the central extension associated to the cocycle c , with the short exact sequence

$$(2.21) \quad 1 \longrightarrow U \xrightarrow{\iota} T_c \longrightarrow G \longrightarrow 1.$$

Changing σ by a coboundary is equivalent to rescaling the section s by a function

$$(2.22) \quad b : G \longrightarrow U, \quad b(1) = 0,$$

so that $s'(\sigma) = b(\sigma)s(\sigma)$ and replacing $c(\sigma, \tau)$ by

$$(2.23) \quad c'(\sigma, \tau) = b(\sigma) + \sigma(b(\tau)) - b(\sigma\tau) + c(\sigma, \tau).$$

This gives an isomorphism $T_{c'} \cong T_c$ that respects the exact sequence (2.21) and its counterpart for T_c .

We refer to Brown [Bro94] for more information on group cocycles and cohomology. The group $H^2(G, U)$ can be interpreted as the second cohomology group of the Eilenberg–MacLane space $K(G, 1)$ with coefficients in the local system given by U .

Evaluation α_c . To a normalized 2-cocycle c we associate an evaluation α_c of diagrams as shown in Figure 2.4.1. It extends to type II vertices via their definition in Figure 2.3.15.

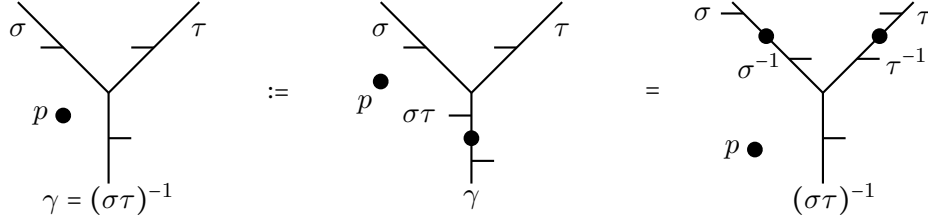


FIGURE 2.4.3. Consistency check for a type II vertex evaluation.

Proposition 2.15. *This evaluation function is invariant under isotopies of diagrams.*

Proof. We will show the invariance under rotation of a vertex in Figure 2.4.2. The element of U associated to the diagram on the left hand side in Figure 2.4.2 is

$$(2.24) \quad -\omega(p_2)c(\tau^{-1}, \sigma^{-1}) + \omega(p_1)c(\sigma, \sigma^{-1}) + \omega(p_3)c(\tau, \tau^{-1}) - \omega(p_1)c(\sigma\tau, (\sigma\tau)^{-1}).$$

We also have

$$(2.25) \quad \omega(p_2) = \omega(p_1)\sigma\tau \quad \text{and} \quad \omega(p_3) = \omega(p_1)\sigma.$$

Rewrite (2.25) as

$$(2.26) \quad \omega(p_2)c(\tau^{-1}, \sigma^{-1}) = \sigma\tau\omega(p_1)c(\tau^{-1}, \sigma^{-1})$$

and

$$(2.27) \quad \omega(p_3)c(\tau, \tau^{-1}) = \sigma\omega(p_1)c(\tau, \tau^{-1}).$$

Applying the 2-cocycle condition (2.16) to the right hand side of (2.26), we have

$$(2.28) \quad \sigma\tau c(\tau^{-1}, \sigma^{-1}) = c(\sigma\tau, \tau^{-1}) + c(\sigma\tau\tau^{-1}, \sigma^{-1}) - c(\sigma\tau, \tau^{-1}\sigma^{-1}).$$

Similarly, we apply (2.16) to the right hand side of (2.27) to obtain

$$(2.29) \quad \sigma c(\tau, \tau^{-1}) = c(\sigma, \tau) + c(\sigma\tau, \tau^{-1}) - c(\sigma, \tau\tau^{-1}).$$

Combine (2.28) and (2.29) into (2.24) to obtain

$$\begin{aligned} & -\cancel{\omega(p_1)c(\sigma\tau, \tau^{-1})} - \cancel{\omega(p_1)c(\sigma, \sigma^{-1})} + \omega(p_1)c(\sigma\tau, \tau^{-1}\sigma^{-1}) + \omega(p_1)c(\sigma, \sigma^{-1}) \\ & + \omega(p_1)c(\sigma, \tau) + \cancel{\omega(p_1)c(\sigma\tau, \tau^{-1})} - \cancel{\omega(p_1)c(\sigma, 1)} - \cancel{\omega(p_1)c(\sigma\tau, (\sigma\tau)^{-1})} \\ & = \omega(p_1)c(\sigma, \tau) \end{aligned}$$

since $c(\sigma, 1) = 0$. We therefore conclude

$$-\omega(p_2)c(\tau^{-1}, \sigma^{-1}) + \omega(p_1)c(\sigma, \sigma^{-1}) + \omega(p_3)c(\tau, \tau^{-1}) - \omega(p_1)c(\sigma\tau, (\sigma\tau)^{-1}) = \omega(p_1)c(\sigma, \tau).$$

For the counterclockwise rotation in Figure 2.4.2, the proof that the diagrams in the middle and the right hand side of Figure 2.4.2 have the same evaluation is similar. This proves the compatibility under rotations of vertices.

Now, consider Figure 2.4.3. To evaluate the left hand side, introduce a flip point at the bottom so that the co-orientations about the vertex are all pointing in the same direction. Then move the flip point through the vertex, resulting in two flip points along

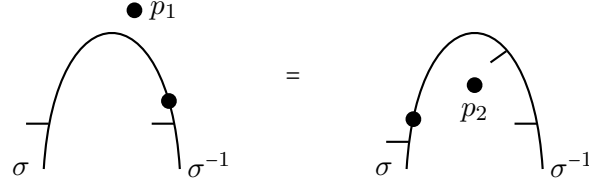


FIGURE 2.4.4. Sliding a flip point across an extremum.

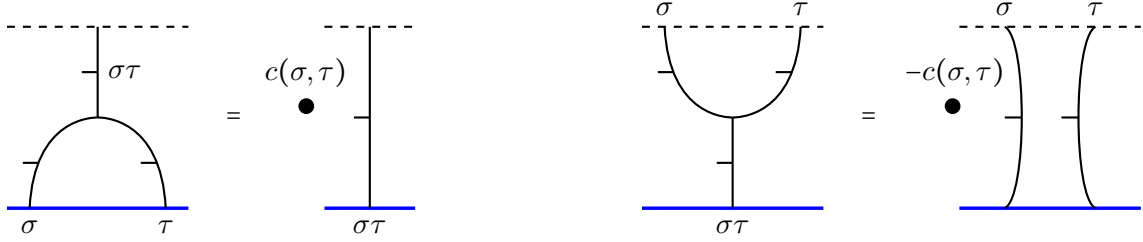


FIGURE 2.4.5. Left: boundary wall absorbs a (σ, τ) triangle and emits $c(\sigma, \tau)$ dot to the region on the left (where co-orientation points out). Right: Boundary wall absorbs a $\sigma\tau$ line with a vertex, at the cost of adding $c(\sigma, \tau)^{-1}$ to the region on the left.

the two edges above the vertex. Using Figure 2.4.1, the evaluation in the middle of Figure 2.4.3 is $-\omega(p)c(\sigma, \tau)$ while the evaluation on the right is $-\omega(p)c((\sigma^{-1})^{-1}, (\tau^{-1})^{-1})$. Since $-\omega(p)c(\sigma, \tau) = -\omega(p)c((\sigma^{-1})^{-1}, (\tau^{-1})^{-1})$, this case is complete.

We will now check the invariance of the evaluation function when moving a flip point across a local extremum, see Figure 2.4.4. Using Figure 2.4.1, the left hand side of Figure 2.4.4 evaluates to $\omega(p_1)c(\sigma, \sigma^{-1})$ while the right hand side evaluates to $\omega(p_2)c(\sigma^{-1}, \sigma)$. Sliding p_2 across the σ edge gives $\omega(p_2) = \omega(p_1)\sigma$. This gives $\omega(p_2)c(\sigma^{-1}, \sigma) = \omega(p_1)\sigma c(\sigma^{-1}, \sigma)$. Since $c(\sigma, \sigma^{-1}) = \sigma c(\sigma^{-1}, \sigma)$ by (2.18), we are done.

Remaining details are left to the reader. \square

Boundary wall. One way to interpret local evaluation rules in Figure 2.4.1 and similar rules for a one-cocycle in Figure 2.3.1 and 2.3.12 is by introducing a boundary wall that can absorb and emit parts of a diagram at the cost of producing dots. Namely, we add the following rules for modifying networks at the boundary (and discuss only the two-cocycle case here).

We introduce relations in Figure 2.4.5. The first relation says that the wall (the boundary of the half-plane, shown in blue) can absorb a (σ, τ) vertex at the cost of adding a dot $c(\sigma, \tau) \in U$ floating to the left of the $\sigma\tau$ line. The second relation absorbs an interval $\sigma\tau$ and a vertex in the opposite way, at the cost of $-c(\sigma, \tau)$ floating in the left region. These two relations interpret the first two entries in the Figure 2.4.1 table via the absorbing wall.

The two relations are equivalent modulo the relation in Figure 2.1.5 on the right, as explained in Figure 2.4.6.

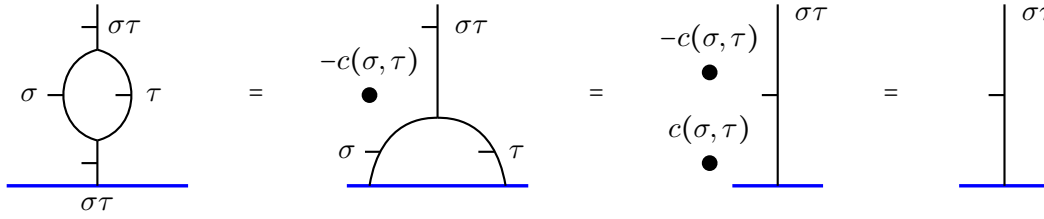


FIGURE 2.4.6. First equality is the relation in Figure 2.4.5 on the right. The second equality is the relation in Figure 2.4.5 on the left. The leftmost diagram in this figure also reduces to the one on the right via the right relation in Figure 2.1.5.

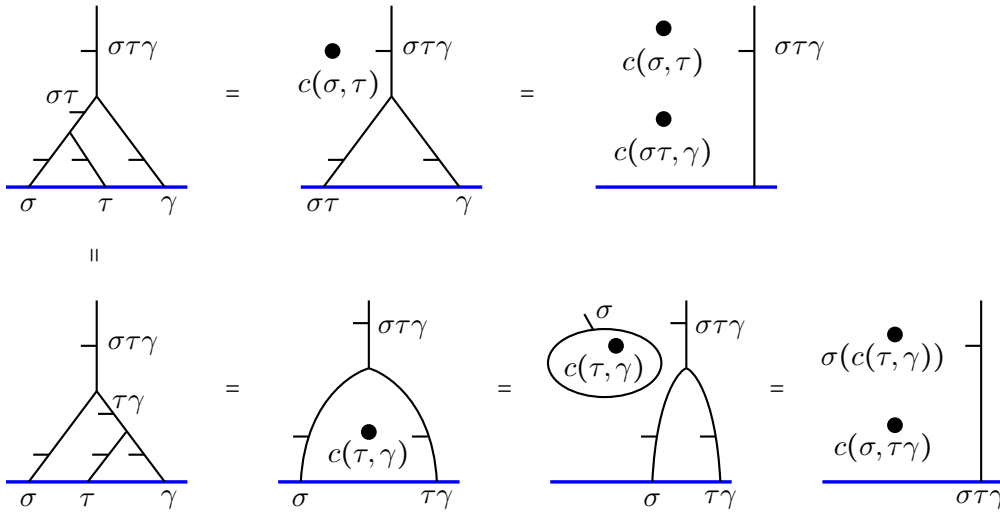


FIGURE 2.4.7. Associativity of merging (or splitting) of G -lines near the boundary is equivalent to the 2-cocycle condition (2.16). Vertical equality on the left is the associativity relation (2.1.3).

Figure 2.4.7 shows that a version of Figure 2.1.3 associativity relation at the wall is equivalent to the 2-cocycle condition (2.16) on c . Note that a dot labelled $c(\tau, \gamma)$ gets twisted by σ when it crosses the σ -line.

We add the relation that a flip point can be absorbed or emitted from the wall, at no cost, see Figure 2.4.8 on the left and the corresponding entry in Figure 2.4.1. The relation on the right of Figure 2.4.8 follows as shown in Figure 2.4.9.

Example 2.16. Figure 2.4.10 shows two ways to simplify a pair of parallel arcs at the wall labelled σ and σ^{-1} . Naturally, the resulting elements of U are equal, due to the relation $c(\sigma, \sigma^{-1}) = \sigma(c(\sigma^{-1}, \sigma))$, which is (2.18).

In Figure 2.4.5 on the left the triangle with sides σ and τ lines and a boundary interval as the base is simplified to a dot $c(\sigma, \tau)$ in the leftmost region and a vertical $\sigma\tau$ line. Alternatively, it can be simplified in two other ways, using the Figure 2.4.5 relation on the right to absorb either the σ or the τ line and then reduce the arc with two endpoints on the boundary line.

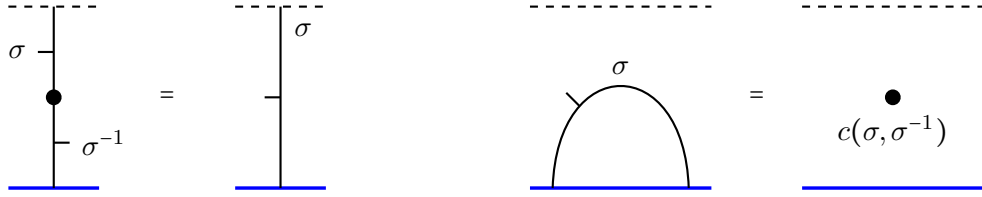


FIGURE 2.4.8. Left: a flip point can be created or absorbed into the boundary at no cost. Right: a boundary σ -labelled out-cooriented arc evaluates to $c(\sigma, \sigma^{-1})$. Both of these rules are from the table in Figure 2.4.1.

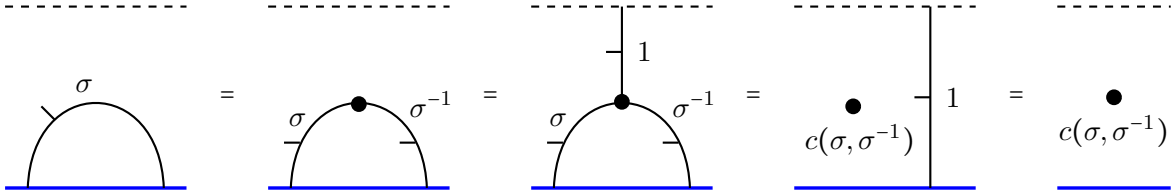


FIGURE 2.4.9. Rule for the arc can be viewed as a special case of the vertex absorption rule, when the upward line out of the vertex is labelled $1 \in G$. Lines labelled by the trivial element of G can usually be erased from the diagram.

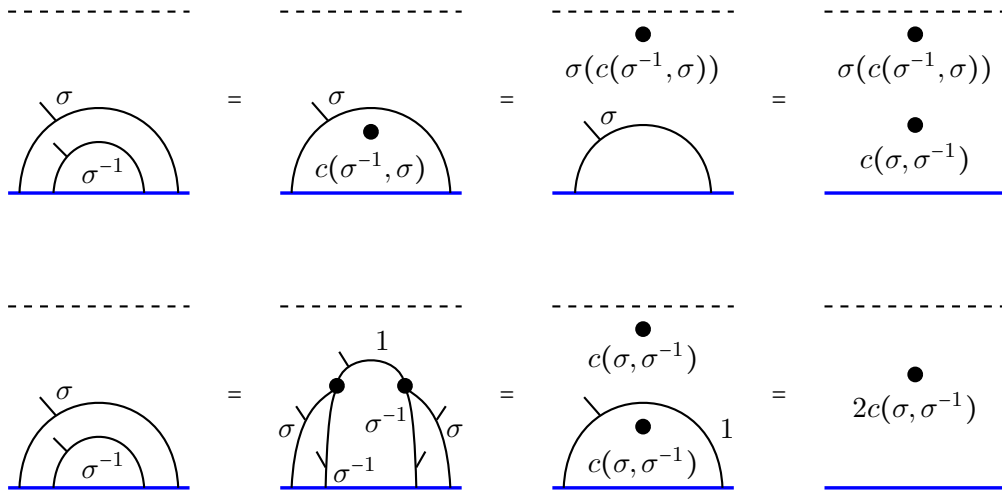


FIGURE 2.4.10. Two ways to compute the evaluation of a pair of concentric arcs at the boundary, with labels σ and σ^{-1} . In the second equality in the bottom row, we use two reductions as in Figure 2.4.5 on the left, resulting in $c(\sigma, \sigma^{-1})$ floating outside the 1-line, and another dot floating inside. A 1-line can be erased. The two computations give the same answer, see (2.18).

In Figure 2.4.11 we check that the simplification along the τ -line yields the same answer, and a similar computation gives the same answer for the reduction along the σ -line. This is part of checking that the rules in Figure 2.4.1 are consistent.

Proposition 2.17. *Any closed diagram without dots evaluates to 0.*

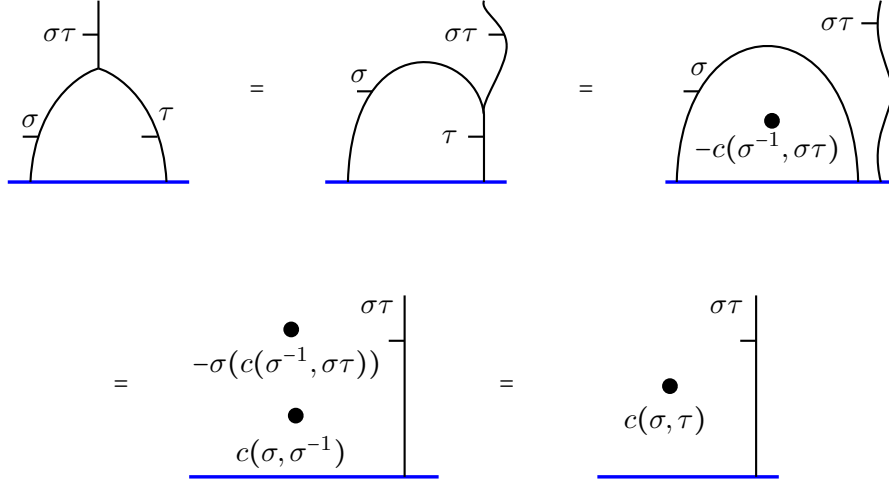


FIGURE 2.4.11. Reduction along the τ -line gives the same answer as Figure 2.4.5 on the left. Plugging $(\sigma, \sigma^{-1}, \sigma\tau)$ in place of (σ, τ, γ) in (2.16) implies the last equality above.

Proof. To check that any closed diagram D evaluates to 0, pick a bounded region r of D with k sides. Cancel the co-orientation reversal dots on the sides in pairs so that each side has at most one dot. The idea is to use associativity relations in Figures 2.1.3 and 2.1.4 and their variations to reduce the number of sides of r without changing the evaluation. Note that two diagrams D_1, D_2 that differ by an edge flip as in Figure 2.1.3 on the left (vertical equality) have equal evaluation, due to the 2-cocycle property.

For instance, evaluation invariance under the move on the left in Figure 2.1.4 is the relation

$$c(\sigma, \tau) - c(\gamma, \gamma^{-1}\sigma\tau) = -\sigma(c(\sigma^{-1}\gamma, \sigma^{-1}\gamma\tau)) + c(\sigma, \sigma^{-1}\gamma),$$

which is equivalent to the 2-cocycle property (2.16). The move on the right in Figure 2.1.4 is the relation

$$-\sigma(c(\sigma^{-1}\gamma, \gamma^{-1}\sigma\tau)) + c(\sigma, \sigma^{-1}\gamma) = -c(\gamma, \gamma^{-1}\sigma) + \gamma c(\gamma^{-1}\sigma, \tau).$$

This relation follows by expanding the two terms with the action of σ and γ into signed sums of cocycles via (2.16) and canceling the resulting terms.

Using these two relations and moving the flip points on edges of r through vertices, if needed, we can keep shrinking the number of edges of r until it has only one edge left, as shown in Figure 2.4.12 on the left. The remaining edge is a circle labelled by $\tau \in G$. This circle and the attached 1-edge can be deleted from the diagram since $c(\tau, 1) = 1$. The opposite endpoint of the 1-edge contributes $c(\sigma, 1) = 0$ for some σ , allowing to delete this configuration without changing the evaluation.

An example of dealing with dots is shown in Figure 2.4.12 on the right, where in a digon region a flip point is present on the boundary. We bend the diagram to evaluate it, resulting in $\sigma\tau(c(\tau^{-1}, \tau)) - c(\sigma, \tau) - c(\sigma\tau, \tau^{-1}) = 0$, matching the evaluation of the vertical line $\sigma\tau$.

This chain of transformations reduces the number of regions of D by one without introducing any dots and preserving the evaluation. Note also that a circle evaluates to 0 and flip

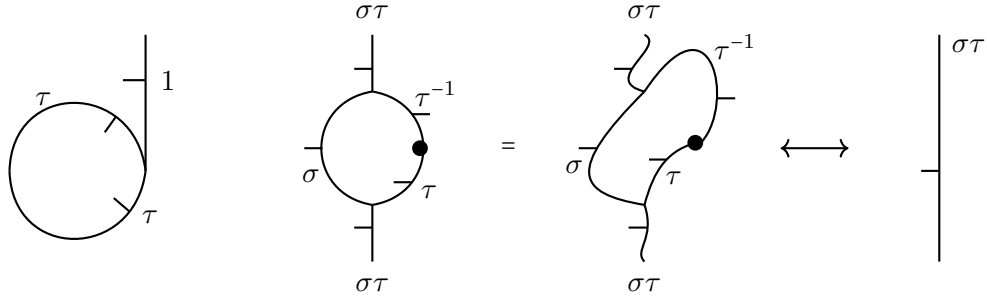


FIGURE 2.4.12. Left: a region with a single boundary edge. Right: example of a digon region with a single flip point. The diagram is deformed to compute the evaluation via the rules in Figure 2.4.1.

points contribute 0 to the evaluation, see Figure 2.4.8. These facts together imply that any closed diagram evaluates to 0. \square

Remark 2.18. The 2-cocycle evaluation α_c has a different flavor from the 1-cocycle evaluation in Section 2.3, for there a closed diagram without dots can evaluate to a nonzero element of U .

Remark 2.19. Proposition 2.17 implies that, given two dotless diagrams D_1, D_2 with the same top and bottom boundaries, having the bottom (blue) line swallow them results in the same value $x \in U$ for the dot in the terminal diagram that consists of vertical lines and a single floating dot in the leftmost region. Consequently, the evaluation x of a dotless diagram D with boundary depends only on the boundary of D . In this way, the function that to a dotless diagram D assigns its evaluation x can be viewed as a one-dimensional theory, depending only on the sequences of labels and co-orientations at the top and bottom lines of D .

Corollary 2.20. *The category \mathcal{C}_c associated to a normalized cocycle c is isomorphic to \mathcal{C}_U as a monoidal category.*

Proof. This is immediate due to Proposition 2.17, since the evaluation of a closed dotless diagram is trivial, and dots are transformed in the same way in both twisted and untwisted diagrammatics. The significance of c is in a different evaluation for diagrams with boundary. \square

Remark 2.21. A 2-cocycle c as above gives a monoidal automorphism of \mathcal{C}_U , where each generating morphism is twisted by a dot placed in the region marked by p in Figure 2.4.1, and the dot is labelled by the coefficient given in the table in that figure (for instance, coefficient $-c(\sigma, \tau)$ for the second entry in the first row of the table).

Remark 2.22. Elements of the central extension T_c of G by U in (2.21) have an interpretation as shown in Figure 2.4.13, where an element is represented by a vertical line σ and a dot $x \in U$. The multiplication of two such diagrams is given by merging the lines and reducing the diagram to a dot and a vertical line, as shown in the same figure. Elements of the central normal subgroup $U \subset G$ correspond to the diagrams with $\sigma = 1$, and the vertical line then can be erased, leaving us with a dot labelled $x \in U$.

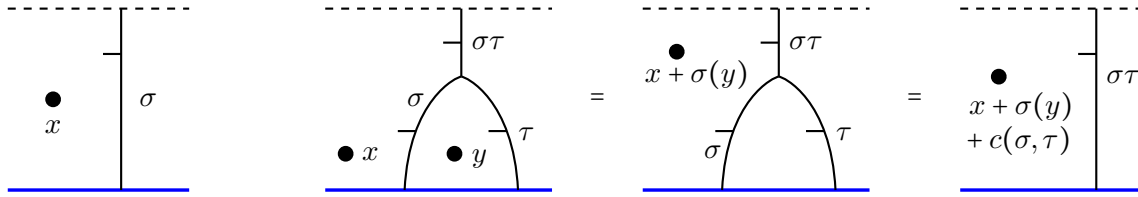


FIGURE 2.4.13. Left: diagram for an element $x\sigma \in T_c$. Middle: multiplication of two elements is given by placing them next to each other and merging the strands. The diagram simplifies as shown.

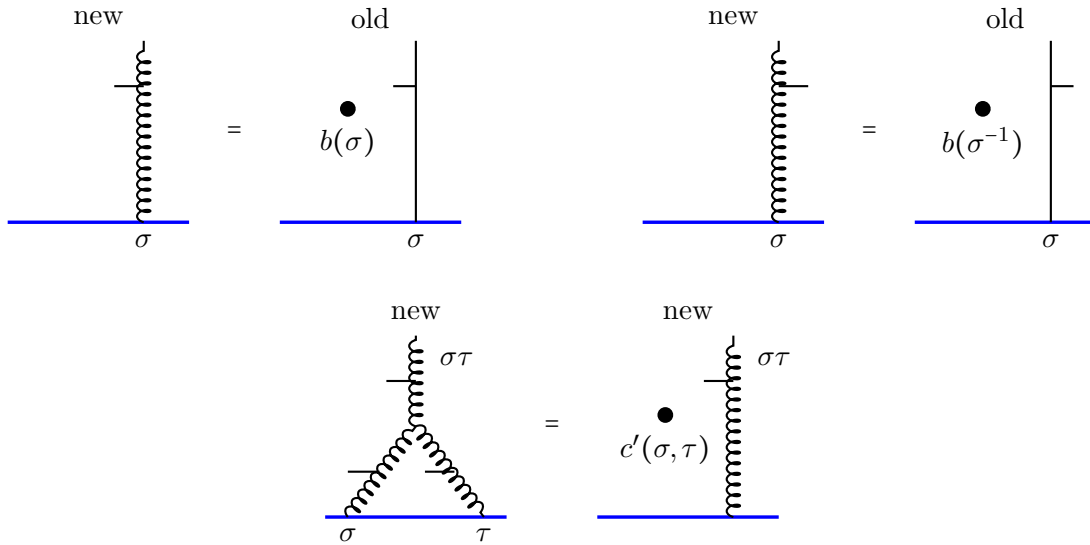


FIGURE 2.4.14. Top row: twisting diagrammatical calculus at the boundary by rescaling at each boundary point of the network. Bottom row: new cocycle $c'(\sigma, \tau)$, computed in the next figure.

Changing by a coboundary. Given a rescaling b as in (2.22), consider the locally defined map

$$r_b : \text{Net} \longrightarrow \text{Net}$$

given by scaling each boundary point of the diagram by placing $b(\sigma)$ to the region on the left if the corresponding edge is co-oriented to the left, and $b(\sigma^{-1})$ if the edge is co-oriented to the right, see Figures 2.4.14 and 2.4.15, where new lines (after rescaling) are shown as spirals.

For a network of spiral lines, each endpoint at the boundary is rescaled as above. In particular, if an interval enters at both endpoints, both endpoint are rescaled. The rest of the diagram is left untouched (intervals and circles disjoint from the boundary and dots do not contribute to the scaling).

We show in Figures 2.4.14 and 2.4.15 how the cocycle changes after this twisting, matching the formula (2.23).

Proposition 2.23. *There is a commutative diagram with horizontal arrow isomorphisms – the rescaling r_b and the isomorphism $T_{c'} \cong T_c$ described earlier and evaluation maps as vertical*

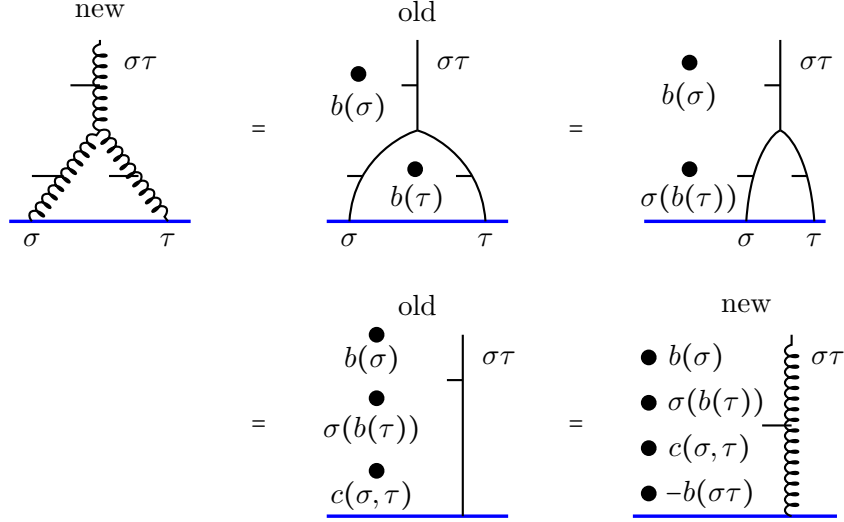


FIGURE 2.4.15. Computation of the cocycle value $c'(\sigma, \tau)$, also see Figure 2.4.14 bottom row. The value is equal to the sum of labels of the four dots in the last diagram. This results in the formula (2.23).

arrows:

$$\begin{array}{ccc}
 \text{Net} & \xrightarrow{r_b} & \text{Net} \\
 \langle \rangle_{c'} \downarrow & & \downarrow \langle \rangle_c \\
 T_{c'} & \xrightarrow{\cong} & T_c
 \end{array}$$

Thus, to each element of $H^2(G, U)$ there is assigned an isomorphism class of diagrammatic calculus of G -networks in the half-plane.

Remark 2.24. Given a 1-cocycle $f \in Z^1(G, U)$ and a 2-cocycle $c \in Z^2(G, U)$, the evaluations described in Sections 2.3 and 2.4 can be added and their sum used to define a monoidal category $\mathcal{C}_{c,f}$ that generalizes both \mathcal{C}_c and \mathcal{C}_f .

Remark 2.25. This and the previous sections explain how one-cocycles and normalized two-cocycles allow to twist the graphical calculus for the category \mathcal{C}_U . Zero-cocycles can be added as well. They correspond to G -invariant elements $z \in U^G$. One can add z to an evaluation of a closed diagram for a one-cocycle, by placing z -labelled dot anywhere in the diagram. This does not change the skein relations for the category \mathcal{C}_f , for a one-cocycle f , but it kind of allows to involve 0-cocycles for (G, U) in the construction, albeit in a trivial way.

Remark 2.26. Labeling domain walls in TQFTs by elements of a finite group G and introducing 2-cocycles in relation to codimension two submanifolds (seams) where domain walls for g and h merge into a gh -wall is common in condensed matter and physics TQFT literature, see for instance [BCH⁺23, Figure 25] and [Tac20]. In the physics literature the action of G on U is usually trivial, and floating labelled dots in the regions can then be taken out of the diagram as scalars. Another difference is that in the present paper the action on U is additive, while in the physics literature the action is multiplicative, where one typically considers $H^n(G, \mathbb{C}^*)$ or a similar group. Nontrivial multiplicative actions of a group G on a ring R appear in

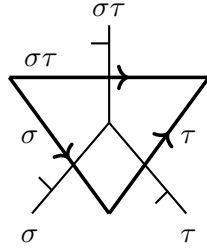


FIGURE 2.4.16. The dual simplex to a vertex of the network, with its edges labelled $\sigma, \tau, \sigma\tau$.

the theory of the Brauer group, and we hope to discuss those in the framework of suitable monoidal categories and their diagrammatics in a follow-up paper.

Remark 2.27. G -networks in the plane, of type I, with or without dots, can be given a topological interpretation. Consider the classifying space BG of a group G . It has a cell decomposition with a single 0-cell x_0 , edges labelled by elements of G , 2-simplices labelled by ordered pairs of elements of G , and so on. A planar G -network \mathcal{N} in a bounded region $X = [a, b] \times [0, 1]$ of the strip $\mathbb{R} \times [0, 1]$ of a plane gives rise to a simplicial map $X \rightarrow BG$. This map is constructed by forming a triangulation of X Poincaré dual to the network \mathcal{N} . Figure 2.4.16 shows the dual simplex to a vertex of a network.

The triangulation is decorated: edges are oriented and labelled by elements of G , so that a 2-simplex carries elements $\sigma, \tau, \sigma\tau \in G$ on its edges. Such a triangulation defines a simplicial map $\phi_{\mathcal{N}} : X \rightarrow BG$.

If network \mathcal{N} is closed (has no boundary points), ∂X is mapped to the base point of BG . The map $\phi_{\mathcal{N}}$ can then be viewed as a simplicial and basepoint-preserving map $\phi_{\mathcal{N}} : \mathbb{S}^2 \rightarrow BG$ of a 2-sphere into the classifying space.

Since the latter is a $K(G, 1)$ -space, map $\phi_{\mathcal{N}}$ is null-homotopic, through a CW-homotopy. The latter homotopy $\phi_{\mathcal{N}}^{\dagger} : \mathbb{S}^2 \times [0, 1] \rightarrow BG$ contracts $\phi_{\mathcal{N}}(\mathbb{S}^2)$ to a point and can be made combinatorial. The corresponding transformations of the network should match relations including those in Figures 2.1.3 through 2.1.6.

Suppose given a representation U of $\mathbb{Z}[G]$. Consider a connected CW-complex Y with

$$\pi_1(Y) \cong G, \quad \pi_2(Y) = U,$$

such that $\pi_1(Y)$ acts on $\pi_2(Y)$ via the representation U . A detailed analysis of related spaces can be found in [MW50]. Form a fibration $p : Y \rightarrow BG$ with fibers homotopy equivalent to a space W with $\pi_1(W) = 1$ and $\pi_2(W) \cong U$. Monodromy action of $G \cong \pi_1(Y) \cong \pi_1(BG)$ on $W_0 := p^{-1}(x_0)$, the fiber above the basepoint $x_0 \in BG$, matches the action of G on U .

Our setup also requires existence of a section $\iota : BG \rightarrow Y$ so that $p\iota = \text{id}_{BG}$. Pick the base point $w_0 = W_0 \cap \iota(BG)$ above x_0 .

Given a diagram D of a type I G -network with floating dots labelled by elements of U , in a patch X of the plane \mathbb{R}^2 , we can construct a map $X \rightarrow Y$ corresponding to D . For a dot $d \in U$ labelled $a \in U$, take a tubular neighbourhood $V(d) \subset X$ and send it to a 2-sphere $\mathbb{S}^2 \in W_0$ representing element a in $U \cong \pi_2(W_0, w_0)$, so that the boundary of the neighbourhood maps to the base point w_0 . Neighbourhood of a trivalent vertex for lines σ, τ merging into $\sigma\tau$

is sent to the 2-simplex for (σ, τ) in the classifying space $BG \subset Y$. Furthermore, points of X away from a tubular neighbourhood of lines and dots in D are sent to the basepoint w_0 .

With this convention, relations on these networks in Section 2.2 can be converted into rel boundary homotopies of maps $X \rightarrow Y$ associated to networks. A 2-cocycle $c : G \times G \rightarrow U$ can be suitably interpreted in this setup as well. We plan to provide a detailed correspondence in another paper.

3. DIAGRAMMATICS FOR TWO TYPES OF LINES

3.1. Crossed products of groups and overlapping networks of two kinds.

Suppose U is a group, not necessarily abelian, and we are given a group homomorphism $\psi : G \rightarrow \text{Aut}(U)$. This data (U, G, ψ) determines a split extension of groups

$$(3.1) \quad 1 \longrightarrow U \longrightarrow T \overset{s}{\dashrightarrow} G \longrightarrow 1,$$

or, equivalently, describes the semidirect product $T = U \rtimes G$. Its elements are $a \cdot \sigma$, with the multiplication $(a \cdot \sigma)(b \cdot \tau) = a\sigma(b) \cdot \sigma\tau$. A refinement of diagrammatics from Section 2.1 gives a graphical calculus for a semidirect product, as follows.

Although G acts on U , since U is no longer abelian one cannot use dots in the plane to denote its elements. Instead, we use co-oriented lines labelled by elements of U which can merge and split, as in Section 2.1. These lines are shown as thin lines in black throughout this section, referred to as *U-lines*, see Figure 3.1.1 top left.

Elements of G are labels of co-oriented lines of the second kind, depicted as thick wavy red lines. They can merge and split as well, in the usual way consistent with the setup of Section 2.1, see Figure 3.1.1 top middle. They are referred to as *G-lines*. A *G-line* and a *U-line* can intersect, and the label of the *U-line* is changed by the action of G on it, see Figure 3.1.1 top right.

There are a number of moves on these diagrams – we leave working out a full set of them to the reader. Moves on networks with edges labelled by elements of a group were discussed in Section 2.1, and the moves there apply to both *U-line* and *G-line* networks. In general, a *U-line* and a *G-line* networks overlap, forming a single network.

There are local moves for these overlapping networks. In particular, *G-lines* and *U-lines* and their vertices can slide through each other as shown in Figure 3.1.1.

Remark 3.1. Additionally, one can allow flip points and vertices of type II for both *G-lines* and *U-lines*, with the obvious modification rules, as discussed in Section 2.1.

An alternative way to get a set of local moves is to consider the simplest evaluation as in Section 2.1, where each closed diagram of overlapping *U-* and *G-*networks is evaluated to $0 \in \{0\}$. For this evaluation any modification of the diagram that preserves its boundary is an allowed move. The result is the monoidal category \mathcal{C}_T for the semi-direct product group T in (3.1), but with a slightly different diagrammatic description, using the above two types of lines.

A general element $a \cdot \sigma$ of T , $a \in U, \sigma \in G$ gives an object of \mathcal{C}_T represented by a pair of dots on a horizontal line, labelled by a and σ , respectively, as shown on the boundaries of Figure 3.1.2 on the left. The figure, also on the left, shows the identity morphism of this object, described by a pair of parallel lines labelled a and σ .

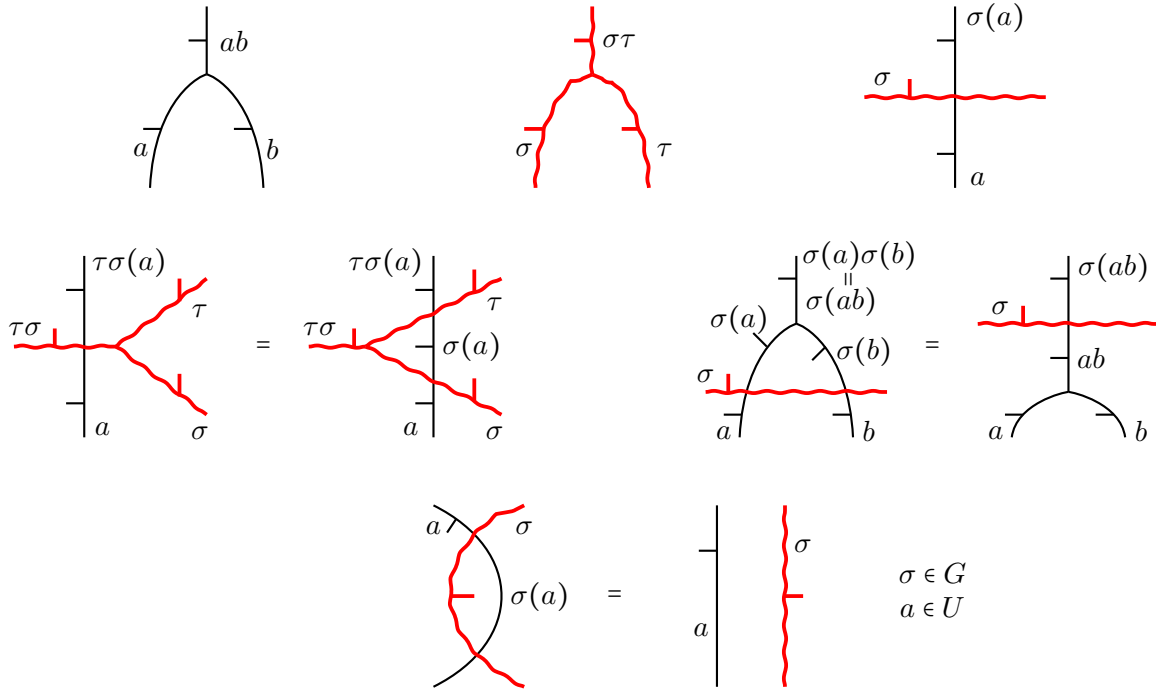


FIGURE 3.1.1. Two types of lines and their interactions. Top left: U -lines a, b merge into ab . Top middle: G -lines σ, τ merge into the line $\sigma\tau$. Top right: label of U -line changes from a to $\sigma(a)$ as it crosses a G -line σ . Middle left: a U -line slides through a G -network crossing. Middle right: a G -line slides through a U -network crossing. Bottom center: a Reidemeister II style move, pulling a U -line and a G -line apart.

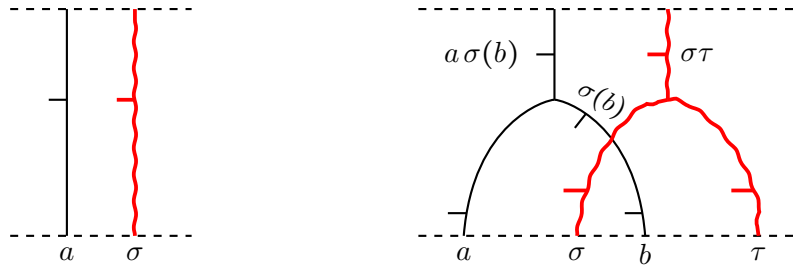


FIGURE 3.1.2. Left: element $a \cdot \sigma \in T$. Right: a diagram describing multiplication (3.1) in the semidirect product T .

An arbitrary object of \mathcal{C}_T is represented by a finite sequence of elements of U and G , together with co-orientation data at these points. Two sequences represent the same element of T if and only if there is a morphism (network) between them, and there is at most one morphism between any two objects of \mathcal{C}_T .

With these conventions, Figure 3.1.2 on the right shows a morphism from the object (a, σ, b, τ) , with all co-orientations to the left, to the object $(a\sigma(b), \sigma\tau)$, again with left co-orientations. This morphism is given by overlapping U - and G -networks, each a merge. Note how the label on the b -edge changes to $\sigma(b)$ as the U -edge crosses G -edge σ .

Given a left $\mathbb{Z}[T]$ -module M , the diagrammatics can be further extended by allowing elements of M to float in regions, subjects to the rules described in Section 2.2. This gives rise to a category equivalent to $\mathcal{C}_{T,M}$ but with a slightly different diagrammatics. Constructions of Sections 2.3 and 2.4 work in this case as well.

Assume now that U is abelian. One can then introduce a crossing of two U -lines, with either co-orientations, as the composition of a merge followed by a split, see Figure 2.1.15. The crossings satisfy the usual permutation relations in the symmetric group, for either co-orientations.

Furthermore, for abelian U , we can introduce dots labelled by U floating in regions of the plane separated by the G -network. These dots can freely cross U -lines and they interact with G -lines as described in Section 2.2. Assume that the lines shown in figures in that section are red. Any point has a G -index as in (2.7) and a closed diagram evaluates to an element of U . Note that the U -network does not contribute to the evaluation, the evaluation is the sum over floating dots of their labels twisted by the action of G via G -winding numbers of the labels.

On the other hand, if U is abelian, we may drop using U -networks and just revert to U -labelled dots and G -networks, as in Section 2.2. Multiplication in the central extension T is then encoded as in Figure 2.4.13 but with the trivial cocycle $c(\sigma, \tau) = 0 \in U$ for all $\sigma, \tau \in G$. The cocycle can be chosen to be trivial since the extension is split. We then recover category \mathcal{C}_c as in Section 2.4, for the zero cocycle c .

Remark 3.2. One can additionally fix a one-cocycle $f \in Z^1(G, U)$ (still assuming abelian U) and change the evaluation by adding contributions as in Figures 2.3.1 and 2.3.12 from the G -lines (which are wavy lines shown in red in this section). One then gets a different monoidal category, which we denote $\mathcal{C}_{G,U}^f$. It has more interactions between dots and G -lines. For example, a G -circle can be converted to a dot, as in Figures 2.3.8 and 2.3.9.

3.2. Two examples: crossed modules and nonabelian one-cocycles.

This section suggests three examples of diagrammatical calculi, one for G -crossed modules and two for noncommutative one-cocycles. In these examples two (three in the last case) types of lines naturally appear, together with some interactions between them. We plan to explore these diagrammatics in a follow-up paper, and this section is not needed for the later parts of the paper.

Crossed modules. A G -crossed module (U, G, ∂) consists of a group homomorphism $\partial : U \rightarrow G$ and an action of G on U subject to conditions:

- (1) ∂ is a homomorphism of G -groups: $\partial(\sigma a) = \sigma \partial(a) \sigma^{-1}$ for all $a \in U, \sigma \in G$,
- (2) the Pfeiffer identity holds: $\partial^b a = bab^{-1}$ for all $a, b \in U$.

Crossed modules were introduced by Whitehead [Whi49]. For a subspace $Y \subset X$ the boundary homomorphism $\partial : \pi_2(X, Y) \rightarrow \pi_1(Y)$ is a crossed module. In any crossed module (an easy exercise or see [Bor16, Lemma 3.2.3], for instance),

- $\ker \partial$ is central in U ,

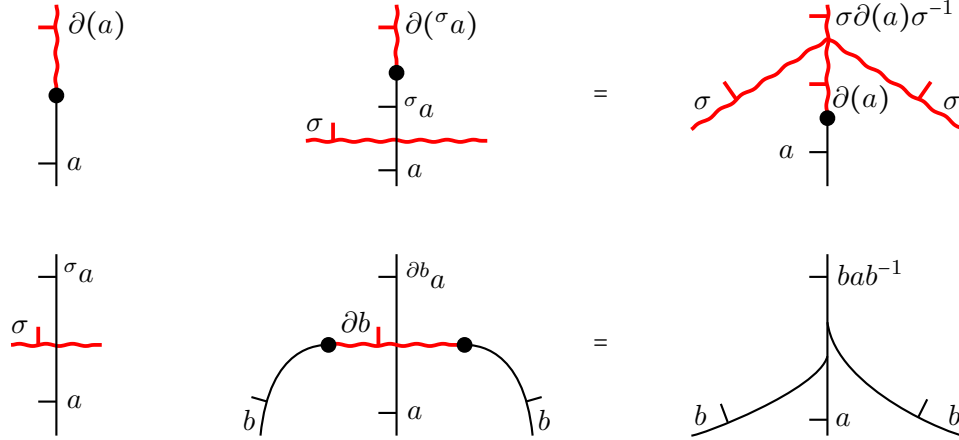


FIGURE 3.2.1. Diagrammatics for a G -crossed module. Top left: map ∂ is encoded by a dot where a U -line turns into a G -line. Bottom left: action of G on U via the intersection point which converts label a to label σa . Top right: diagrammatics for relation (1). Bottom right: diagrammatics for the Pfeiffer identity (2).

- $\text{im } \partial$ is normal in G ,
- $G/\text{im } \partial$ acts on $\ker \partial$.

For relations of crossed modules to nonabelian cohomology see [Bor16] and references therein.

Crossed modules admit a diagrammatics of overlapping networks that refines one for crossed products. Consider networks for cross-product of G by U coming from the action of G on U , so that one has

- Co-oriented thin lines labelled $a \in U$, with merges and splits as in Figure 3.1.1 top left.
- Co-oriented wavy thick lines (shown in red) labelled $\sigma \in G$, with merges and splits as well.

At the intersection of a thin a -line and a thick σ -line the label a of the thin line as it moves across the thick line becomes $\sigma(a)$, see Figure 3.1.1 top right. Other relations from Figure 3.1.1 hold as well. We allow co-orientation reversal points at both thin and thick wavy lines as usual, see Figure 2.1.11.

Now add a vertex where a thin line becomes a thick wavy red line, with label changing from $a \in U$ to $\sigma(a) \in G$, co-orientations pointing in the same direction, see Figure 3.2.1.

Impose the relations in Figure 3.2.1. Note that lines are co-oriented, and a thin line b in the lower center diagram turns into wavy line ∂b , then turns back into b . One should be able to build a monoidal category associated with a crossed module from these diagrammatics.

Nonabelian one-cocycles. Consider groups G, U which are noncommutative, in general. Suppose given a homomorphism $\psi : G \rightarrow \text{Aut}(U)$. A one-cocycle of G with values in U is a

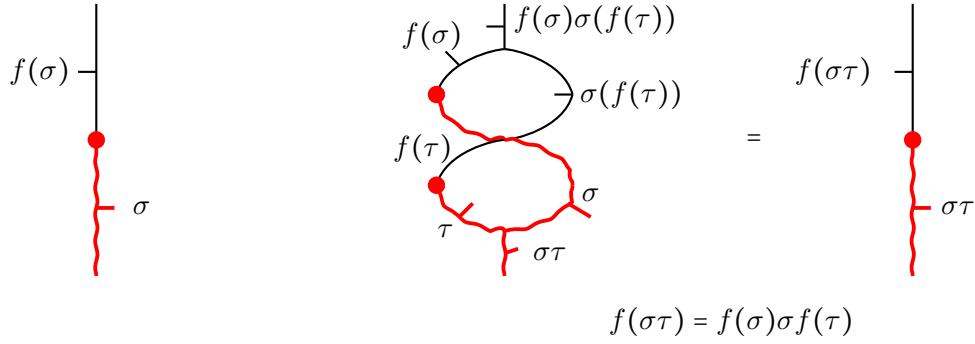


FIGURE 3.2.2. Left: wavy line σ turns into a smooth line $f(\sigma)$, with co-orientation reversal. Right: interpreting noncommutative one-cocycle relation as equality of two diagrams. Notice that line $f(\tau)$ turns into $\sigma f(\tau)$ upon crossing a wavy line.

map $f : G \rightarrow U$ such that

$$(3.2) \quad f(\sigma\tau) = f(\sigma) \cdot \sigma(f(\tau)), \quad \sigma, \tau \in G.$$

We write $f \in Z^1(G, U)$. One-cocycles f_1, f_2 are called *equivalent* if for some $u \in U$,

$$(3.3) \quad f_2(\sigma) = c^{-1} f_1(\sigma) \sigma(c), \quad \sigma \in G.$$

The set of equivalence classes for this relation is denoted $H^1(G, U) = Z^1(G, U) / \sim$ and called the first nonabelian cohomology of G with coefficients in U , see [Mil17, Section 27] and [Ser02]. It is a group only if U is commutative and otherwise has a distinguished element, the class of 1-cocycles of the form

$$(3.4) \quad \sigma \mapsto b^{-1} \cdot \sigma(b), \quad b \in U,$$

also called *principal 1-cocycles*.

To give a diagrammatic interpretation of a nonabelian 1-cocycle f , start with the diagrammatics for the groups G, U and a homomorphism $G \rightarrow \text{Aut}(U)$ as in Section 3.1. Encode the map $f : G \rightarrow U$ by allowing a G -line labelled σ to turn into a U -line labelled $f(\sigma)$ via a valency two vertex, together with reversing co-orientation at it, see Figure 3.2.2 on the left.

The one-cocycle condition can now be interpreted as equality of diagram on the right of that figure. Note that the $f(\tau)$ -line intersects the σ -line and gets rescaled to $\sigma(f(\tau))$. The label at the top of the middle diagram is $f(\sigma)\sigma(f(\tau))$, and the equality forces it to equal $f(\sigma\tau)$.

Figure 3.2.3 shows how to interpret formula (3.4), that is, a twist of a one-cocycle f_1 by a coboundary. One draws a line labelled c and intersecting the σ -line. That changes c at the intersection to $\sigma(c)$. The three smooth lines are then merged into one, which is $c^{-1} f_1(\sigma) \sigma(c)$, and the order of merges is irrelevant. Principal one-cocycles correspond to erasing the line $f_1(\sigma)$, with the diagram being a loop around the vertex where the σ -line terminates, intersecting σ -line once.

Noncommutative one-cocycles are common in mathematics and appear, for instance, in classification of twisted algebraic structures under Galois extensions [Ser02, Mil17], see also [Bor16].

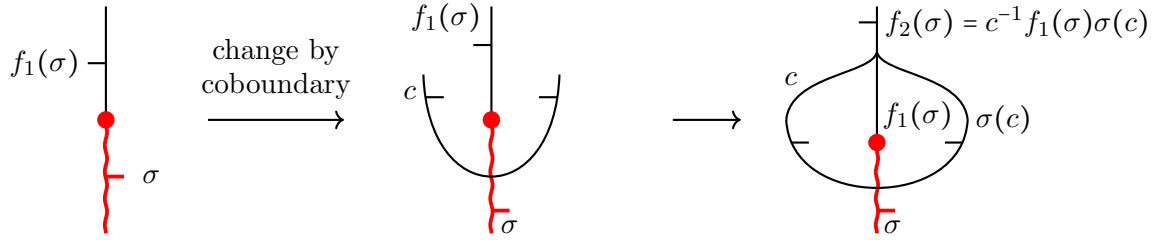


FIGURE 3.2.3. Twisting a noncommutative one-cocycle by a coboundary.

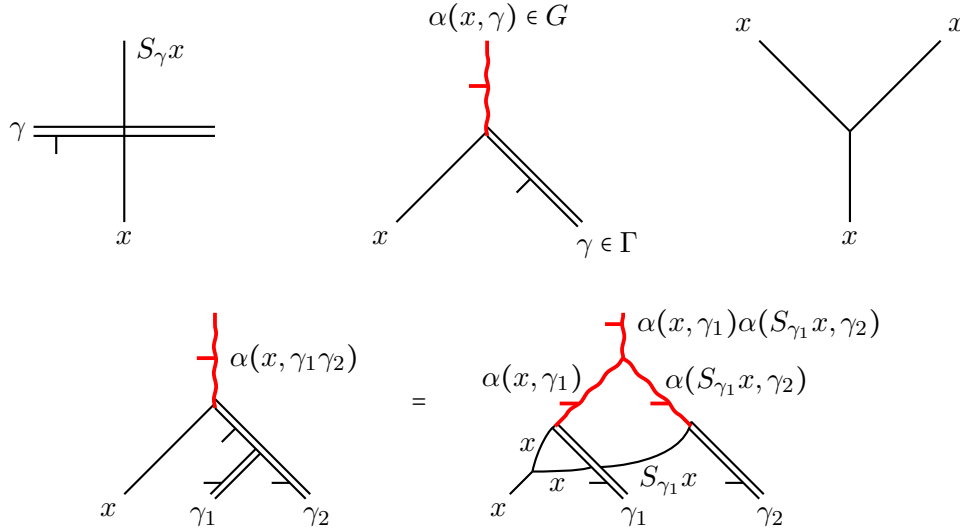


FIGURE 3.2.4. Cocycles in ergodic theory involve a space X , and there are 3 types of lines in the diagrammatics. Thin lines are labelled by elements $x \in X$, double lines by elements $\gamma \in \Gamma$ and thick wavy lines—by elements of G .

Classification of principal G -bundles is via Čech 1-cocycles and cohomology, which is different from cocycles in $Z^1(U, G)$ that we consider, however.

The notion of a noncommutative 1-cocycle in ergodic theory and dynamical systems [Par74, Kat79, Lem97, Arn98] requires a more specialized setup. Following [Kat79], we consider a Lebesgue measure space (X, μ) and two locally compact second countable groups Γ, G . Assume that Γ acts on X in a measure-preserving way, denoting the action by $S_\gamma x$, $\gamma \in \Gamma$, $x \in X$.

A G -cocycle over S is a measurable function $\alpha : X \times \Gamma \rightarrow G$ such that

$$(3.5) \quad \alpha(x, \gamma_1\gamma_2) = \alpha(x, \gamma_1)\alpha(S_{\gamma_1}x, \gamma_2), \quad x \in X, \gamma_1, \gamma_2 \in \Gamma.$$

Such cocycles can be interpreted diagrammatically, via planar networks with lines of three types:

- A line labelled $x \in X$. Network of such lines can have trivalent vertices where three x -lines come together, see Figure 3.2.4.

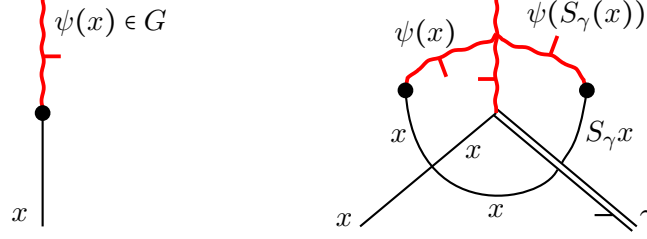


FIGURE 3.2.5. Replacing a non-abelian 1-cocycle by a cohomologous cocycle by twisting it by $\psi : X \rightarrow G$.

- Co-oriented lines labelled by elements Γ that can form a trivalent network as usual, see Section 2, shown as double lines in Figure 3.2.4.
- Co-oriented lines labelled by elements of G and forming trivalent G -networks, as usual.

An X -line can intersect a Γ -line, changing its label from x to $S_\gamma x$, see Figure 3.2.4. A trivalent vertex where all three types of lines come together denotes the 1-cocycle α . The cocycle equation (3.5) has a diagrammatic interpretation shown in Figure 3.2.4.

Figure 3.2.5 shows diagrammatic for replacing a cocycle by a cohomologous cocycle.

Remark 3.3. Rewriting the map $\alpha : X \times \Gamma \rightarrow G$ as a homomorphism $\alpha' : \Gamma \rightarrow \text{Maps}(X, G)$ from Γ to the group of measurable maps $X \rightarrow G$ presents these 1-cocycles as a special case of 1-cocycles in (3.2) with G there replaced by Γ and U by $\text{Maps}(X, G)$.

Abelian and non-abelian 1-cocycles have recently emerged in statistics and graphical models [DBR24] and in graph algorithms and neural networks [DGPV23].

Remark 3.4. Fox derivatives $\partial_i : \mathbb{Z}F \rightarrow \mathbb{Z}F$, where F is a free group, with $\partial_i(x_j) = \delta_{i,j}$ and $\partial_i(fg) = \partial_i(f) + f\partial_i(g)$ are abelian 1-cocycles and play a fundamental role in knot and 3-manifold theory [RRV99, CF77].

Remark 3.5. Differential of a smooth map between manifolds can be interpreted as a non-commutative 1-cocycle, see [Uzm22]. This example is sufficiently general so that many functors from a topological to a linear category can be interpreted as noncommutative 1-cocycles. In the one-dimensional case, the chain rule for the derivative is the 1-cocycle condition [AAKM10] in the monoid of smooth functions $\mathbb{R} \rightarrow \mathbb{R}$. For more sophisticated examples of cocycles in differential geometry we refer to [Tab96] and references therein. Some examples of uses of low-degree cocycles in quantum theory can be found in [Mic10b, Mic10a].

4. ENTROPY AND INFINITESIMAL DILOGARITHMS

4.1. Entropy of a finite random variable and its cohomological interpretation.

The entropy equation. Shannon's entropy of a probability distribution X on a finite space $X = \{x_1, \dots, x_n\}$ that associates probabilities p_1, \dots, p_n , $\sum_{i=1}^n p_i = 1$, $0 \leq p_i \leq 1$ to points x_1, \dots, x_n is given by

$$(4.1) \quad H(X) := - \sum_{i=1}^n p_i \log p_i.$$

When $n = 2$, one can think of $H(X)$ as a function of a single probability $p = p_1$, and the entropy is

$$(4.2) \quad H(p) = -p \log p - (1-p) \log(1-p).$$

It is natural to extend function H from $0 < p < 1$ to all real numbers by

$$(4.3) \quad H(p) := \begin{cases} -p \log |p| - (1-p) \log |1-p| & \text{if } p \neq 0, 1, \\ 0 & \text{if } p = 0, 1. \end{cases}$$

Following Leinster [Lei21b], consider a related function $\psi : \mathbb{R} \rightarrow \mathbb{R}$, denoted $\partial_{\mathbb{R}}$ in [Lei21b] and given by

$$(4.4) \quad \psi(a) = \begin{cases} -a \log |a| & \text{if } a \neq 0, \\ 0 & \text{if } a = 0. \end{cases}$$

Function ψ is a *non-linear derivation*:

$$(4.5) \quad \psi(ab) = \psi(a)b + a\psi(b), \quad a, b \in \mathbb{R}, \quad \psi(1) = 0.$$

For a finite sequence $\underline{a} := (a_1, \dots, a_n)$ of real numbers define

$$(4.6) \quad H(\underline{a}) := \sum_{i=1}^n \psi(a_i) - \psi\left(\sum_{i=1}^n a_i\right)$$

to measure non-additivity of ψ on the sequence \underline{a} . When \underline{a} is a sequence of probabilities for a finite random variable X , the last term is $\psi(1) = 0$, and one recovers the entropy of X .

Entropy function $H : \mathbb{R} \rightarrow \mathbb{R}$ satisfies a four-term functional equation

$$(4.7) \quad H(p) - H(q) + pH\left(\frac{q}{p}\right) + (1-p)H\left(\frac{1-q}{1-p}\right) = 0, \quad q \in \mathbb{R}, \quad p \in \mathbb{R}, \quad p \neq 0, 1$$

and

$$(4.8) \quad H(1-p) = H(p), \quad p \in \mathbb{R}.$$

The functional equation for entropy first appeared in [Tve58]. Introduction to [Vig20] contains more information on the history of the functional equation. Equations (4.7) and (4.8), normalization $H(1/2) = \log 2$, and the continuity (or measurability) property uniquely determine H as a function $\mathbb{R} \rightarrow \mathbb{R}$, see [Lee64].

Setting $q = p$ in (4.7) gives $H(1) = 0$ and, by symmetry, $H(0) = 0$. Setting $q = 1$ in (4.7) implies

$$(4.9) \quad pH\left(\frac{1}{p}\right) = -H(p), \quad p \neq 0,$$

and allows to rewrite (4.7) in a more symmetric form

$$(4.10) \quad H(p) + (1-p)H\left(\frac{q}{1-p}\right) = H(q) + (1-q)H\left(\frac{p}{1-q}\right), \quad p, q \neq 1.$$

Remark 4.1. Uniqueness of the entropy function is lost if measurability condition is dropped. Let $d : \mathbb{R} \rightarrow \mathbb{R}$ be a derivation of \mathbb{R} viewed as a \mathbb{Z} -algebra (so that $d(x+y) = dx + dy$ and $d(xy) = d(x)y + yd(x)$ for all $x, y \in \mathbb{R}$). Such derivations exist (via the Zorn Lemma) due to the transcendental structure of the field \mathbb{R} , see [ZS58, Chapter II] or [Kuc09, Theorem 14.2.2].

Following [Acz79], consider the function

$$(4.11) \quad h(x) = \begin{cases} \frac{(dx)^2}{x(1-x)} & \text{if } x \neq 0, 1, \\ 0 & \text{if } x = 0, 1. \end{cases}$$

This non-measurable function satisfies functional equations (4.7) and (4.8).

Cathelineau–Kontsevich symbol. To relate entropy to group cohomology, following Kontsevich [Kon02] and Cathelineau [Cat88, Cat96, Cat07, Cat11], consider a nonlinear symbol map $\langle \cdot, \cdot \rangle_H : \mathbb{R} \times \mathbb{R} \rightarrow \mathbb{R}$ given by

$$(4.12) \quad \langle a, b \rangle_H := \begin{cases} (a+b)H\left(\frac{a}{a+b}\right) & \text{if } a+b \neq 0, \\ 0 & \text{if } a+b = 0. \end{cases}$$

We have

$$(4.13) \quad \langle a, b \rangle_H = -a \log |a| - b \log |b| + (a+b) \log |a+b| = \psi(a) + \psi(b) - \psi(a+b),$$

so that $\langle a, b \rangle_H$ measures the failure of ψ to be additive for the pair (a, b) . Note that formula

$$(4.14) \quad \langle a, b \rangle_H = \psi(a) + \psi(b) - \psi(a+b), \quad \psi(a) = \begin{cases} -a \log |a| & \text{if } a \neq 0, \\ 0 & \text{if } a = 0. \end{cases}$$

holds for all $a, b \in \mathbb{R}$. A direct computation establishes the following result.

Proposition 4.2. *The symbol satisfies the following relations*

$$(4.15) \quad \langle a, b \rangle_H + \langle a+b, c \rangle_H = \langle a, b+c \rangle_H + \langle b, c \rangle_H,$$

$$(4.16) \quad \langle a, b \rangle_H = \langle b, a \rangle_H,$$

$$(4.17) \quad \langle ca, cb \rangle_H = c \langle a, b \rangle_H.$$

The first relation above is the two-cocycle relation. The second says that the symbol is symmetric in a and b , and the third is a scaling property.

Writing down relation (4.15) for $a+b+c=1$ and replacing $p=a+b, q=a$ gives the equation

$$(4.18) \quad H(p) - H(q) + pH\left(\frac{q}{p}\right) - (1-q)H\left(\frac{1-p}{1-q}\right) = 0, \quad q \in \mathbb{R}, p \in \mathbb{R}, p \neq 0, 1$$

This equation is similar to (4.7) but the last term is different. Applying relation (4.9) with $\frac{1-q}{1-p}$ as the argument converts (4.18) to (4.7).

To understand relation (4.9) cohomologically, write (4.15) for $(a, b, c) = (p, 1-p, p-1)$ to get

$$(4.19) \quad \langle p, 1-p \rangle_H + \langle 1, p-1 \rangle_H = \langle p, 0 \rangle_H + \langle 1-p, p-1 \rangle_H = 0 + 0 = 0.$$

Note that $\langle 1, p-1 \rangle_H = pH(1/p)$ and $\langle p, 1-p \rangle_H = H(p)$, resulting in (4.9).

Equation (4.17) is a scaling property of the 2-cocycle. It indicates that one should add a scaling group \mathbb{R}^* acting on \mathbb{R} . Form the cross-product group of affine symmetries of the real line

$$(4.20) \quad \text{Aff}_1(\mathbb{R}) = \left\{ \begin{pmatrix} c & a \\ 0 & 1 \end{pmatrix} : c \in \mathbb{R}^*, a \in \mathbb{R} \right\},$$

with the multiplication in $\text{Aff}_1(\mathbf{k})$ given by:

$$(4.21) \quad \begin{pmatrix} c_1 & a_1 \\ 0 & 1 \end{pmatrix} \begin{pmatrix} c_2 & a_2 \\ 0 & 1 \end{pmatrix} = \begin{pmatrix} c_1 c_2 & c_1 a_2 + a_1 \\ 0 & 1 \end{pmatrix}.$$

To extend the 2-cocycle $\langle a, b \rangle$ to $\text{Aff}_1(\mathbb{R})$ we use the following formula

$$(4.22) \quad \langle (a_1, c_1), (a_2, c_2) \rangle_H := \langle a_1, c_1 a_2 \rangle_H,$$

which will be motivated later, in Section 5, from the diagrammatic description. One can check that (4.22) is a (normalized) 2-cocycle on $\text{Aff}_1(\mathbb{R})$ valued in \mathbb{R} ,

$$\text{Aff}_1(\mathbb{R}) \times \text{Aff}_1(\mathbb{R}) \longrightarrow \mathbb{R},$$

where the action of $\text{Aff}_1(\mathbb{R})$ on \mathbb{R} is $(a, c)x = cx$.

Relation (4.14) shows [Kon02] that the 2-cocycle $\langle a, b \rangle_H$ on \mathbb{R} is the coboundary of the 1-cochain $\psi : \mathbb{R} \rightarrow \mathbb{R}$.

Proposition 4.3. *Two-cocycle (6.4) on $\text{Aff}_1(\mathbb{R})$ is not a coboundary.*

Proof. This is due to lack of solutions $\phi : \mathbb{R} \times \mathbb{R}^* \rightarrow \mathbb{R}$ of the equation

$$(4.23) \quad \langle a_1, c_1 a_2 \rangle_H = \phi((a_1, c_1)) + \phi((a_2, c_2)) - \phi((a_1 + c_1 a_2, c_1 c_2)).$$

Indeed, any other solution ψ_1 of (4.14) has the form $\psi_1 = \psi + \rho$ where $\rho : \mathbb{R} \rightarrow \mathbb{R}$ is homomorphism (not necessarily continuous). Then $\phi((a, 1)) = \psi(a) + \rho(a)$ for some ρ and all $a \in \mathbb{R}$. Specializing $c_1 = 1$ gives

$$(4.24) \quad \langle a_1, a_2 \rangle_H = \phi((a_1, 1)) + \phi((a_2, c_2)) - \phi((a_1 + a_2, c_2))$$

and

$$(4.25) \quad \phi((a_2, c_2)) - \phi((a_2, 1)) = \phi((a_1 + a_2, c_2)) - \phi((a_1 + a_2, 1))$$

so that

$$(4.26) \quad \phi((a, c)) = \phi((a, 1)) + \tau(c) = \psi(a) + \rho(a) + \tau(c)$$

for some function $\tau : \mathbb{R}^* \rightarrow \mathbb{R}$ and a homomorphism ρ . Substituting formula (4.26) in (4.23) quickly leads to a contradiction. \square

Thus, the 2-cocycle (6.4) is a coboundary for the group \mathbb{R} but not a coboundary for the larger group $\text{Aff}_1(\mathbb{R})$.

4.2. Cathelineau's infinitesimal dilogarithm. Infinitesimal dilogarithms were defined by Cathelineau [Cat88, Cat96] and Bloch–Esnault [BE03]. These two types of infinitesimal dilogarithms are slightly different. The relation is clarified in Bloch–Esnault [BE03] (also see Garoufalidis [Gar09] for the case of a characteristic 0 field, a survey by Ünver [Ü21], and Elbaz-Vincent and Gangl [EVG02]). Throughout the paper we consider the Cathelineau dilogarithm, following [Cat11, Cat96]. Bloch–Esnault dilogarithm carries an additional parameter of higher degree which we do not discuss.

Starting with a field \mathbf{k} , Cathelineau defines $J(\mathbf{k})$ as a \mathbf{k} -vector space generated by symbols $\langle a, b \rangle$, over $a, b \in \mathbf{k}$, subject to the relations in Proposition 4.2:

$$(4.27) \quad \langle a, b \rangle = \langle b, a \rangle,$$

$$(4.28) \quad \langle ca, cb \rangle = c \langle a, b \rangle,$$

$$(4.29) \quad \langle a, b \rangle + \langle a + b, c \rangle = \langle b, c \rangle + \langle a, b + c \rangle,$$

thus generalizing the symbol from \mathbb{R} to an arbitrary field. The relations imply that $\langle a, 0 \rangle = \langle 0, a \rangle = 0$ and, if $\text{char}(\mathbf{k}) \neq 2$, $\langle a, -a \rangle = 0$. Cathelineau also introduces the \mathbf{k} -vector space $\beta(\mathbf{k})$ generated by symbols $[a]$, $a \in \mathbf{k}^\times$ subject to defining relations

$$[1] = 0$$

and

$$(4.30) \quad [a] - [b] + a \left[\frac{b}{a} \right] + (1 - a) \left[\frac{1 - b}{1 - a} \right] = 0, \quad a \in \mathbf{k} \setminus \{0, 1\}, \quad b \in \mathbf{k}^\times.$$

We write $\mathbf{k}^\times = \mathbf{k} \setminus \{0\}$ for the multiplicative group of \mathbf{k} and \mathbf{k}^* for the \mathbf{k} -vector space dual of \mathbf{k} .

Cathelineau proves that, if $\text{char}(\mathbf{k}) \neq 2$, there is an isomorphism of \mathbf{k} -vector spaces

$$(4.31) \quad R : \beta(\mathbf{k}) \xrightarrow{\cong} J(\mathbf{k}), \quad [a] \mapsto \langle a, 1 - a \rangle$$

with the inverse map R^{-1} given by

$$(4.32) \quad \langle a, -a \rangle \mapsto 0, \quad \langle a, b \rangle \mapsto (a + b) \left[\frac{a}{a + b} \right] \text{ if } a + b \neq 0.$$

If $\text{char}(\mathbf{k}) = 2$, the isomorphism is given by

$$R_2 : \beta(\mathbf{k}) \longrightarrow J(\mathbf{k}), \quad [a] \mapsto \langle 1, 1 + a \rangle,$$

with the inverse

$$R_2^{-1} : J(\mathbf{k}) \longrightarrow \beta(\mathbf{k}),$$

We state Theorem 8.10 in [Cat07].

Theorem 4.4 (Cathelineau). *Let $\Omega_{\mathbf{k}}^1$ be the space of degree one absolute Kähler differentials. If $\text{char}(\mathbf{k}) = 0$, the following sequence of \mathbf{k} -vector spaces is exact.*

$$(4.33) \quad 0 \longrightarrow \beta(\mathbf{k}) \xrightarrow{f} \mathbf{k}^+ \otimes \mathbf{k}^\times \xrightarrow{g} \Omega_{\mathbf{k}}^1 \longrightarrow 0.$$

If $\text{char}(\mathbf{k}) = p > 0$, the following sequence of \mathbf{k} -vector spaces is exact

$$(4.34) \quad 0 \longrightarrow \mathbf{k} \xrightarrow{h} \beta(\mathbf{k}) \xrightarrow{f} \mathbf{k}^+ \otimes \mathbf{k}^\times \xrightarrow{g} \Omega_{\mathbf{k}}^1 \longrightarrow 0.$$

In these sequences the maps are

$$f([a]) = a \otimes a + (1 - a) \otimes (1 - a), \quad \text{for } a \neq 0, 1; \quad f([0]) = 0,$$

$$g(b \otimes a) = b \frac{da}{a} = b d \log(a), \quad h(1) = \sum_{c \in \mathbf{k}_0} [c].$$

Here $\mathbf{k}_0 = \mathbf{F}_p$ is the prime subfield of \mathbf{k} . The composition

$$(4.35) \quad f \circ R^{-1} : J(\mathbf{k}) \longrightarrow \mathbf{k}^+ \otimes \mathbf{k}^\times$$

is given by

$$(4.36) \quad \langle a, b \rangle \longmapsto a \otimes a + b \otimes b - (a + b) \otimes (a + b).$$

Remark 4.5. Consider the cross-product group

$$(4.37) \quad \text{Aff}_1(\mathbf{k}) = \left\{ \begin{pmatrix} c & a \\ 0 & 1 \end{pmatrix} : c \in \mathbf{k}^\times, a \in \mathbf{k} \right\}$$

of affine transformations of \mathbf{k} that send $x \mapsto cx + a$. Write its elements as (a, c) . This group fits into the short exact sequence of groups

$$(4.38) \quad 0 \longrightarrow \mathbf{k} \longrightarrow \text{Aff}_1(\mathbf{k}) \longrightarrow \mathbf{k}^\times \longrightarrow 0.$$

Denote by \mathbf{k}_r the *left* Aff_1 -module which is \mathbf{k} with the action $(a, c).u = c^{-1}u$. Cathelineau [Cat11, Theorem 6.1] establishes a canonical isomorphism

$$(4.39) \quad \Theta : H_2(\text{Aff}_1(\mathbf{k}), \mathbf{k}_r) \xrightarrow{\cong} \beta(\mathbf{k}),$$

and tributes Chi-Han Sah with observing the isomorphism for infinite \mathbf{k} . The isomorphism is induced by the map that takes a 2-chain $b[(a, c)|(a', c')]$ in the non-homogeneous complex for the homology of $\text{Aff}_1(\mathbf{k})$ to $b(ca', a) \in J(\mathbf{k})$ and then to the corresponding element of $\beta(\mathbf{k})$ by composing with R^{-1} in (4.31), see [Cat11] for details.

Summarizing, there are natural isomorphisms of \mathbf{k} -vector spaces

$$(4.40) \quad \beta(\mathbf{k}) \cong J(\mathbf{k}) \cong H_2(\text{Aff}_1(\mathbf{k}), \mathbf{k}_r).$$

Next, form \mathbf{k} -vector space duals of the spaces and exact sequences (4.33) and (4.34), in characteristic 0 and p , respectively. The first sequence dualizes to the exact sequence (when $\text{char}(\mathbf{k}) = 0$)

$$0 \longrightarrow \text{Der}(\mathbf{k}) \xrightarrow{g^*} \text{Log}(\mathbf{k}) \xrightarrow{f^*} \text{Dil}(\mathbf{k}) \longrightarrow 0,$$

and to the exact sequence

$$0 \longrightarrow \text{Der}(\mathbf{k}) \xrightarrow{g^*} \text{Log}(\mathbf{k}) \xrightarrow{f^*} \text{Dil}(\mathbf{k}) \xrightarrow{h^*} \mathbf{k}^* \longrightarrow 0$$

(when $\text{char}(\mathbf{k}) = p > 0$). Here $\text{Der}(\mathbf{k})$ is the vector space of derivations, that is, additive maps $d : \mathbf{k} \longrightarrow \mathbf{k}$ with $d(xy) = x d(y) + y d(x)$. The next term, $\text{Log}(\mathbf{k})$, the dual of $\mathbf{k} \otimes \mathbf{k}^\times$, can be identified with the space of group homomorphisms $\rho : \mathbf{k}^\times \longrightarrow \mathbf{k}^*$.

The \mathbf{k} -vector space $\text{Dil}(\mathbf{k}) := J(\mathbf{k})^*$ is called the space of *infinitesimal dilogarithms*.

Cathelineau [Cat11] establishes isomorphisms

$$(4.41) \quad \text{Dil}(\mathbf{k}) \cong \text{Ext}_{\mathbf{k}^\times}^1(\mathbf{k}, \mathbf{k}) \cong H^2(\text{Aff}_1(\mathbf{k}), \mathbf{k}_\ell).$$

Note that \mathbf{k} is naturally a $\mathbb{Z}[\mathbf{k}^\times]$ -module, and the corresponding ext group is considered in the isomorphism above. Left $\text{Aff}_1(\mathbf{k})$ -module $\mathbf{k}_\ell \cong \mathbf{k}$ has the action $(a, c).u = cu$. Isomorphism between the first and the last terms in (4.41) is dual to the second isomorphism in (4.40).

In Figure 4.2.1 we write down various maps involved in the Cathelineau construction, for ours and the reader's convenience.

$\beta(\mathbf{k})$: relations: $[a] - [b] + a \left[\frac{b}{a} \right] + (1-a) \left[\frac{1-b}{1-a} \right] = 0, a \neq 0, 1, [1] = 0$
 generators: $[a], a \in \mathbf{k}$

$$\begin{array}{ccccccc}
 & & & & a \otimes b & \xrightarrow{\quad} & a \frac{db}{b} = a d \log b \\
 0 & \longrightarrow & \beta(\mathbf{k}) & \xrightarrow{f} & \mathbf{k}^+ \otimes_{\mathbb{Z}} \mathbf{k}^\times & \xrightarrow{g} & \Omega_{\mathbf{k}}^1 \longrightarrow 0 \\
 & & \begin{array}{c} \uparrow \\ (a+b) \left[\frac{a}{a+b} \right] \\ \uparrow \\ 0 \\ \uparrow \\ \langle a, -a \rangle \end{array} & \begin{array}{c} \xrightarrow{[a]} \\ \downarrow \\ \langle a, 1-a \rangle \\ \downarrow \\ \langle a, b \rangle \end{array} & \begin{array}{c} \xrightarrow{[a]} \\ \downarrow \\ \langle a, b \rangle \end{array} & & \\
 & & R & \simeq & \begin{array}{c} a \otimes a + \\ (1-a) \otimes (1-a) \\ - (a+b) \otimes (a+b) + \\ a \otimes a + b \otimes b \end{array} & & \\
 & & \downarrow & & \uparrow & & \\
 & & J(\mathbf{k}) & & J(\mathbf{k}) & & \\
 & & \uparrow & & \text{generators: } \langle a, b \rangle & & \\
 & & \simeq & & \text{relations: } \langle a, b \rangle = \langle b, a \rangle & & \\
 & & H_2(\text{Aff}_1(\mathbf{k}), \mathbf{k}_r) & & \langle ca, cb \rangle = c \langle a, b \rangle & & \\
 & & \mathbf{k}_r: \text{ left module, } (a, c)u = c^{-1}u, & & \langle a, b \rangle + \langle a+b, c \rangle = \langle a, b+c \rangle + \langle b, c \rangle & & \\
 & & (a, c) \in \text{Aff}_1(\mathbf{k}), (a, c)x = cx + a & & \text{weaker relation than} & & \\
 & & & & \langle a_1 + a_2, b \rangle \neq \langle a_1, b \rangle + \langle a_2, b \rangle & & \\
 & & & & \text{(the symbol is not bilinear)} & &
 \end{array}$$

FIGURE 4.2.1. Cathelineau's exact sequence and related maps when $\text{char} \mathbf{k} = 0$. The spaces $\beta(\mathbf{k})$ and $J(\mathbf{k})$ are \mathbf{k} -vector spaces.

Remark 4.6. (Cathelineau [Cat11]) If \mathbf{k} is a perfect field of finite characteristic p then $\text{Dil}(\mathbf{k}) \cong \mathbf{k}$ is one-dimensional, with a generator coming from the equivariant 2-cocycle $\chi^{\frac{1}{p}}$, where

$$\chi : \mathbf{k} \times \mathbf{k} \longrightarrow \mathbf{k}, \quad \chi(x, y) = \sum_{i=1}^{p-1} \frac{1}{p} \binom{p}{i} x^i y^{p-i}.$$

Cocycle χ also describes the addition on the space $W_2(\mathbf{k})$ of length 2 Witt vectors [Cat11, Section 4.4]. The infinitesimal dilogarithm θ_p represented by the cocycle is given by

$$\theta_p(x) = \sum_{i=1}^{p-1} \frac{1}{p} \binom{p}{i} x^{i/p} (1-x)^{(p-i)/p}$$

for $p \neq 2$, $\theta_2(x) = 1 + x^{1/2}$, and it restricts to the Kontsevich $1\frac{1}{2}$ logarithm [Kon02, Lei21b] on the prime subfield of \mathbf{k} .

Cathelineau [Cat11, Corollary 4.9] provides examples of fields where $J(\mathbf{k})$ is infinite dimensional over \mathbf{k} , including $\overline{\mathbb{Q}}$ and $F(X)$ for any field F .

Cocycle χ above is closely related to the successful attack by Satoh–Araki, Smart, and Semaev [SA98, Sma99, Sem98, Vol] on the discrete logarithm problem on anomalous elliptic curves over \mathbb{F}_p (i.e., curves with exactly p points), see [GMP04, Section 4].

Remark 4.7. The entropy function H is a rather special element of the \mathbb{R} -vector space

$$\text{Dil}(\mathbb{R}) = \text{Hom}_{\mathbb{R}}(J(\mathbb{R}), \mathbb{R})$$

given by

$$(4.42) \quad H(\langle a, b \rangle) = \langle a, b \rangle_H.$$

Elements of $\text{Dil}(\mathbb{R})$ not proportional to H do not correspond to measurable functions.

Remark 4.8. A surprising connection between the Dehn invariant of polyhedra in \mathbb{R}^3 and the infinitesimal dilogarithm and entropy is developed in [Cat88, Section 1.4]. The Dehn invariant \mathcal{D} of a polyhedron in \mathbb{R}^3 is the first map in the scissor congruence short exact sequence

$$0 \longrightarrow \mathcal{P}/\mathcal{L} \xrightarrow{\mathcal{D}} \mathbb{U} \otimes_{\mathbb{Z}} i\mathbb{R} \longrightarrow \Omega_{\mathbb{R}}^1 \longrightarrow 0,$$

where \mathcal{P}/\mathcal{L} is the \mathbb{R} -vector space of polyhedra in \mathbb{R}^3 modulo scissor congruence and prisms, see [Cat88, Syd65, Jes68, Sch13, Dup01, Sah79, Cal22a]. Cathelineau [Cat88] constructs a natural homomorphism from this short exact sequence into the one in (4.33) for $\mathbf{k} = \mathbb{C}$. Homomorphism of fields $\mathbb{R} \rightarrow \mathbb{C}$ induces a corresponding map of short exact sequences (4.33) from $\mathbf{k} = \mathbb{R}$ to $\mathbf{k} = \mathbb{C}$. This results in a diagram of three short exact sequences and maps between them, also see [Cat88].

$$\begin{array}{ccccccccc} 0 & \longrightarrow & \mathcal{P}/\mathcal{L} & \xrightarrow{\mathcal{D}} & i\mathbb{R} \otimes_{\mathbb{Z}} \mathbb{U} & \longrightarrow & \Omega_{\mathbb{R}}^1 & \longrightarrow & 0 \\ & & \downarrow & & \downarrow & & \downarrow & & \\ 0 & \longrightarrow & \beta(\mathbb{C}) & \xrightarrow{f_{\mathbb{C}}} & \mathbb{C}^+ \otimes \mathbb{C}^\times & \xrightarrow{g_{\mathbb{C}}} & \Omega_{\mathbb{C}}^1 & \longrightarrow & 0 \\ & & \uparrow & & \uparrow & & \uparrow & & \\ 0 & \longrightarrow & \beta(\mathbb{R}) & \xrightarrow{f_{\mathbb{R}}} & \mathbb{R}^+ \otimes \mathbb{R}^\times & \xrightarrow{g_{\mathbb{R}}} & \Omega_{\mathbb{R}}^1 & \longrightarrow & 0. \end{array}$$

The entropy relates to the bottom left term in this diagram, being a function $H : \beta(\mathbb{R}) \rightarrow \mathbb{R}$. The analogue of symbols $\langle a, b \rangle$ in the scissor congruence group \mathcal{P}/\mathcal{L} are special tetrahedra $T(a, b)$, for $0 < a, b < 1$. These are Euclidean tetrahedra $ABCD$ such that the edges AB, BC, CD are pairwise orthogonal, $AB = \cot \alpha$, $BC = \cot \alpha \cot \beta$, $CD = \cot \beta$, where $0 < \alpha, \beta < \frac{\pi}{2}$ are angles such that $\sin^2 \alpha = a, \sin^2 \beta = b$. One then has the 2-cocycle relation

$$T(a, b) + T(ab, c) = T(b, c) + T(a, bc)$$

in the scissor congruence group \mathcal{P}/\mathcal{L} , see [Jes68, Sch13]. The scaling law $T(ca, cb) = cT(a, b)$ and the commutativity condition $T(a, b) = T(b, a)$ hold as well (compare with the relations (4.27)-(4.29)), which allows to interpret the scissor congruence group cohomologically. We refer to [Cat88, Section 1.4] for more details about this relation and to [Jes68, Sch13, Cal22a] and the other references above for the background on the Dehn invariant.

In the above construction, parameters a, b belong to a semigroup rather than a group. Extension of 2-cocycles from certain abelian semigroups to groups is studied in [JKT68, Eba79]. A similar extension of a 2-cocycle from $(\mathbb{R}_{>0}, +)$ to $(\mathbb{R}, +)$ appears in [IK24a], where

the 2-cocycle is antisymmetric and comes from the cobordism group of unoriented weighted 1-foams embedded in \mathbb{R}^2 .

D. Calegari points out in [Cal22b] that $-a \log a$ can be interpreted as the hyperbolic area of a suitable trapezoid in the upper half-plane, gives a scissor congruence proof of the entropy functional equation (4.7), and interprets his construction via a symplectic action of $\text{Aff}_1^+(\mathbb{R}) \times \mathbb{R}$ on $T^*\mathbb{R}$.

We refer the reader to the end of Section 7 in [Sah79] for analogies pointed out to Sah by Chern between the Dehn invariant and structures in geometric probability, including integrals of mean curvature and quermassintegrals, in particular see formula (13.58) in [San04]. These formulas may also have been a motivation for Dehn to introduce his invariant.

5. DIAGRAMMATICS OF INFINITESIMAL DILOGARITHMS

In this section we develop diagrammatics for the cohomological interpretation of infinitesimal dilogarithm, with an eye towards a similar interpretation of entropy in Section 6. Following Cathelineau, we work over any field \mathbf{k} and use his universal 2-cocycle generated by symbols $\langle a, b \rangle \in J(\mathbf{k})$. Later on, we specialize the diagrammatics to $\mathbf{k} = \mathbb{R}$ and the entropy 2-cocycle.

5.1. Motivation for the diagrammatics. The 2-cocycle $\langle a, b \rangle$ with $a, b \in \mathbf{k}$ can be represented diagrammatically as discussed in Section 2.4. When lines $a, b \in \mathbf{k}$ merge into the $(a + b)$ -line, the vertex contributes $\langle a, b \rangle$ to the evaluation, see Figure 5.1.1 top left. It is natural to allow the opposite vertex, splitting $(a + b)$ -line into a, b -lines. This vertex should then contribute $-\langle a, b \rangle$ to the evaluation, see Figure 5.1.1 top middle. As usual, the 2-cocycle property in (4.15) corresponds to relation in Figure 5.1.2 top left.

The symmetry property (4.16) indicates that we should allow the lines to intersect, with the intersection point contributing 0 to the evaluation, but adding a skein relation in Figure 5.1.2 top right, i.e., $\langle b, a \rangle = \langle a, b \rangle$. The intersection can also be defined as a composition of a split and a merge, as shown in Figure 5.2.6 in top left. We refer to these lines as *additive lines* and to split and merge vertices as *additive vertices*, and in this section use oriented rather than co-oriented additive lines, for convenience.

In the previous section, we discussed the scaling property (4.28) of the 2-cocycle $\langle a, b \rangle$ and passed to the affine group $\text{Aff}_1(\mathbf{k})$ in (4.37), which is a cross-product of \mathbf{k}^\times and \mathbf{k} . Diagrammatics of cross-product groups was introduced in Section 3.1. We follow that diagrammatics as a guide and introduce lines of the second kind – *multiplicative lines*, labelled by elements of \mathbf{k}^\times . These are shown as red wavy lines in the diagrams, labelled by elements $c \in \mathbf{k}^\times$ and co-oriented. At an intersection point of an additive and a multiplicative line, the weight of the additive line is scaled by the weight of the multiplicative line, see the bottom left diagram in Figure 5.1.1. The scaling happens in the direction of the co-orientation of the multiplicative line.

We allow multiplicative lines to merge and split, while respecting their co-orientation and multiplying the labels when two lines merge or a line splits into two lines, see the bottom middle Figure 5.1.1.

Thus, we consider planar networks of diagrams where lines have two types:

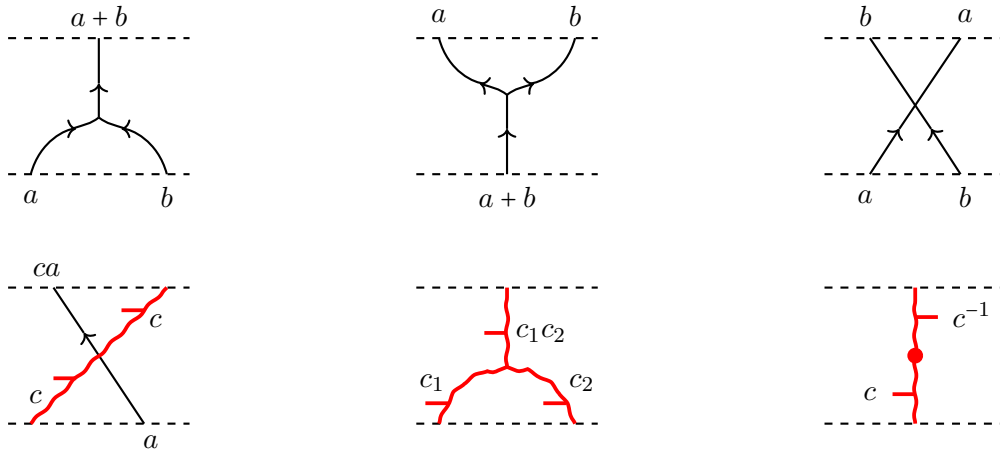


FIGURE 5.1.1. Generators of the diagrammatical calculus for the entropy 2-cocycle. Top left: a merge of additive lines, where $a, b \in \mathbf{k}$. Top middle: a split of an additive line. Top right: intersection of additive lines. Bottom left: intersection of additive and multiplicative lines (one out of two possible orientations of the additive and one co-orientation of the multiplicative line is shown). Bottom middle: merging of multiplicative lines, where $c_1, c_2 \in \mathbf{k}^\times$. Bottom right: co-orientation reversal node on a multiplicative line $c \in \mathbf{k}^\times$.

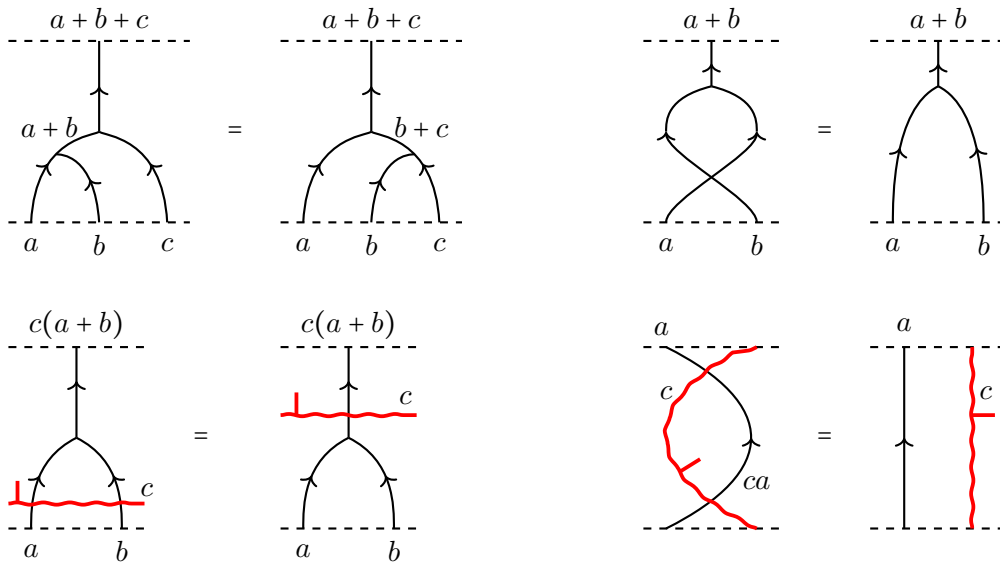


FIGURE 5.1.2. Top left: associativity of merges, for the 2-cocycle equation (4.15). Top right: commutativity of a merge, see (4.16). Bottom left: moving a multiplicative line through a merge of additive lines, equation (4.17). Bottom right: splitting a multiplicative and an additive line apart.

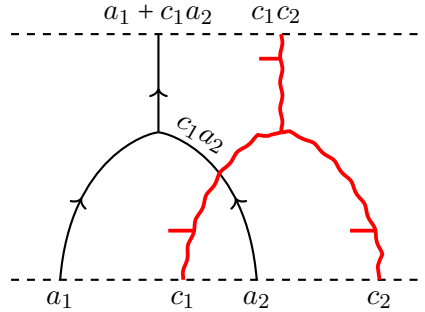


FIGURE 5.1.3. This network corresponds to multiplication in the group $\text{Aff}_1(\mathbf{k})$. It also shows an isomorphism from $X_{a_1}^+ \otimes Y_{c_1}^+ \otimes X_{a_2}^+ \otimes Y_{c_2}^+$ to $X_{a_1+c_1 a_2}^+ \otimes Y_{c_1 c_2}^+$ in categories $\mathcal{C}_{\mathbf{k}}$ and $\mathcal{C}_{\mathbf{k}}^\circ$.

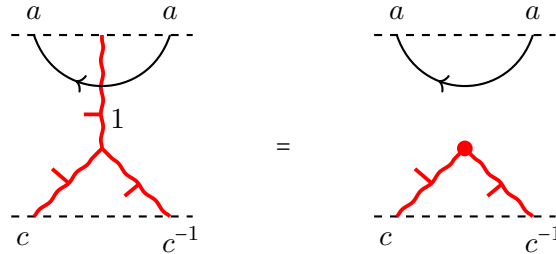


FIGURE 5.1.4. Multiplicative (red) 1-line can be erased with co-orientation reversal marks, where the line ends, added to the rest of the multiplicative network. (See Figure 6.1.5 for additive lines labelled 0, allowing for reversal labels on the additive network.)

- *Additive lines* that are oriented and carry elements of \mathbf{k} . Two such lines labelled a, b can merge into a line $a + b$, preserving orientation. Additive lines can intersect. They can also merge or split, preserving orientation, with their weights added.
- *Multiplicative lines*, shown as wavy red lines, that are co-oriented and carry an element of \mathbf{k}^\times . Multiplicative lines can merge or split, respecting co-orientations, with the weights multiplied in a merge (and likewise for a split).
- Arbitrary isotopies of diagrams are allowed.

Co-orientation reversal nodes are allowed on multiplicative lines, see Figure 5.1.1 bottom right. At such a node label c is reversed to c^{-1} . A merge of two multiplicative lines with the co-orientations opposite to that in Figure 5.1.1 is allowed as well. Splits of a red line into two are given by rotating the corresponding merge diagram in Figure 5.1.1 (middle of bottom row) by 180° .

Multiplicative (red) 1-line can be erased, see Figure 5.1.4. Points where it splits into c and c^{-1} multiplicative lines become co-orientation reversal nodes, as in Figure 5.1.1 bottom right.

Additive vertex in Figure 5.1.1 top left that contributes $\langle a, b \rangle$ represents the addition operation in \mathbf{k} . It extends to the group operation in the cross-product as shown in the multiplication diagram in Figure 5.1.3 for $\text{Aff}_1(\mathbf{k})$ or in Figure 3.1.2 on the right (for general cross-products).

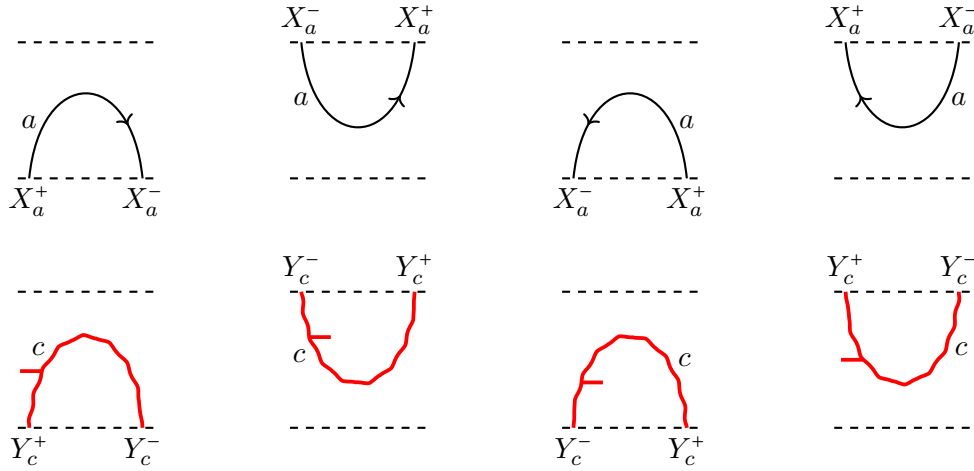


FIGURE 5.2.1. Pivotal structure morphisms in $\mathcal{C}_{\mathbf{k}}$ with X_a^- the dual of X_a^+ and Y_c^- the dual of Y_c^+ .

In Figure 5.1.3 the bottom endpoints alternate between additive and multiplicative, and they are a_1, c_1, a_2, c_2 in that order. In the diagram additive a_2 -line crosses multiplicative c_1 -line and gets rescaled to additive $c_1 a_2$ -line. After that the two additive lines become adjoint and can be merged into the additive line labelled $a_1 + c_1 a_2$. Likewise, multiplicative lines become adjoint and can be moved into the multiplicative line $c_1 c_2$. At the top boundary of the diagram we see an additive endpoint $a_1 + c_1 a_2$ followed by the multiplicative endpoint $c_1 c_2$. Note that all three additive endpoints at the boundary of the diagram are upward oriented and all three multiplicative endpoints at the boundary are left-cooriented. The diagram matches the multiplication rule (4.21) in the affine group $\text{Aff}_1(\mathbf{k})$.

5.2. Monoidal categories for the infinitesimal dilogarithm. We would like to define two pivotal monoidal categories $\mathcal{C}_{\mathbf{k}}, \mathcal{C}_{\mathbf{k}}^\circ$ that are based on the above diagrammatical calculi. Generating objects in both categories correspond to possible endpoints in the diagrams. The objects are $X_a^+, X_a^-, a \in \mathbf{k}$ and $Y_c^+, Y_c^-, c \in \mathbf{k}^\times$. An object Z of $\mathcal{C}_{\mathbf{k}}$ or $\mathcal{C}_{\mathbf{k}}^\circ$ is a finite tensor product of objects of these four types over various a 's and c 's. The empty product is the unit object $\mathbf{1}$. Generating morphisms in $\mathcal{C}_{\mathbf{k}}$ include the morphisms in Figure 5.1.1 and pivotal structure morphisms (*cups* and *caps*) in Figure 5.2.1.

In more detail, the generating morphisms in $\mathcal{C}_{\mathbf{k}}$ are the following:

- Morphisms for the pivotal structure, with X_a^- the dual of X_a^+ and Y_c^- the dual of Y_c^+ , see Figure 5.2.1.
- Merge and split morphisms $\rho_m : X_a^+ \otimes X_b^+ \longrightarrow X_{a+b}^+$ and $\rho_s : X_{a+b}^+ \longrightarrow X_a^+ \otimes X_b^+$ for additive lines shown in the top row (left and middle) of Figure 5.1.1. Dual merge and split morphisms $X_b^- \otimes X_a^- \longrightarrow X_{a+b}^-$ and $X_{a+b}^- \longrightarrow X_b^- \otimes X_a^-$ can be obtained by rotating diagrams for ρ_s and ρ_m by 180° .
- Permutation morphism $X_a^+ \otimes X_b^+ \longrightarrow X_b^+ \otimes X_a^+$ in Figure 5.1.1 top right and its variations given by reversing one or both orientations, corresponding to intersections of additive lines. (We do not introduce intersections of multiplicative lines, although it is possible to do that due to commutativity of \mathbf{k}^\times .)

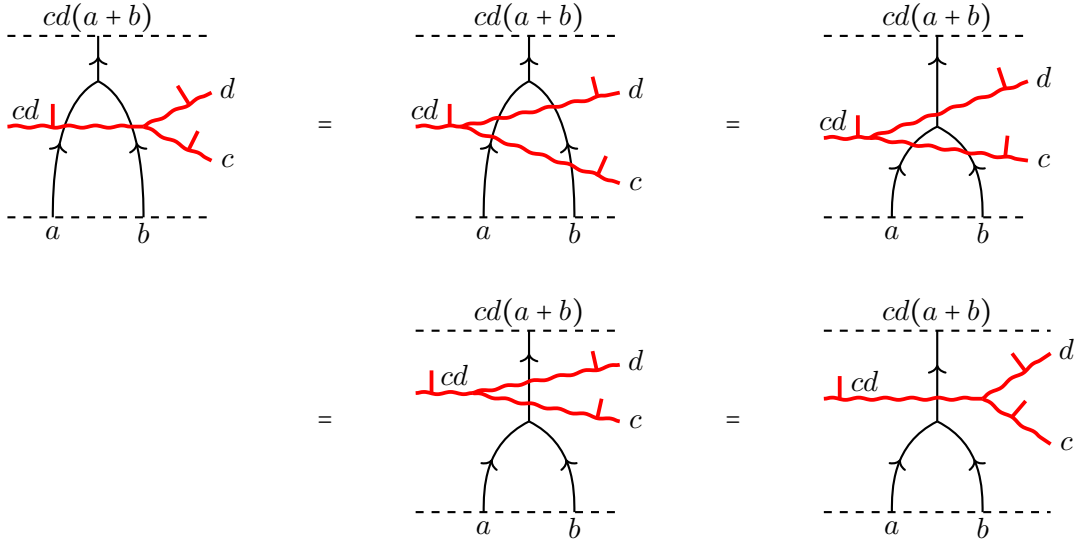


FIGURE 5.2.3. Multiplicative (c, d) -crossing can pass through an additive crossing in various ways.

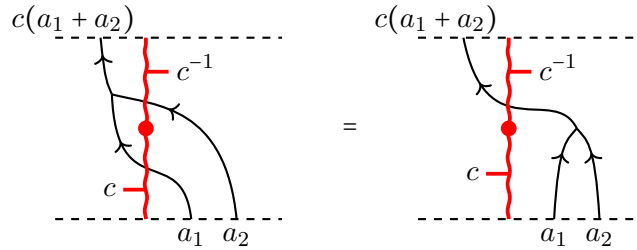
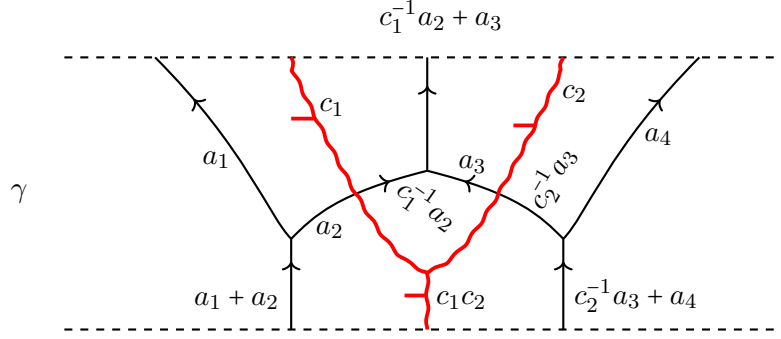


FIGURE 5.2.4. Moving an additive vertex past a co-orientation reversal point.

In the category $\mathcal{C}_{\mathbf{k}}^{\circ}$, where dots are present, we should add analogues of the relations in Figure 2.3.7: (1) dots labelled x, y and floating in the same region can be merged into $x + y$ dots; (2) moving an x -dot through a red line c co-oriented away from the dot scales the dot by c to an cx -dot.

To avoid listing a full defining set of relations we instead define morphisms in these categories using a suitable evaluation function and the universal construction. Consider a planar diagram, representing a morphism in $\mathcal{C}_{\mathbf{k}}$ from a tensor product Z to Z' and built out of the above generators, see Figure 5.2.5 for a representative example.

In Section 4.1 we defined the \mathbf{k} -vector space $J(\mathbf{k})$ associated to the field \mathbf{k} . To a morphism γ in $\mathcal{C}_{\mathbf{k}}$ from Z to Z' assign an element $j(\gamma) \in J(\mathbf{k})$ as follows. First, each point p of the diagram of γ not on a multiplicative line has the \mathbf{k}^{\times} -winding number $\omega(p, \gamma) \in \mathbf{k}^{\times}$ relative to the leftmost region of γ . It is defined just as in Section 2.1, also see Figure 2.1.2. To compute it, draw a generic path from p to the leftmost region of the diagram and multiply labels c of wavy (red) lines that the path crossed, using the inverse c^{-1} if the co-orientation of the wavy line at the intersection points towards p .



$$\begin{aligned}
 j(\gamma) &= -\langle a_1, a_2 \rangle + c_1 \langle c_1^{-1} a_2, a_3 \rangle - c_1 c_2 \langle c_2^{-1} a_3, a_4 \rangle \\
 &= -\langle a_1, a_2 \rangle + \langle a_2, c_1 a_3 \rangle - \langle c_1 a_3, c_1 c_2 a_4 \rangle
 \end{aligned}$$

FIGURE 5.2.5. Computing element $j(\gamma) \in J(\mathbf{k}) \cong \beta(\mathbf{k})$ associated to a morphism γ . Each vertex of the additive lines network contributes a signed symbol acted upon by an element of \mathbf{k}^\times . Additive lines are shown as thin black lines; the additive network has three vertices in this example.

The element $j(\gamma)$ is a sum over all merges and splits of additive lines. Denote by $\text{add}(\gamma)$ the set of such merges and splits. For $p \in \text{add}(\gamma)$, define its sign $s(p) = 1$ if p is a merge and $s(p) = -1$ if p is a split. Denote by a_p and b_p the labels a and b of the two lines that merge or split, following the order in Figure 5.1.1 top left and middle diagrams.

Define

$$(5.1) \quad j(\gamma) = \sum_{p \in \text{add}(\gamma)} s(p) \omega(p, \gamma) \langle a_p, b_p \rangle \in J(\mathbf{k}).$$

As an example, consider the morphism γ in Figure 5.2.5, with three additive vertices, which we label p_1, p_2, p_3 from left to right. The leftmost point p_1 is a split, so $s(p_1) = -1$, and has \mathbf{k}^\times -winding number 1, since it is already in the leftmost region of the wavy red network. It contributes $-\langle a_1, a_2 \rangle$ to $j(\gamma)$. Point p_2 in the middle is a merge, $s(p_2) = 1$, the winding number $\omega(p_2, \gamma) = c_1$, and it contributes $c_1 \langle c_1^{-1} a_2, a_3 \rangle = \langle a_2, c_1 a_3 \rangle$ to $j(\gamma)$. Finally, the rightmost point p_3 has $s(p_3) = -1$ and $\omega(p_3, \gamma) = c_1 c_2$. The invariant $j(\gamma)$ is written down in Figure 5.2.5.

Define $\mathcal{C}_{\mathbf{k}}$ to be the quotient of $\tilde{\mathcal{C}}_{\mathbf{k}}$ by the relation: two morphisms $\gamma_1, \gamma_2 : Z \rightarrow Z'$ in $\tilde{\mathcal{C}}_{\mathbf{k}}$ are equal as morphisms in $\mathcal{C}_{\mathbf{k}}$ if and only if $j(\gamma_1) = j(\gamma_2)$. To be precise, we first define the hom set $\text{Hom}_{\mathcal{C}_{\mathbf{k}}}(Z, Z') := \text{Hom}_{\tilde{\mathcal{C}}_{\mathbf{k}}}(Z, Z') / \sim$ as the quotient of the corresponding hom set in $\tilde{\mathcal{C}}_{\mathbf{k}}$ by this equivalence relation and later (Proposition 5.6) check that composition in $\mathcal{C}_{\mathbf{k}}$ is well-defined.

Proposition 5.1. *Relations in Figures 5.1.2, 5.2.6, 5.2.7, and 5.2.8 hold in $\mathcal{C}_{\mathbf{k}}$. Modifications of these relations given by reversing orientations of additive lines or the co-orientation of the multiplicative line (simultaneously with replacing c by c^{-1} , bottom row in Figure 5.1.2) hold as well.*

Proof. Top left relation is the 2-cocycle equation (4.29). Orientation reversal corresponds to adding minus sign to all terms of the equation, thus the corresponding diagrammatic relation

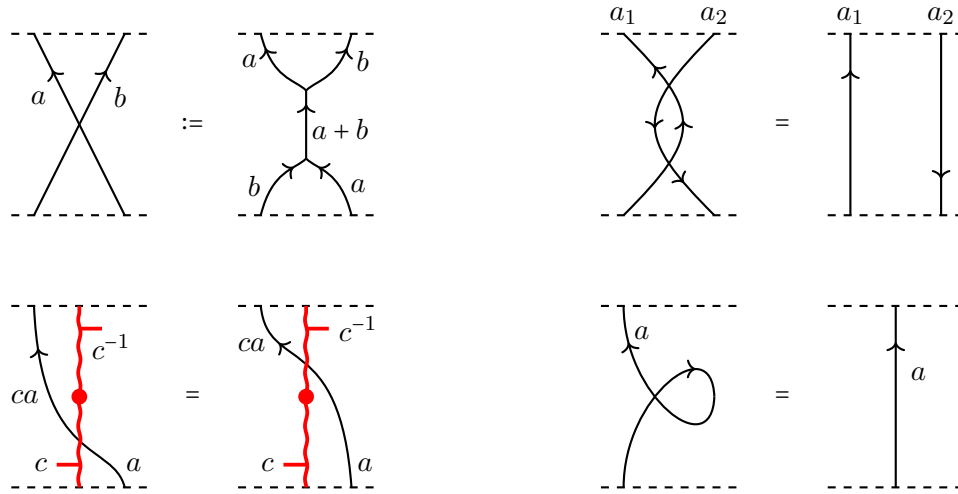


FIGURE 5.2.6. Top left: defining a crossing as a composition of a merge and a split. Top right: Pulling apart a double intersection (holds for arbitrary strand orientation). Bottom left: moving an additive line through a co-orientation reversal point on a multiplicative line. Bottom right: removing a curl on an additive line.

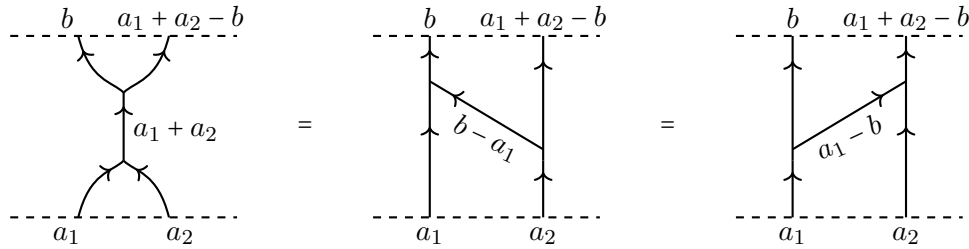


FIGURE 5.2.7. A skein relation on additive lines, cf. Figure 2.1.4.

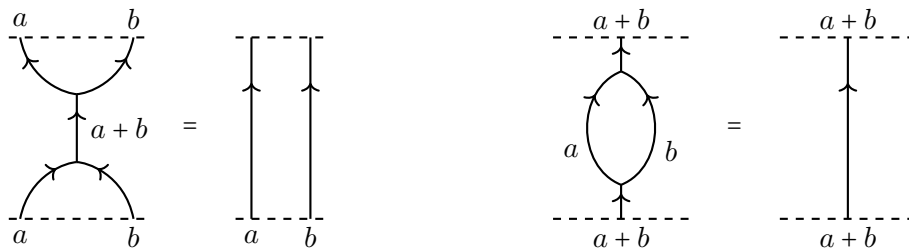


FIGURE 5.2.8. Another skein relation (cancellation moves), cf. Figure 2.1.5.

holds as well. Top right relation is the commutativity (4.27). Bottom left relation is the equation (4.28). Bottom right relation holds since both diagrams contribute 0 to $j(\gamma)$. \square

Proposition 5.2. *Suppose that $\gamma : \mathbf{1} \rightarrow \mathbf{1}$ is an endomorphism of the identity object in $\mathcal{C}_{\mathbf{k}}$. Then $j(\gamma) = 0$.*

Proof. An endomorphism γ is given by two overlapping networks of additive and multiplicative lines, with the empty boundary. Using relations discussed above we can isotop the additive network away from the multiplicative network (possibly changing weights on additive lines in the process). After the isotopy additive and multiplicative networks become disjoint. The multiplicative network evaluates to 0. An additive network γ_0 evaluates to the signed sum $j(\gamma_0) = \sum_{p \in \text{add}(\gamma_0)} s(p) \langle a_p, b_p \rangle \in J(\mathbf{k})$, since \mathbf{k}^\times -winding numbers of its vertices are all 1. We claim that $j(\gamma_0) = 0$. This can be shown by converting γ_0 to a network $\widehat{\gamma}_1$ which is the closure of a braid-like network γ_1 , with all lines pointed up and no U-turns. An example of a braid-like additive network and its closure is shown in Figure 5.2.11. In a braid-like (additive) network all lines are oriented upward so that no tangent line to the network is horizontal, and the network is a composition of merges, splits and transpositions of lines.

The Alexander theorem [Bir74] says that any oriented link in \mathbb{R}^3 is the closure of a braid. It is straightforward to derive a weak analogue of the Alexander theorem: for any closed additive network γ_0 , there exists a braid-like network γ_1 such that $j(\gamma_0) = j(\widehat{\gamma}_1)$. This can be proved by mimicking the proof of the Alexander theorem:

- Convert γ_0 to a piecewise-linear (PL) form and choose a generic base point p_0 in the plane. Further deform γ_0 so that near each intersection, merge and split point orientations of intervals of γ_0 all point clockwise around p_0 .
- Any interval in γ_0 which goes clockwise around p_0 is left alone. An interval I that goes counterclockwise around p_0 is modified into a PL curve by moving some portions of I towards p_0 and some all the way around the diagram as schematically shown in Figure 5.2.9. These moves do not change the invariant j .

Network $\widehat{\gamma}_1$ is analogous to a braid closure. We claim that $j(\widehat{\gamma}_1) = 0$ for any braid-like network γ_1 . To see this, consider merges, splits, and transposition points of γ_1 . Put them in general position so that their y -coordinates are all different. Using moves that do not change the j -invariant we can modify γ_1 to a braid-like network γ_2 with no transposition points by replacing the latter with merges followed by splits as in Figure 5.2.6 bottom left. Then, using isotopies and the move in Figure 5.2.7, network γ_2 is modified to a braid-like network γ_3 which consists of merges and splits with all merges happening before the splits (all having smaller y -coordinates than those of the split points). The bottom and top boundaries of γ_3 are given by the same sequence $a_1, \dots, a_k \in \mathbf{k}$ of weights.

Network γ_3 splits the i -line, of weight a_i , into a sequence of lines of weights $a_{i,1}, \dots, a_{i,\ell_i}$. Then these lines, over $i = 1, \dots, k$ and in this order are merged back into the same sequence a_1, \dots, a_k . Using associativity moves (Figure 5.1.2 top left and its reflection) and cancellation moves in Figure 5.2.8 network γ_3 can be reduced to a network γ_4 which consists of vertical lines of weights a_1, \dots, a_k , with two consecutive lines (of weights a_i, a_{i+1}) exchange at most one line of weight 0, see Figure 5.2.10. Then $j(\widehat{\gamma}_4) = 0$ since $\langle a, 0 \rangle = 0$ for all $a \in \mathbf{k}$.

Another way to show that a braid-like network γ has zero j invariant is to merge all upward-oriented lines of $\widehat{\gamma}$ that intersect a given horizontal line into a single line and then split it back (this does not change the invariant). The network then starts and ends with a single line and it can be gradually simplified to the vertical line, without changing the invariant. A simple example is shown in Figure 5.2.12.

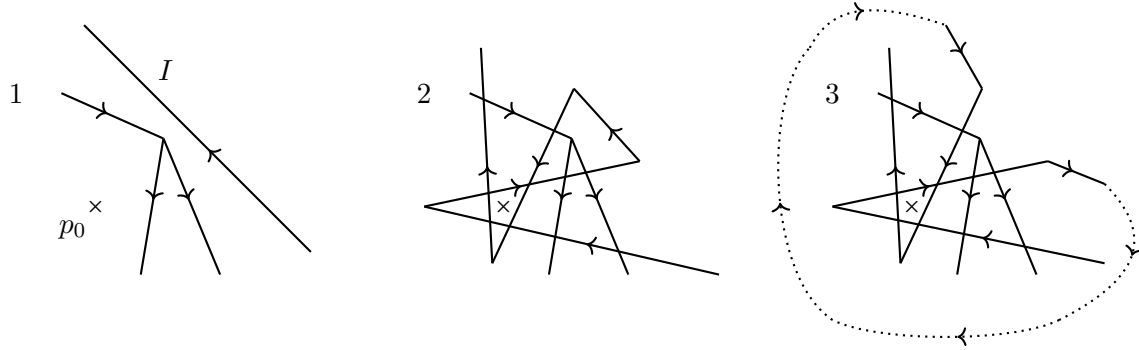


FIGURE 5.2.9. Counterclockwise interval I is broken into subintervals I_i . If the triangle with base I_i and vertex p_0 does not contain merge or split vertices, I_i is converted into a zigzag that wraps around p_0 clockwise. These transformations $1 \Rightarrow 2$ in the Figure create pairs of intersections via “Reidemeister II” moves as in Figure 5.2.6 top right and do not change j . Subintervals I_i with a merge or split vertex in the corresponding triangle are converted into “outside” paths that go around p_0 clockwise (transformations $2 \Rightarrow 3$ in the Figure). Likewise, j is not changed by these transformations. Doing these sequentially for all counterclockwise intervals results in a braid-like closed diagram. Minor details are left to the reader.

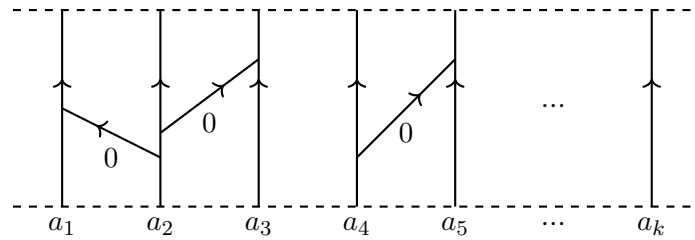


FIGURE 5.2.10. A braid-like network γ_4 made of vertical lines, with at most one weight 0 line connecting consecutive lines. The invariant $j(\widehat{\gamma}_4) = 0$.

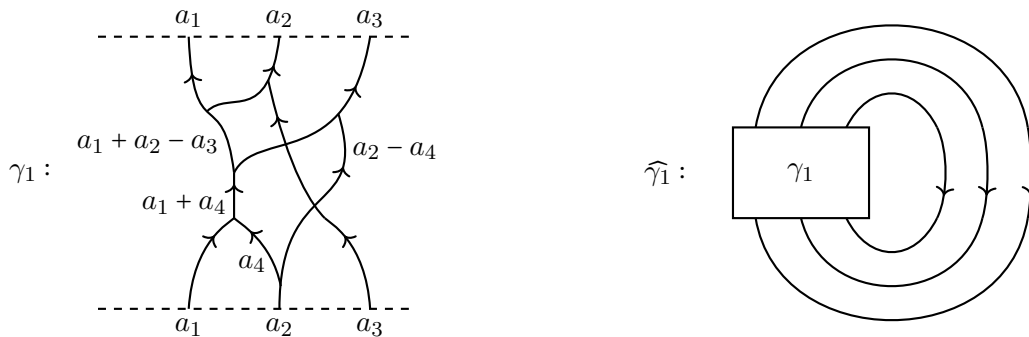


FIGURE 5.2.11. Left: a braid-like network γ_1 . Not shown weights for the remaining two edges are $a_2 - a_3$ and $a_3 + a_4 - a_2$. Right: its closure (network γ_1 is shown as a box).

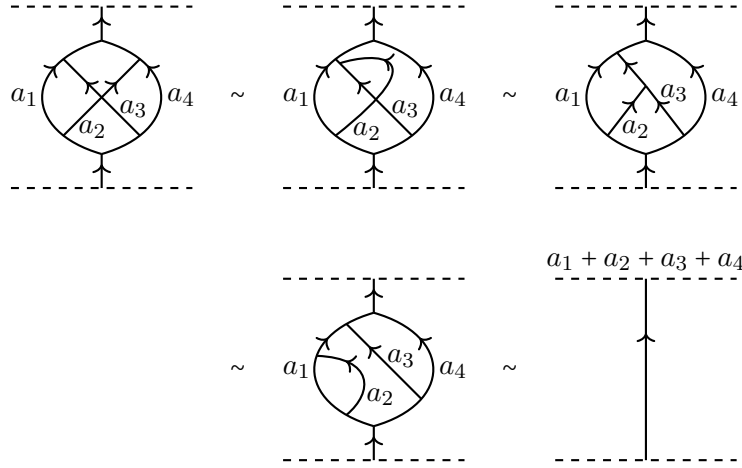


FIGURE 5.2.12. An example of simplifying a braid-like network that starts and ends with a single line.

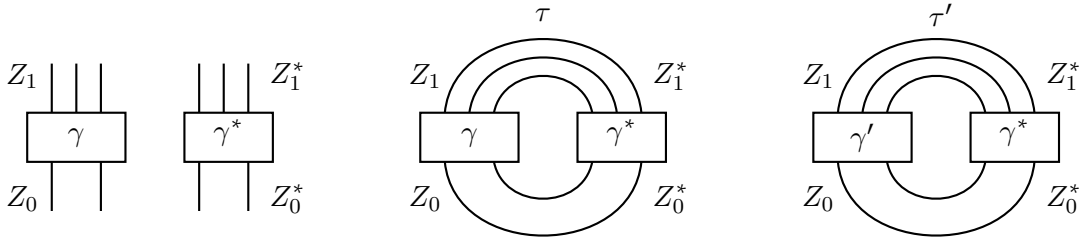


FIGURE 5.2.13. Left to right: morphism γ , its dual γ^* , closures τ and τ' of γ and γ' .

One then gradually simplifies this modification of γ_1 without changing j until it is a vertical diagram, with $j = 0$. An example of such modification, reducing a crossing squeezed between a full split and a full merge, is shown in Figure 5.2.12. \square

Remark 5.3. One should be able to prove the above proposition more directly, using a variation on Proposition 2.17. Here we use two networks, one for the multiplicative and one for the additive subgroups of $\text{Aff}_1(\mathbf{k})$, while Proposition 2.17 uses a single network for all elements of a group G .

Corollary 5.4. *We have the following:*

- (1) Given a morphism $\gamma : Z_0 \rightarrow Z_1$ in $\mathcal{C}_{\mathbf{k}}$, the invariant $j(\gamma)$ depends only on Z_0 and Z_1 .
- (2) $j(\gamma) = 0$ for any endomorphism γ of an object Z .

Proof. Consider two morphisms $\gamma, \gamma' : Z_0 \rightarrow Z_1$. Reflect the morphism γ about the y -axis and reverse the orientation of all additive lines. Denote the resulting morphism by $\gamma^* : Z_0^* \rightarrow Z_1^*$ ($*$ operation on morphisms is part of the pivotal structure on $\mathcal{C}_{\mathbf{k}}$). Note that $j(\gamma^*) = -c(Z)^{-1} \cdot j(\gamma)$.

Compose morphisms γ, γ' with γ^* and the duality morphisms and to get endomorphisms τ, τ' of $\mathbf{1}$, see Figure 5.2.13. We have

$$(5.2) \quad j(\tau) = j(\gamma) + c(Z).j(\gamma^*) = j(\gamma) - c(Z).c(Z)^{-1}.j(\gamma) = 0,$$

$$(5.3) \quad j(\tau') = j(\gamma') + c(Z).j(\gamma^*) = j(\gamma') - j(\gamma) = 0.$$

The last equality holds since j is 0 on any endomorphism of $\mathbf{1}$, including τ' . Consequently, $j(\gamma') = j(\gamma)$ and part (1) of the corollary follows.

Part (2) holds since $j(\text{id}_Z) = 0$, where id_Z is the identity endomorphism of Z (the diagram of id_Z consists of vertical parallel lines, which do not contribute to j). Consequently, $j(\gamma) = 0$ for any endomorphism γ of Z . \square

An object $Z \in \text{Ob}(\mathcal{C}_{\mathbf{k}})$ is a tensor product of objects X_a^\pm and Y_c^\pm , over various $a \in \mathbf{k}$ and $c \in \mathbf{k}^\times$. Define *the weight* of Z , denoted $w(Z)$, to be the unique pair $(a(Z), c(Z))$, with $a(Z) \in \mathbf{k}$ (*additive weight*) and $c(Z) \in \mathbf{k}^\times$ (*multiplicative weight*) such that there exists a morphism

$$(5.4) \quad Z \longrightarrow X_{a(Z)}^+ \otimes Y_{c(Z)}^+$$

in $\mathcal{C}_{\mathbf{k}}$. To determine the weight of Z , first move all X -terms in the product for Z to the left of all Y -terms using permutation morphisms

$$(5.5) \quad Y_c^\pm \otimes X_a^+ \longrightarrow X_{c^\pm a}^+ \otimes Y_c^\pm, \quad Y_c^\pm \otimes X_a^- \longrightarrow X_{c^\mp a}^+ \otimes Y_c^\pm$$

given by the morphism in Figure 5.1.1, bottom left corner, and its modifications with reversed orientation and co-orientation. The new product

$$Z_0 = X_{a_1}^{\epsilon_1} \otimes \cdots \otimes X_{a_n}^{\epsilon_n} \otimes Y_{c_1}^{\mu_1} \otimes \cdots \otimes Y_{c_m}^{\mu_m}, \quad \epsilon_i, \mu_j \in \{+, -\}.$$

Define

$$(5.6) \quad a(Z) = \sum_{i=1}^n \epsilon_i a_i \in \mathbf{k}, \quad c(Z) = \prod_{j=1}^m c_j^{\mu_j} \in \mathbf{k}^\times,$$

where in the formula μ_j stands for 1 or -1 depending on whether $\mu = +$ or $\mu = -$, and likewise for ϵa . With this choice of parameters there is a morphism (5.4). The weight $w(Z) = (a(Z), c(Z))$ of Z is naturally an element of the affine group $\text{Aff}_1(\mathbf{k})$.

Weights of the tensor product $Z \otimes Z'$ are given by:

$$(5.7) \quad a(Z \otimes Z') = a(Z) + c(Z)a(Z'), \quad c(Z \otimes Z') = c(Z)c(Z'),$$

which we can also write as $w(Z \otimes Z') = w(Z)w(Z')$, where the product is just the multiplication in $\text{Aff}_1(\mathbf{k})$.

Weights of the source and target objects of any morphism $\gamma : Z \longrightarrow Z'$ in $\mathcal{C}_{\mathbf{k}}$ are equal: $a(Z) = a(Z'), c(Z) = c(Z')$. The following propositions are clear.

Proposition 5.5. *A morphism $\gamma : Z \longrightarrow Z'$ from Z to Z' in $\mathcal{C}_{\mathbf{k}}$ exists if and only if the weights of Z and Z' are equal.*

Proposition 5.6. *For composable morphisms, $j(\gamma_2 \gamma_1) = j(\gamma_2) + j(\gamma_1)$. For two morphisms $\gamma_i : Z_i \longrightarrow Z'_i$, $i = 1, 2$, the invariant $j(\gamma_1 \otimes \gamma_2) = j(\gamma_1) + c(Z_1)j(\gamma_2)$.*

Corollary 5.7. *Composition of morphisms in $\mathcal{C}_{\mathbf{k}}$ is well-defined. Category $\mathcal{C}_{\mathbf{k}}$ is pivotal monoidal.*

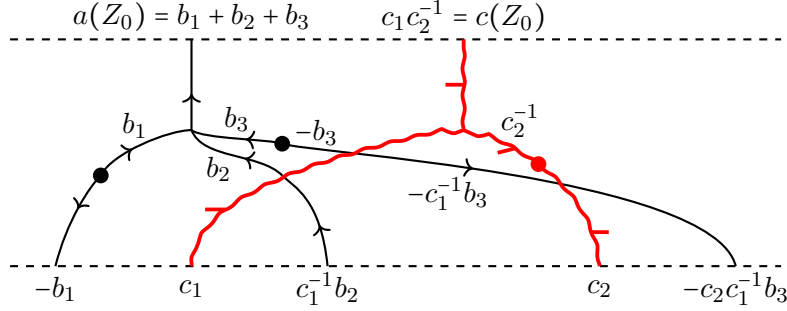


FIGURE 5.2.14. An example of morphism γ_0 in the factorization of a morphism γ . Additive lines, all pointed upwards, are collected on the left, multiplicative lines, all cooriented to the left, are merged together on the right.

Proof. If $j(\gamma_0) = j(\gamma'_0)$ for $\gamma_0, \gamma'_0 : Z_0 \rightarrow Z_1$ and $j(\gamma_1) = j(\gamma'_1)$ for $\gamma_1, \gamma'_1 : Z_1 \rightarrow Z_2$, then $j(\gamma_1 \gamma_0) = j(\gamma'_1 \gamma'_0)$ due to Proposition 5.6. This implies that composition in $\mathcal{C}_{\mathbf{k}}$ is well-defined and $\mathcal{C}_{\mathbf{k}}$ is a category.

The monoidal structure in $\mathcal{C}_{\mathbf{k}}$ is inherited from that of $\mathcal{C}_{\mathbf{k}}$. That it is well-defined follows from the formula for the j invariant of the tensor product in Proposition 5.6. \square

Corollary 5.8. *Any morphism γ in $\mathcal{C}_{\mathbf{k}}$ is invertible. For any two objects Z, Z' of $\mathcal{C}_{\mathbf{k}}$ there exist at most one morphism $\gamma : Z \rightarrow Z'$ in $\mathcal{C}_{\mathbf{k}}$. A morphism $\gamma : Z \rightarrow Z'$ exists if and only if Z and Z' have equal weights: $w(Z) = w(Z')$. For any object Z there exists an isomorphism*

$$(5.8) \quad Z \xrightarrow{\cong} X_{a(Z)}^+ \otimes Y_{c(Z)}^+.$$

Proof. Two morphisms $\gamma_0, \gamma_1 : Z \rightarrow Z'$ have the same j invariant: $j(\gamma_0) = j(\gamma_1)$ so they are equal. The inverse of γ is given by reflecting γ in a horizontal plane. The existence condition follows from that in Proposition 5.5 for the category $\mathcal{C}'_{\mathbf{k}}$. \square

Category $\mathcal{C}_{\mathbf{k}}$ is small and morphisms in it are in a bijection with pairs of objects (Z, Z') of equal weight. The j invariant of morphisms in $\mathcal{C}_{\mathbf{k}}$ takes values in the \mathbf{k} -vector space $J(\mathbf{k})$. It extends the entropy and the Cathelineau invariant to morphisms in $\mathcal{C}_{\mathbf{k}}$.

To compute $j(\gamma)$ for a morphism $\gamma : Z_0 \rightarrow Z_1$ (equivalently, for a pair (Z_0, Z_1) with $a(Z_0) = a(Z_1)$ and $c(Z_0) = c(Z_1)$), factor γ as

$$(5.9) \quad Z_0 \xrightarrow{\gamma_0} X_{a(Z_0)}^+ \otimes Y_{c(Z_0)}^+ \xrightarrow{\gamma_1} Z_1$$

Morphism γ_0 can be represented by the diagram where all additive points of Z_0 cross to the left of all multiplicative points of Z_0 . Downward-oriented additive lines then reverse orientation (and their weights). Right-co-oriented multiplicative lines reverse coorientation and their weights. Finally all additive lines merge into a single upward additive line that carries weight $a(Z_0)$ and all multiplicative lines merge into a single left cooriented line that carries weight $c(Z_0)$, see Figure 5.2.14. Additive weights get rescaled upon crossing multiplicative lines.

Suppose that the additive weights are b_1, \dots, b_n , after the crossings and switches to upward orientation on additive strands are done. Then the invariant

$$j(\gamma_0) = \sum_{k=1}^{n-1} \langle \sum_{i=1}^k b_i, b_{k+1} \rangle.$$

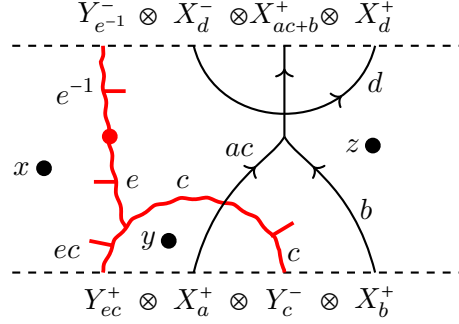


FIGURE 5.3.1. A morphism γ' in $\mathcal{C}_{\mathbb{R}}^{\circ}$ extending the morphism γ in $\mathcal{C}_{\mathbb{R}}$ shown in Figure 5.2.2. The invariant $j(\gamma')$ is given in (5.10).

A similar diagram and computation gives the formula

$$j(\gamma_1) = - \sum_{k=1}^{m-1} \langle \sum_{i=1}^k b'_i, b'_{k+1} \rangle,$$

where b'_1, \dots, b'_m are the weights of Z_1 upon moving all additive points to the leftmost region. The diagram for γ_1 is given by reflecting a suitable diagram as in Figure 5.2.14 about the x -axis and reversing orientations of all additive lines. Finally, $j(\gamma) = j(\gamma_0) + j(\gamma_1)$.

Proposition 5.9. *Pivotal monoidal category $\mathcal{C}_{\mathbf{k}}$ is equivalent to the category \mathcal{C}_G for $G = \text{Aff}_1(\mathbf{k})$ as defined in Section 2.1.*

Proof. This is immediate from our results on $\mathcal{C}_{\mathbf{k}}$. \square

The interesting part of the construction of $\mathcal{C}_{\mathbf{k}}$ is the invariant j of morphisms related to the 2-cocycle $\langle a, b \rangle$.

5.3. Monoidal category $\mathcal{C}_{\mathbf{k}}^{\circ}$.

We now extend $\mathcal{C}_{\mathbf{k}}$ to the monoidal category $\mathcal{C}_{\mathbf{k}}^{\circ}$ by keeping the same objects as in $\mathcal{C}_{\mathbf{k}}$ by adding dots labelled by elements of $J(\mathbf{k})$ floating in regions to the morphism diagrams, see Section 4.2. First, we consider category $\mathcal{C}_{\mathbb{R}}^{\circ}$ mentioned earlier and introduce a function j evaluating a morphism in $\mathcal{C}_{\mathbb{R}}^{\circ}$ to an element of $J(\mathbf{k})$. A morphism γ' in $\mathcal{C}_{\mathbb{R}}^{\circ}$ is given by a morphism γ in $\mathcal{C}_{\mathbb{R}}$ together with a collection of $J(\mathbf{k})$ -labelled dots in regions of γ . Denote by $D(\gamma')$ the set of dots of γ' . For each dot d of γ' let $\ell(d) \in J(\mathbf{k})$ be its label and recall from the discussion of (5.1) the function $\omega(d, \gamma) \in \mathbf{k}^{\times}$ that to a point d of γ not on a multiplicative line assigns its winding index relative to the leftmost region. Define

$$(5.10) \quad j(\gamma') := j(\gamma) + \sum_{d \in D(\gamma')} \omega(d, \gamma) \ell(d) \in J(\mathbf{k}),$$

where $j(\gamma)$ is given by (5.1) and $\omega(d, \gamma) \ell(d)$ is the element $\ell(d)$ of $J(\mathbf{k})$ scaled by $\omega(d, \gamma)$.

For example, consider the morphism γ' in $\mathcal{C}_{\mathbb{R}}^{\circ}$ in Figure 5.3.1 extending the morphism γ in Figure 5.2.2 by three dots. These dots have winding numbers $1, ec, e$ relative to the leftmost region of the diagram. Consequently,

$$(5.11) \quad j(\gamma') = j(\gamma) + x + ec \cdot y + e \cdot z = e \langle ac, b \rangle + x + ec \cdot y + e \cdot z$$

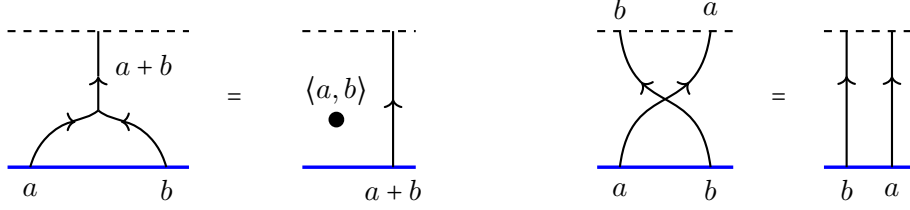


FIGURE 5.3.2. Left: absorbing an intersection point and emitting an $\langle a, b \rangle$ -dot. Right: absorbing an additive crossing at no cost.

Define the category $\mathcal{C}_{\mathbf{k}}^{\circ}$ as the quotient of $\mathcal{C}_{\mathbb{R}}^{\circ}$ by the relation: two morphisms $\gamma_1, \gamma_2 : Z_0 \rightarrow Z_1$ in $\mathcal{C}_{\mathbb{R}}^{\circ}$ are equal in $\mathcal{C}_{\mathbf{k}}^{\circ}$ if and only if $j(\gamma_1) = j(\gamma_2)$. Category $\mathcal{C}_{\mathbf{k}}^{\circ}$ shares many properties with $\mathcal{C}_{\mathbf{k}}$ and contains $\mathcal{C}_{\mathbf{k}}$ as a subcategory. Category $\mathcal{C}_{\mathbf{k}}^{\circ}$ is monoidal, with the tensor product given by placing diagrams in parallel. Any morphism in $\mathcal{C}_{\mathbf{k}}^{\circ}$ is invertible. There exists a morphism $\gamma : Z_0 \rightarrow Z_1$ in $\mathcal{C}_{\mathbf{k}}^{\circ}$ if and only if $j(Z_0) = j(Z_1)$.

Given a morphism $\gamma_0 : Z_0 \rightarrow Z_1$, any morphism $\gamma_1 : Z_0 \rightarrow Z_1$ has a unique presentation as γ_0 with an additional dot labelled by some $x \in J(\mathbf{k})$ in the leftmost region. In other words, $\text{Hom}_{\mathcal{C}_{\mathbf{k}}^{\circ}}(Z_0, Z_1)$, when nonempty, is naturally a $J(\mathbf{k})$ -torsor, for the action given by placing dots in the leftmost region.

Given a diagram D of a morphism γ in $\mathcal{C}_{\mathbf{k}}^{\circ}$, it can be replaced by a diagram where all the dots are collected in the leftmost region, with the label of each dot twisted by its winding number relative to that region. The labels can then be added to replace several dots by a single dot.

Factorization of morphisms in $\mathcal{C}_{\mathbf{k}}$ in (5.9) extends to those in $\mathcal{C}_{\mathbf{k}}^{\circ}$, adding a dot with an arbitrary label in $J(\mathbf{k})$ in the leftmost region.

Category $\mathcal{C}_{\mathbf{k}}^{\circ}$ is similar to the category described in Section 2.2, where $G = \text{Aff}_1(\mathbf{k})$ and representation $U = J(\mathbf{k})$ with the action of $\text{Aff}_1(\mathbf{k})$ given earlier. Evaluation j is analogous to the 2-cocycle evaluation in Section 2.4.

By analogy with Section 2.4, we can introduce a “blue line”, the bottom boundary of a diagram, that can absorb part of the network describing a morphism, in exchange emitting elements of $J(\mathbf{k})$. Figure 5.3.2 shows that absorbing an (a, b) -merge requires emitting $\langle a, b \rangle$ -dot, while an additive crossing can be absorbed at no cost. Figure 5.3.3 interprets commutativity of $\langle a, b \rangle$ via emission and absorption of a merge and an additive crossing.

The two-cocycle property of $\langle a, b \rangle$ is demonstrated in Figure 5.3.4, which is similar to the computation in Figure 2.4.7 except that in the present case \mathbb{R} acts trivially on $J(\mathbf{k})$.

Figure 5.3.5 shows that a crossing of an additive and a multiplicative line is absorbed at no cost. Likewise, Figure 5.3.6 says that a local maximum or minimum of a red line can be absorbed at no cost, and likewise for a merge and orientation reversal of red (multiplicative) lines. Split of a multiplicative line into two lines can be absorbed at no cost as well.

Remark 5.10. If one prefers, additive 0-lines can be removed from diagrams, see Figure 5.3.7.

6. DIAGRAMMATICS OF ENTROPY

6.1. A monoidal category for entropy. Let us specialize $\mathbf{k} = \mathbb{R}$. Real vector space $J(\mathbb{R})$ is enormous, and we reduce the complexity by using the entropy function $H : J(\mathbb{R}) \rightarrow \mathbb{R}$ given

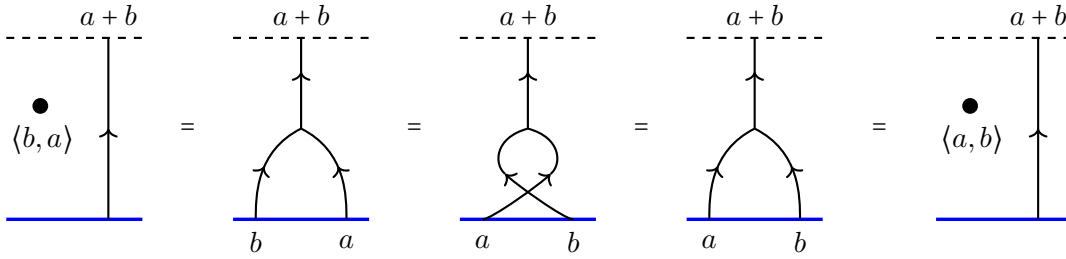


FIGURE 5.3.3. The boundary line absorbs an (a, b) -vertex, in two ways (compare with Figure 2.4.5, left half). This chain of relations shows the symmetry of the symbol, $\langle b, a \rangle = \langle a, b \rangle$.

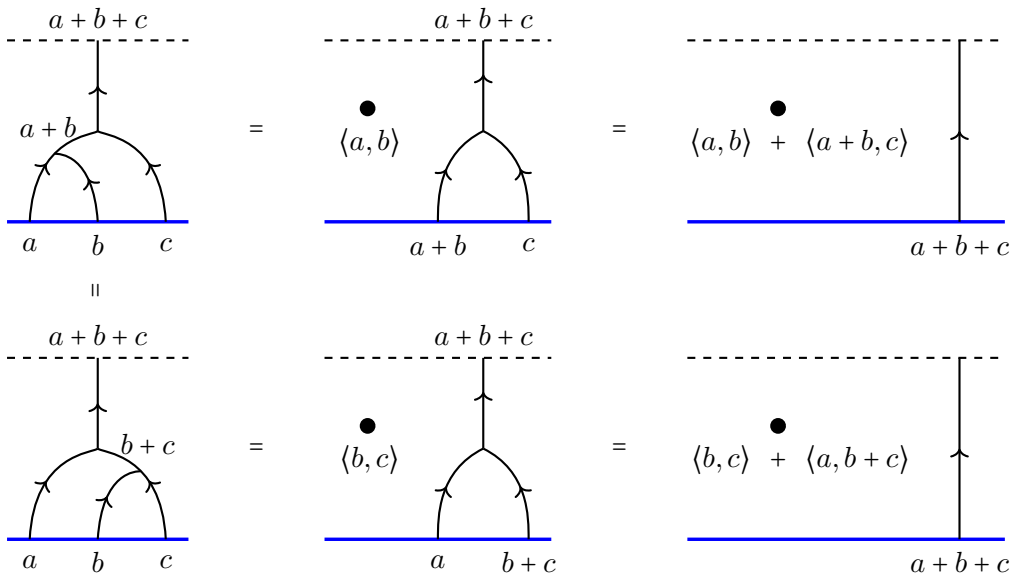


FIGURE 5.3.4. Relation (4.29) follows from the associativity of the merge operation (compare with Figure 2.4.7).

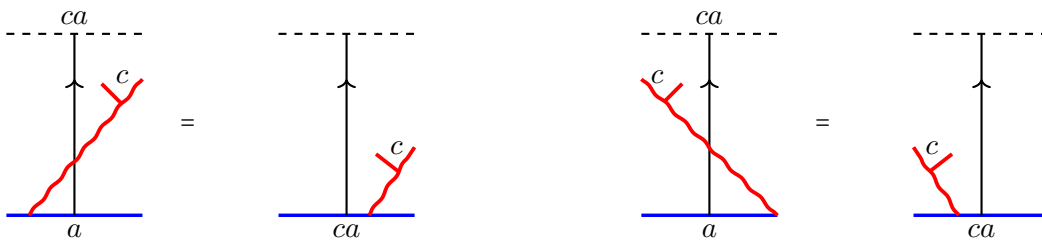


FIGURE 5.3.5. The blue line absorbs an additive-multiplicative intersection at no cost. The relation holds for the other co-orientation of the multiplicative line and for the downward orientation of the additive line as well.

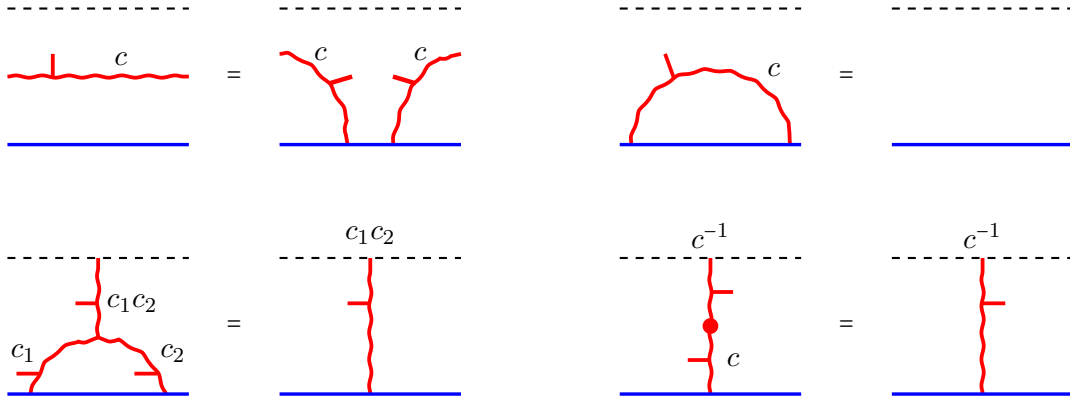


FIGURE 5.3.6. Blue line absorbs a local maximum or minimum of a red line and a black-red crossing at no cost.

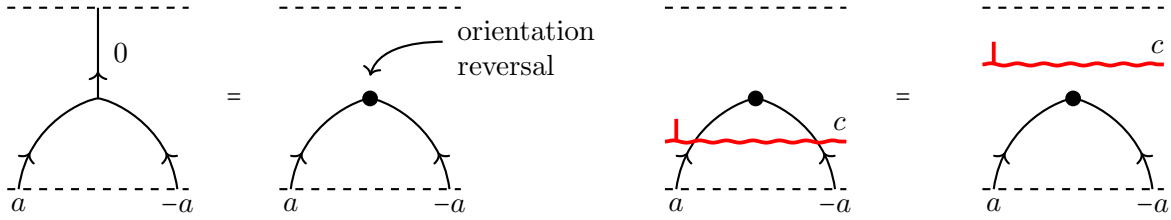


FIGURE 5.3.7. Left: removing an additive 0-line and remembering just its endpoints, where orientations and labels of a pair of additive edges are reversed (flip points). Right: a multiplicative line can slide through an orientation reversal point.

on generators of $J(\mathbb{R})$ by (4.42) and (4.12). Start with the category $\mathcal{C}_{\mathbb{R}}^{\circ}$, where elements of $J(\mathbb{R})$ float in regions of morphism diagrams and for two objects Z_0, Z_1 with $w(Z_0) = w(Z_1)$ the space of homs $\text{Hom}_{\mathcal{C}_{\mathbb{R}}^{\circ}}(Z_0, Z_1)$ is a $J(\mathbb{R})$ -torsor. Recall the invariant j that takes a morphism in $\mathcal{C}_{\mathbb{R}}^{\circ}$ to $J(\mathbb{R})$ and compose it with the entropy function to get an invariant

$$(6.1) \quad j_H : \text{Hom}_{\mathcal{C}_{\mathbb{R}}^{\circ}}(Z_0, Z_1) \longrightarrow \mathbb{R},$$

$$(6.2) \quad j_H := H \circ j, \quad \text{Hom}_{\mathcal{C}_{\mathbb{R}}^{\circ}}(Z_0, Z_1) \xrightarrow{j} J(\mathbb{R}) \xrightarrow{H} \mathbb{R}.$$

Take the quotient of the category $\mathcal{C}_{\mathbb{R}}^{\circ}$ by identifying two morphisms $\gamma_0, \gamma_1 : Z_0 \longrightarrow Z_1$ iff $j_H(\gamma_0) = j_H(\gamma_1)$ and denote the resulting category \mathcal{C}_H° .

A related way to define \mathcal{C}_H° is to consider a version of the category $\mathcal{C}_{\mathbb{R}}^{\circ}$ where dots are labelled by elements of \mathbb{R} rather than $J(\mathbb{R})$. Otherwise it is the same setup with a morphism γ given by a pair of overlapping multiplicative and additive networks together with a finite set of dots $D(\gamma)$, disjoint from the multiplicative network, and labelled by elements of \mathbb{R} . For a morphism γ in this category there is a well-defined evaluation, which can also be denoted $j_H(\gamma)$, given by

$$(6.3) \quad j_H(\gamma) = \sum_{p \in \text{add}(\gamma)} s(p)\omega(p, \gamma)\langle a_p, b_p \rangle_H + \sum_{d \in D(\gamma)} \omega(d, \gamma)\ell(d) \in \mathbb{R}.$$

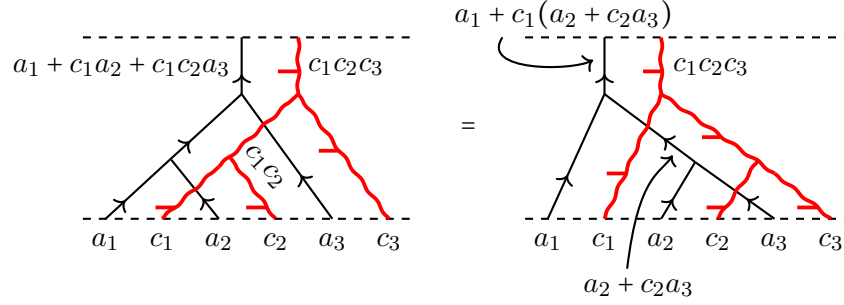


FIGURE 6.1.1. 2-cocycle property of the symbol $\text{Aff}_1(\mathbb{R}) \times \text{Aff}_1(\mathbb{R}) \xrightarrow{\langle \cdot, \cdot \rangle} \mathbb{R}$ in (6.4).

This formula is analogous to (5.1) and (5.10), with $\langle a, b \rangle_H$ given by (4.12). We sum over vertices p of the additive network, multiplying the value of the symbol $\langle a_b, b_p \rangle_H \in \mathbb{R}$ by the winding number $\omega(p, \omega) \in \mathbb{R}^\times$ and the sign. In addition, sum over dots, scaling the label $\ell(d)$ of a dot ℓ by its winding number.

Category \mathcal{C}_H° is monoidal, with the same objects as in categories $\mathcal{C}_{\mathbb{R}}$ and $\mathcal{C}_{\mathbb{R}}^\circ$. There is a morphism $\gamma : Z_0 \rightarrow Z_1$ iff $w(Z_0) = w(Z_1)$. In the latter case, the set of homs from Z_0 to Z_1 is an \mathbb{R} -torsor. For a morphism $\gamma_0 : Z_0 \rightarrow Z_1$, any morphism $\gamma_1 : Z_0 \rightarrow Z_1$ has a unique presentation as γ_0 with an extra dot labelled by some $x \in \mathbb{R}$ in the leftmost region. Furthermore, all dots in a diagram can be moved to the leftmost region, twisted by winding numbers, and added into a single dot. Factorization of morphisms works in the same way as for categories $\mathcal{C}_{\mathbf{k}}$ and $\mathcal{C}_{\mathbf{k}}^\circ$.

Define \mathcal{C}_H to be the subcategory of \mathcal{C}_H° consisting of dotless diagrams. In \mathcal{C}_H there is a unique morphism $Z_0 \rightarrow Z_1$ iff $w(Z_0) = w(Z_1)$, and \mathcal{C}_H is equivalent to the category \mathcal{C}_G in Section 2.1 for $G = \text{Aff}_1(\mathbb{R})$.

Entropy is incorporated in the symbols $\langle a, b \rangle_H$ via (4.12). Entropy, when viewed as the function $j_H(\gamma)$ on morphisms γ in \mathcal{C}_H , depends only the source and target objects of the morphisms γ . In this sense, it may be viewed as a one-dimensional topological theory with defects, which are endpoints of additive and multiplicative lines on the boundary of a network (corresponding to objects X_a^\pm and Y_c^\pm).

Remark 6.1. The extension of the 2-cocycle $\langle a, b \rangle_H$ from \mathbb{R} to $\text{Aff}_1(\mathbb{R})$ in (4.22) can be motivated by Figure 5.1.3 representation of the multiplication in $\text{Aff}_1(\mathbb{R})$ (and, more generally, in $\text{Aff}_1(\mathbf{k})$). For the extension considered in the present paper we make only the additive vertex in that diagram to contribute to the cocycle, and one extends the 2-cocycle from \mathbb{R} to $\text{Aff}_1(\mathbb{R})$ via

$$(6.4) \quad \langle (a_1, c_1), (a_2, c_2) \rangle_H := \langle a_1, c_1 a_2 \rangle_H,$$

and likewise replacing \mathbb{R} by \mathbf{k} . That it is a (normalized) 2-cocycle on $\text{Aff}_1(\mathbb{R})$ can be encoded by the skein relation in Figure 6.1.1. The same relation encodes the associativity of the multiplication in $\text{Aff}_1(\mathbb{R})$. This relation follows from the diagrammatic relations listed earlier.

In Section 5.3 we described category $\mathcal{C}_{\mathbf{k}}^\circ$ and a way to evaluate a morphism in $\mathcal{C}_{\mathbf{k}}^\circ$ by using the bottom boundary line of a diagram to absorb parts of a diagram while emitting elements of $J(\mathbf{k})$. Essentially the same construction applies to evaluate and manipulate morphisms in \mathcal{C}_H° , replacing $\langle a, b \rangle$ in Figures 5.3.2, 5.3.3 and 5.3.4 by $\langle a, b \rangle_H \in R$.

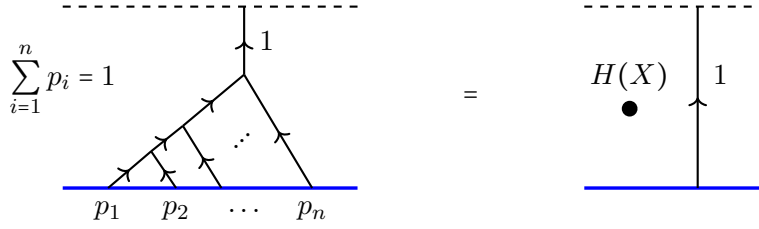


FIGURE 6.1.2. The diagram on the left, when swallowed by the blue line, reduces to the dot labelled by the entropy $H(X) = -\sum_{i=1}^n p_i \log p_i$ of the random variable $X = (p_1, \dots, p_n)$ next to a 1-vertical line.

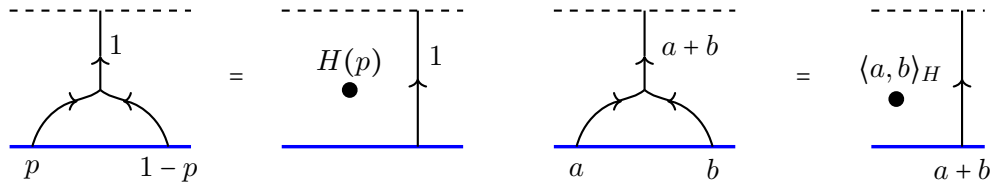


FIGURE 6.1.3. Left: a $(p, 1-p)$ -vertex can be absorbed by the bottom boundary, emitting an $H(p)$ dot. More generally, (a, b) -vertex can be absorbed into the boundary at the cost of emitting $\langle a, b \rangle_H$.

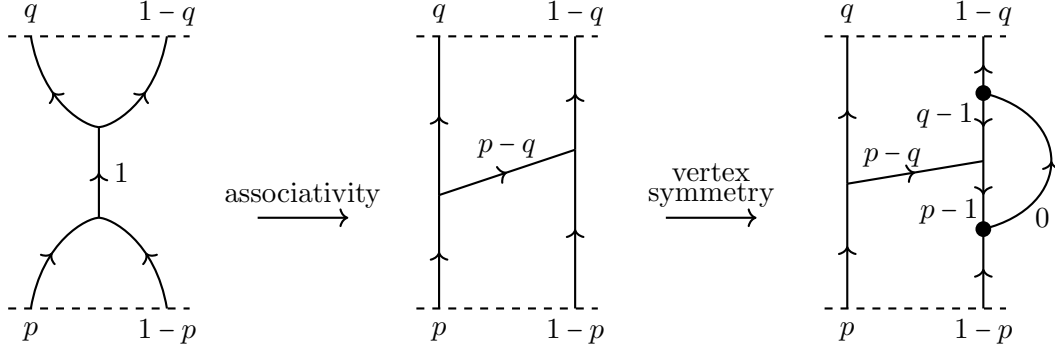


FIGURE 6.1.4. Diagram transformations that match the entropy relation (4.7).

The network in Figure 6.1.2 on the left is an example of a morphism in \mathcal{C}_H^2 from the object $X_{p_1}^+ \otimes \dots \otimes X_{p_n}^+$ to X_1^+ . When the bottom boundary absorbs this network, it produces several dots that add up to the entropy $H(X)$ of a random variable X . Here X takes some values x_1, \dots, x_n with probabilities p_1, \dots, p_n , with $p_1 + \dots + p_n = 1$, and we may also write $X = (p_1, \dots, p_n)$.

A special case of this relation is shown in Figure 6.1.3 on the left.

Functional equation (4.7) for the entropy and its variations (4.10), (4.18) can be interpreted diagrammatically as equalities of evaluations of the following diagrams. Consider the transformation labelled “associativity” in Figure 6.1.4 from the diagram on the right to the

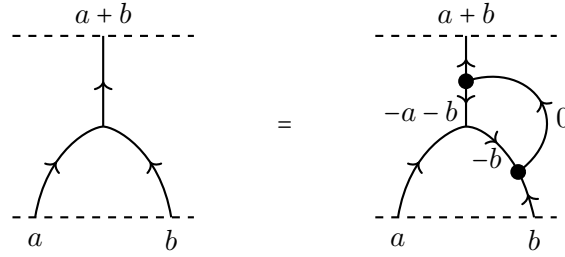


FIGURE 6.1.5. A local symmetry transformation around a trivalent vertex reverses orientation of one *in* and one *out* edge at the vertex, adding 0-line connecting two orientation-reversal points. The two diagrams have the same evaluation.

$$\begin{array}{ccccc}
 H(p) & \xleftrightarrow{\text{inverse}} & -pH(p^{-1}) & \xleftrightarrow{\text{minus}} & -pH(1-p^{-1}) \\
 \updownarrow \text{minus} & & & & \updownarrow \text{inverse} \\
 H(1-p) & \xleftrightarrow{\text{inverse}} & (p-1)H((1-p)^{-1}) & \xleftrightarrow{\text{minus}} & (p-1)H(\frac{p}{1-p})
 \end{array}$$

FIGURE 6.1.6. S_3 -action on the space \mathbb{R} of parameters preserving scaled entropy. Generators act by $p \rightarrow 1-p$ (labelled as *minus* and $p \rightarrow p^{-1}$ (labelled as *inverse*)).

middle. It can indeed be viewed as a version of the associativity for the addition, with one orientation of one of the edges reversed, see Figures 2.1.3 and 2.1.4 for similar transformations in an arbitrary group G rather than in \mathbb{R} .

The merge and the split in the leftmost diagram in Figure 6.1.4 evaluate to $\langle p, 1-p \rangle_H - \langle q, 1-q \rangle_H = H(p) - H(q)$. The middle diagram, obtained via the associativity transformation from the one on the left evaluates to $-\langle q, p-q \rangle_H + \langle p-q, 1-p \rangle_H = -pH(\frac{q}{p}) + (1-q)H(\frac{p-q}{1-q})$. Inserting weight 0 line, whose endpoints contribute 0, as shown in the rightmost diagram, results in the evaluation $-\langle q, p-q \rangle_H + \langle q-1, p-q \rangle_H + \langle p-1, 1-p \rangle_H - \langle q-1, 1-q \rangle_H = -pH(\frac{q}{p}) + (p-1)H(\frac{q-1}{p-1}) + 0 - 0$. This gives the 4 term relation in (4.7).

Transformation of diagrams in Figure 6.1.5 corresponds to the relation $\langle a, b \rangle_H = -\langle -a-b, a \rangle_H$ (modulo the relations $\langle u, -u \rangle_H = 0$). It also corresponds to the symmetry property (4.9) of the entropy (modulo (4.8)), which corresponds to the transformation in Figure 5.1.2 top right).

These symmetries of the bracket $\langle a, b \rangle_H$ and the entropy $H(p)$ are described by an action of S_3 on the space of parameters $p \in \mathbb{R}$ as shown in Figure 6.1.6.

Chain rule for the entropy. The entropy function for finite random variables can be described via the formula (4.2) for random variables that take two values and the chain rule [Fad56, Fad19, Hc56, BFL11].

Figure 6.1.7 interprets diagrammatically the simplest instance of the chain rule. Label Y near a vertex denotes a random variable $(p, 1-p)$, with the line going out of the corresponding

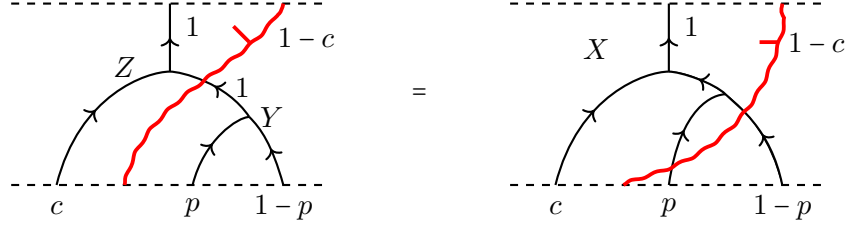


FIGURE 6.1.7. The isotopy of the red line can be interpreted as the simplest instance of the chain rule for entropy, see also Figure 6.1.8.

vertex labelled 1. The line gets rescaled by the $1 - c$ red line. The other additive vertex on the LHS represents a random variable $Z = (c, 1 - c)$. Diagram on the right corresponds to the random variable $X = (c, p(1 - c), (1 - p)(1 - c))$. The equality of evaluations in Figure 6.1.8 is the simplest instance of the chain rule:

$$(6.5) \quad H(X) = H(Z) + (1 - c)H(Y).$$

This example can be generalized in various ways. Consider the LHS of Figure 6.1.9 encoding finite random variables Y_1, \dots, Y_n with $Y_i = (p_{1,i}, \dots, p_{k_i,i})$ and a random variable $Z = (p_1, \dots, p_n)$. Each variable Y_i is represented by a collection of additive lines that merge into an vertex located below the corresponding multiplicative (wavy) line. The lines merge into a line that carries label 1. Upon crossing the i -th multiplicative line, of weight p_i , the additive line get scaled to p_i . Next, additive lines p_1, \dots, p_n merge into additive line 1, describing a random variable Z . This merge (and the merges for Y_i 's) is shown as a single merge, but it can be more accurately defined as a composition of pairs of lines merging and adding their weights, see Figure 6.1.2 on the left, for instance.

On the RHS of Figure 6.1.9 additive lines at the bottom of the diagram first cross multiplicative lines, then merge in groups, then eventually merge into a single line 1. This composition of merges is denoted by a single variable

$$X = (p_1 p_{1,1}, \dots, p_1 p_{k_1,1}, p_2 p_{1,2}, \dots, p_2 p_{k_2,2}, \dots, p_n p_{k_n,1}, \dots, p_n p_{k_n,n}).$$

To go from the left to the right figure we pull the red lines on the LHS of Figure 6.1.9 downward until they are below corresponding additive vertices. The LHS diagram evaluates to the sum of the entropy of Z and entropies of Y_i scaled by p_i , due to the presence of multiplicative lines.

The equality of the two evaluations is then the chain rule for the entropy:

$$(6.6) \quad H(X) = H(Z) + \sum_{i=1}^n p_i H(Y_i).$$

Extending the category of finite probabilistic spaces. Category \mathcal{C}_H° contains a subcategory equivalent to the Baez-Fritz-Leinster category FinProb as defined in [BFL11]. Objects of FinProb are finite sets equipped with probability measures (X, p) and morphisms are measure-preserving functions on finite sets $f : (X, p) \rightarrow (Y, q)$ with $q_j = \sum_{i \in f^{-1}(j)} p_i$. Any morphism $f : X \rightarrow Y$ is surjective onto points of Y of strictly positive measure.

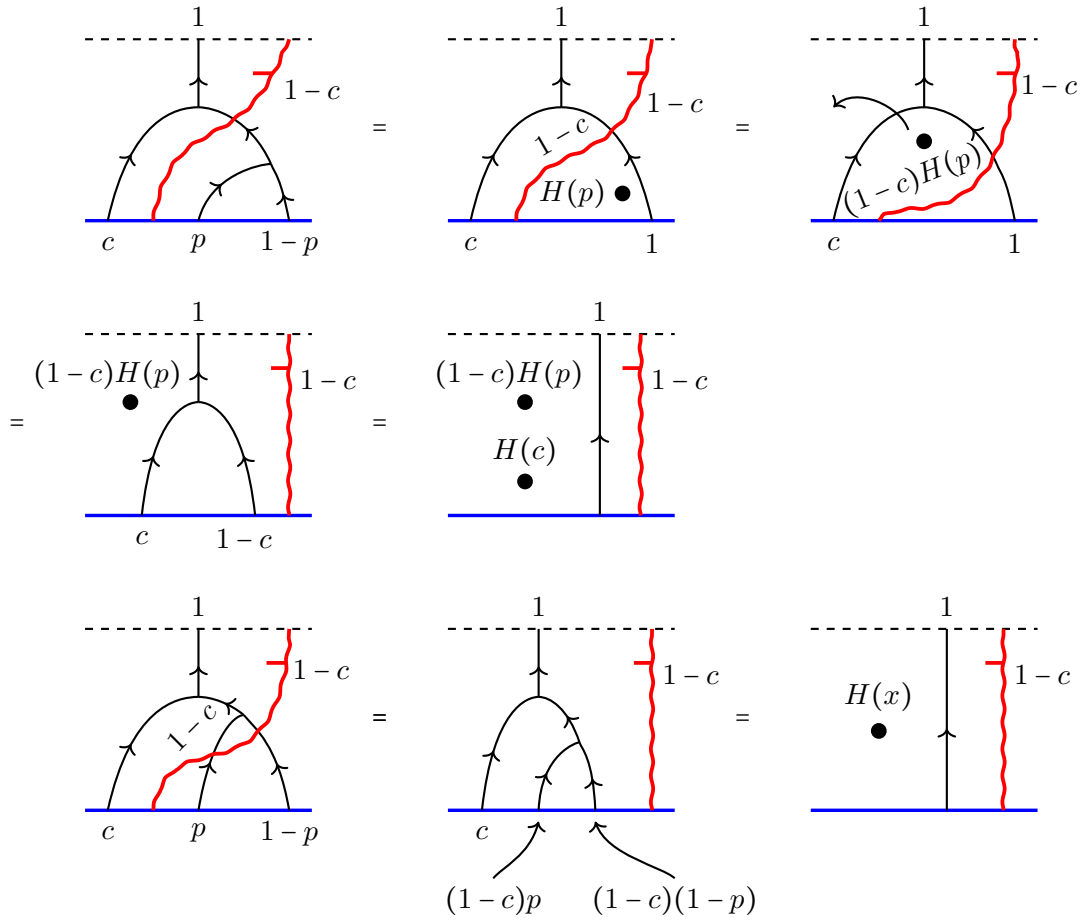


FIGURE 6.1.8. An equivalent deduction of the chain rule (6.5), by having the bottom boundary swallow the diagram.

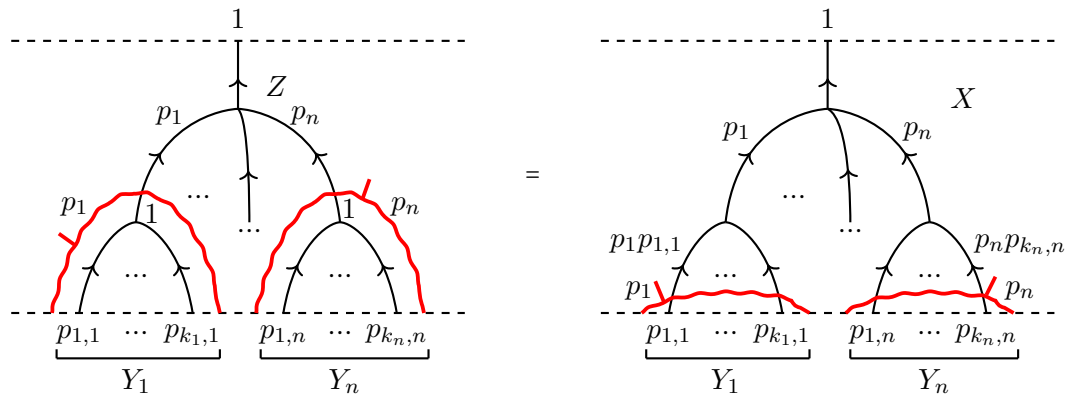


FIGURE 6.1.9. A graphical interpretation of the chain rule (6.6).

Consider the subcategory \mathcal{C}_{Fin} of \mathcal{C}_H° with objects given by tensor products

$$X_{\underline{p}}^+ := X_{p_1}^+ \otimes \cdots \otimes X_{p_n}^+, \quad 0 \leq p_i \leq 1, \quad \sum_{i=1}^n p_i = 1, \quad \underline{p} := (p_1, \dots, p_n).$$

Morphisms are generated by merges $X_p^+ \otimes X_{p'}^+ \rightarrow X_{p+p'}^+$, for $p + p' \leq 1$ and transpositions $X_p^+ \otimes X_{p'}^+ \rightarrow X_{p'}^+ \otimes X_p^+$ (see Section 5.2 for a list of generating morphisms).

These are exactly dotless diagrams made only of additive upward-oriented lines of non-negative weight p with $0 \leq p \leq 1$ with no splits, with the total weight 1 in any cross-section by a horizontal line. Equivalently, these are upward-oriented additive line diagrams with merges and permutations of strands only, total weight 1, and weight restriction $0 \leq p \leq 1$ for each line.

Subcategory \mathcal{C}_{Fin} is equivalent to FinProb . An equivalence is given by the functor $F : \mathcal{C}_{\text{Fin}} \rightarrow \text{FinProb}$ that takes $X_{\underline{p}}^+$ to a finite n -point set with probabilities p_1, \dots, p_n assigned to the points. It is clear how to extend the functor to morphisms. Notice that \mathcal{C}_{Fin} is also a subcategory in $\mathcal{C}_H \subset \mathcal{C}_H^\circ$, since diagrams describing morphisms in \mathcal{C}_{Fin} are dotless.

Functoriality property of entropy in FinProb corresponds to additivity of the entropy on the composition of morphisms, including in the larger category \mathcal{C}_H° , that is, $j(\gamma'\gamma) = j(\gamma') + j(\gamma)$. Convex linearity of entropy in FinProb , see [BFL11], says that

$$H(\lambda Y_1 \oplus (1 - \lambda) Y_2) = \lambda H(Y_1) + (1 - \lambda) H(Y_2),$$

where random variable $\lambda Y_1 \oplus (1 - \lambda) Y_2$ is associated to random variables Y_1, Y_2 and $\lambda, 0 < \lambda < 1$ in the obvious way. Convex linearity corresponds to the equality of evaluations in Figure 6.1.9 when $n = 2$ and $\lambda = p_1$.

The category \mathcal{C}_{Fin} , while equivalent to the Baez–Fritz–Leinster category, is a small part of \mathcal{C}_H . It is natural to wonder whether the bigger categories \mathcal{C}_H and \mathcal{C}_H° , closely related to the affine group $\text{Aff}_1(\mathbb{R})$, may be relevant to probability or whether some modification of \mathcal{C}_H and \mathcal{C}_H° could extend probability as it appears in the quantum world. We refer to [BFL11, Bra21, Lei21a, Gro13, Vig20, BB15] and follow-up papers for more on the categorical meaning of entropy. Operadic interpretation of entropy by Bradley [Bra21] and Leinster [Lei21a] is closely related to the diagrams in Figure 6.1.9.

In this section we offered a different categorical interpretation of entropy of a finite probability space from what exists in the literature. Our interpretation does not have an immediate application to probability. Still, we hope that the present paper complements existing work in a useful way.

6.2. More entropy and cocycle remarks.

Remark 6.2. Consider the action of $\text{Aff}_1(\mathbb{R})$ on the abelian group $(\mathbb{R}, +)$ via $(a, c)u = c|c|^{\alpha-1}u$, where $\alpha \in \mathbb{R}_{>0} \setminus 1$. Note that $c|c|^{\alpha-1} = \text{sign}(c)|c|^\alpha$. One can recover the Tsallis entropy by looking at a suitable 2-cocycle on $\text{Aff}_1(\mathbb{R})$. Tsallis entropy is given by

$$H_\alpha(X) = \frac{1}{\alpha - 1} \left(1 - \sum_{i \in X} p_i^\alpha \right).$$

Interpreting $1 = (\sum_{i \in X} p_i)^\alpha$ we can define

$$\psi_\alpha(x) = \begin{cases} x|x|^{\alpha-1}, & \text{if } x \in \mathbb{R}^*, \\ 0 & \text{if } x = 0 \end{cases}$$

and

$$\langle a, b \rangle_\alpha := \psi_\alpha(a) + \psi_\alpha(b) - \psi_\alpha(a + b).$$

Observe that $\psi_\alpha : \mathbb{R} \rightarrow \mathbb{R}$ is a homomorphism. Then

$$(\alpha - 1)H_\alpha(p) = \pm \langle p, 1 - p \rangle_\alpha.$$

Symmetry property holds: $\langle b, a \rangle_\alpha = \langle a, b \rangle_\alpha$. For the scaling property we have $\psi_\alpha(ca) = \psi_\alpha(c)\psi_\alpha(a)$ and

$$\langle ca, cb \rangle_\alpha = \psi_\alpha(c) \langle a, b \rangle_\alpha.$$

We extend the cocycle to the entire $\text{Aff}_1(\mathbb{R})$ group via

$$(6.7) \quad \langle (a_1, c_1), (a_2, c_2) \rangle_\alpha := \langle a_1, c_1 a_2 \rangle_\alpha$$

In the diagrammatics for the analogue of category \mathcal{C}_H° in this setup, an additive line a crossing a multiplicative line c co-oriented away from it still gets rescaled to ca . But a dot labelled $x \in \mathbb{R}$ moving through a multiplicative c -line co-oriented away from the dot is scaled to $\psi_\alpha(c)x$. In the evaluation function J_α the 2-cocycle $\langle a, b \rangle$ in (5.1) and the 2-cocycle $\langle a, b \rangle_H$ in (4.12) should be replaced by $\langle a, b \rangle_\alpha$ and the action of \mathbb{R}^\times on \mathbb{R} by the action via ψ_α , so that $c\dot{x} = \psi_\alpha(c)x$:

$$(6.8) \quad J_\alpha(\gamma) = \sum_{p \in \text{add}(\gamma)} s(p) \psi_\alpha(\omega(p, \gamma)) \langle a_p, b_p \rangle_\alpha \in \mathbb{R}.$$

and, by analogy with (5.10),

$$(6.9) \quad J_\alpha(\gamma') = J_\alpha(\gamma) + \sum_{d \in \gamma'} \psi_\alpha(\omega(d, \gamma)) \ell(d) \in \mathbb{R}$$

in the presence of \mathbb{R} -weighted dots.

A cohomological interpretation of the Tsallis entropy is discussed in Vigneaux [Vig20]. Another interesting problem is to look for cohomological interpretation of other entropies, including the Rényi entropy. P. Tempesta [Tem16] has discovered a relation between entropies and formal groups, and it is a natural question whether this relation can be given a cohomological meaning.

Remark 6.3. Recall a non-measurable entropy-like function in (4.11) given by

$$h(x) = ((dx)^2)/(x(1-x)) \text{ for } x \in \mathbb{R}, x \neq 0, 1 \text{ and } h(0) = h(1) = 0,$$

where $d : \mathbb{R} \rightarrow \mathbb{R}$ is a \mathbb{Q} -linear derivation. Noting that $1/(x(1-x)) = 1/x + 1/(1-x)$, introduce a function $\psi : \mathbb{R} \rightarrow \mathbb{R}$ given by

$$(6.10) \quad \psi(a) = \begin{cases} (da)^2/a & \text{if } a \neq 0, 1, \\ 0 & \text{if } a = 0, 1. \end{cases}$$

Then $h(x) = \psi(x) + \psi(1-x)$. Function ψ is not a non-linear derivation, unlike (4.5), since $\psi(ab) \neq \psi(a)b + a\psi(b)$. Instead, we compute

$$d(a/(a+b)) = ((da)(a+b) - a(da+db))/(a+b)^2 = ((da)b - a(db))/(a+b)^2$$

and define

$$\begin{aligned} \langle a, b \rangle &:= (a+b)h(a/(a+b)) = (a+b)^3(d(a/(a+b))^2)/(ab), \\ &= (a+b)^{-1}((da)b - a(db))^2/ab \\ &= (da)^2b/(a(b+a)) + (db)^2a/(b(a+b)) - 2(da)(db)/(a+b) \end{aligned}$$

Next,

$$\begin{aligned}\psi(a) + \psi(b) - \psi(a+b) &= (da)^2/a + (db)^2/b - (da+db)^2/(a+b) \\ &= (b^2(da)^2 + a^2(db)^2 - 2ab(da)(db))/(ab(a+b)) = \langle a, b \rangle\end{aligned}$$

Consequently,

$$(6.11) \quad \langle a, b \rangle = \psi(a) + \psi(b) - \psi(a+b),$$

and the 2-cocycle $\langle a, b \rangle$ on \mathbb{R} is the coboundary of ψ . The bracket is symmetric, $\langle a, b \rangle = \langle b, a \rangle$, and a direct computation shows the scaling property

$$\langle ca, cb \rangle = c \langle a, b \rangle.$$

On the field \mathbb{R} , function $h(x)$ and the 2-cocycle $\langle a, b \rangle$ are not measurable and cannot be written down explicitly. Instead, start with a base field \mathbf{k} and form the field $K = \mathbf{k}(y)$, where y is a formal variable. Pick $r = r(y) \in K$ and define $dy = r$, $d(f/g) = (d(f)g - fd(g))/g^2$, for polynomials $f, g \in \mathbf{k}[y]$, resulting in a derivation $d : K \rightarrow K$. Via formula (6.10) we get a null-homologous \mathbf{k} -linear 2-cocycle $\langle a, b \rangle : K \times K \rightarrow K$.

This cocycle extends to a 2-cocycle on the group $\text{Aff}_1(K)$ by

$$(6.12) \quad \langle (a_1, c_1), (a_2, c_2) \rangle := \langle a_1, c_1 a_2 \rangle, \quad a_i \in K, c_i \in K^*,$$

as in (6.4). We do not classify r 's that give rise to non-homologous 2-cocycles in this case but refer to Cathelineau's result [Cat11, Corollary 4.9] that the space $H_2(\text{Aff}_1(K), K_r)$ is infinite-dimensional over K .

Remark 6.4. The unrolled quantum group $\mathfrak{sl}(2)$, see [CGPM15, CGPM17], contains both elements H and $K = q^H$. The trace of the element HK on a representation of the modified quantum $\mathfrak{sl}(2)$ has the flavor of the von Neumann entropy, being the sum $\sum_i \lambda_i \log(\lambda_i)$, where λ_i 's are the eigenvalues of K .

Remark 6.5. Generalized binomials as 2-cocycles. The binomial coefficient $c(k_1, k_2) := \binom{k_1+k_2}{k_1} = \frac{(k_1+k_2)!}{k_1!k_2!}$ satisfies the 2-cocycle equation

$$c(k_1, k_2)c(k_1+k_2, k_3) = c(k_2, k_3)c(k_1, k_2+k_3).$$

Consequently, it can be viewed as a 2-cocycle on the monoid $(\mathbb{Z}_+, +)$ of non-negative integers under addition, taking values in the abelian group \mathbb{Q}^* . The binomial cocycle is null-homologous, since $c(k_1, k_2) = f(k_1+k_2)f(k_1)^{-1}f(k_2)^{-1}$. It is the coboundary of 1-cochain $f : \mathbb{Z}_+ \rightarrow \mathbb{Q}^*$ given by $f(k) = k!$.

Likewise, the q -binomial coefficient $c_q(k_1, k_2) := \frac{[k_1+k_2]!}{[k_1]![k_2]!}$, where $[k]! := [k] \cdots [2][1]$ and $[n] := \frac{q^n - q^{-n}}{q - q^{-1}} = q^{n-1} + q^{n-3} + \dots + q^{1-n}$ is a 2-cocycle $c_q : \mathbb{Z}_+ \times \mathbb{Z}_+ \rightarrow \mathbb{Q}(q)^*$, valued in the group of invertible elements of the field of rational functions in q with rational coefficients. Again, this 2-cocycle is null-homologous, being the coboundary of the 1-cochain $f : \mathbb{Z}_+ \rightarrow \mathbb{Q}^*$, $f(k) = [k]!$.

Binomials and generalized binomials are interpreted cohomologically in [Vig23] in a more sophisticated way, and we are not aware of a reference or use for this trivial interpretation, as null-homologous 2-cocycles on the monoid \mathbb{Z}_+ with values in \mathbb{Q}^* .

More generally, pick a function $g : \mathbb{Z}_+ \rightarrow \mathbf{k}^\times$, where \mathbf{k} is a field, and define a 1-cochain $f : \mathbb{Z}_+ \rightarrow \mathbf{k}^*$ by $f(0) = 1$ and $f(k) = g(1)g(2)\cdots g(k)$ for $k > 0$. Then the generalized binomial coefficient (the Fontené–Ward coefficient [Vig23])

$$c_g(k_1, k_2) := f(k_1 + k_2)f(k_1)^{-1}f(k_2)^{-1}$$

is the coboundary of f .

Note that [Gor13, Gar09] for $a > b > 0$

$$aH\left(\frac{b}{a}\right) = \lim_{n \rightarrow \infty} \frac{1}{n} \log \left(\binom{an}{bn} \right),$$

realizing the entropy as a limit via binomial coefficients (set $a = 1$ to get $H(b)$).

The factorial function extends to the Gamma function $\Gamma : \mathbb{R}_{>0} \rightarrow \mathbb{R}_{>0}$ by

$$\Gamma(x) := \int_0^\infty t^{x-1} e^{-t} dt,$$

with $n! = \Gamma(n+1)$. Beta function

$$B(x_1, x_2) := \frac{\Gamma(x_1)\Gamma(x_2)}{\Gamma(x_1+x_2)} = \int_0^1 t^{x_1-1} (1-t)^{x_2-1} dt$$

gives rise to a null-homologous 2-cocycle

$$\beta : \mathbb{R}_+ \times \mathbb{R}_+ \rightarrow \mathbb{R}^*, \quad \beta(x_1, x_2) = B(x_1+1, x_2+1).$$

Monoid \mathbb{R}_+ can be replaced by the larger monoid $\mathbb{C}_+ = \{z \in \mathbb{C} \mid \operatorname{Re} z \geq 0\}$, under addition, which still avoids the poles of $\Gamma(z+1)$, resulting in a null-homologous 2-cocycle $\beta : \mathbb{C}_+ \times \mathbb{C}_+ \rightarrow \mathbb{C}^*$. Poles of $\Gamma(z)$ provide an obstruction to extending the 2-cocycle β to all of \mathbb{C} .

Remark 6.6. The PMI cocycle. Pointwise Mutual Information (PMI) between a pair of discrete outcomes x and y of random variables X and Y is given by

$$(6.13) \quad \text{PMI}(x, y) = \log \frac{p(x, y)}{p(x)p(y)}.$$

Here it makes sense at first to restrict to $p(x), p(y) \neq 0$, to avoid a possible zero in the denominator. Even with that restriction, $\text{PMI}(x, y)$ may take value $-\infty$, if x and y are disjoint, that is, $p(x, y) = 0$. Thus, $\text{PMI}(x, y) \in \mathbb{R} \cup \{-\infty\}$.

Pointwise Mutual Information is commonly used in linguistics and natural language processing (NLP) [Wik24, Fan68, CH90, Bou09]. The original word embedding construction of Mikolov et al. [MCCD13, MSC+13] is interpreted as factorizations of the PMI matrix and its variations in Levy and Goldberg [LG14].

Observe that PMI is a null-homologous 2-cocycle, since

$$\text{PMI}(x, y) = \log p(x, y) - \log p(x) - \log p(y) = \log p(x \cap y) - \log p(x) - \log p(y).$$

Here x, y are viewed as elements of the commutative monoid $\mathbf{M}(\Omega)$ of measurable subsets of a probability space Ω , with $x \sim x'$ if $p(x \Delta x') = 0$ and $x + y := x \cap y$. Random variables X and Y above are discrete measurable functions on Ω . Map

$$(6.14) \quad \text{PMI} : \mathbf{M}(\Omega) \times \mathbf{M}(\Omega) \rightarrow \widetilde{\mathbb{R}}, \quad \widetilde{\mathbb{R}} := \mathbb{R} \cup \{-\infty\}$$

is a null-homologous 2-cocycle on the commutative monoid $\mathbf{M}(\Omega)$ taking values in the commutative monoid $\widetilde{\mathbb{R}}$. For consistency, we can set $\text{PMI}(\emptyset, y) = -\log p(y)$. Nevertheless, one

runs into the issue that subtraction is not well-defined in $\widetilde{\mathbb{R}}$ when claiming that cocycle PMI is null-homologous, see a related short discussion close to the end of Remark 6.8 below.

Remark 6.7. Penrose impossibility cocycle. R. Penrose [Pen93] gave an amusing proof of the impossibility of the Escher *tribar* shape via the first cohomology group of a non-simply connected plane region, with coefficients in \mathbb{R} . It is an interesting question whether such methods may have a practical use, for instance, for detection of computer and AI generated images and videos.

We discovered this reference by browsing through online threads [Cor12, Gia17] dedicated to appearances of cocycles and cohomology and refer to these threads for more examples.

Remark 6.8. The carry cocycle. When adding two numbers represented in base N there is the carry map on digits $\mathbb{Z}/N \times \mathbb{Z}/N \rightarrow \{0, 1\} \subset \mathbb{Z}/N$ given by $(i, j) \mapsto \lfloor \frac{i+j}{N} \rfloor$. It has been pointed out and rediscovered several times [Dol23, Isa02, DGPV23] that the map is a 2-cocycle which defines a nontrivial extension $0 \rightarrow \mathbb{Z}/N \rightarrow \mathbb{Z}/(N^2) \rightarrow \mathbb{Z}/N$ of abelian groups. This 2-cocycle is *not* null-homologous and gives a generator of the cohomology group $H^2(\mathbb{Z}/N, \mathbb{Z}/N)$.

The carry $\lfloor \frac{i+j}{N} \rfloor$ can be thought of as *excess* that digits i and j produce when added. Upon reflection, one realizes that many operations with “excess” in them can be interpreted as 2-cocycles. Let us provide some examples.

(a) Consider a set \mathcal{S} of companies. Denote by $p(A)$ yearly profit of a company $A \in \mathcal{S}$. Suppose that if two companies merge, they can streamline operations and produce excess profit $e(A, B)$ per year. Denote by $A + B$ the merged company. Then the excess profit

$$(6.15) \quad e(A, B) = p(A + B) - p(A) - p(B).$$

The excess profit is a symmetric 2-cocycle: A, B, C can merge into $A + B + C$ in different orders, with

$$p(A, B) + p(A + B, C) = p(B, C) + p(A, B + C),$$

where both sides show the total excess profit of going from A, B, C to $A + B + C$. The 2-cocycle equation also follows at once from (6.15). Equation (6.15) tells us that 2-cocycle p is null-homologous: $e = dp$, the differential of the one-cochain p . To phrase this carefully, consider the Boolean monoid \mathcal{PS} of all subsets of \mathcal{S} , with addition being the disjoint union. In particular, $A + A = A$ (if a company A merges with itself, it remains A). Then $p : \mathcal{PS} \rightarrow \mathbb{R}$ is a one-cochain (a function) from the abelian idempotent monoid \mathcal{PS} to the abelian group of real numbers. Here, for a subset $\mathcal{U} \subset \mathcal{S}$, we define $p(\mathcal{U})$ as the profit of the company given by merging all companies in \mathcal{U} . Furthermore, $e = dp$ is a null-homologous \mathbb{R} -valued 2-cocycle,

$$e : \mathcal{PS} \times \mathcal{PS} \rightarrow \mathbb{R}.$$

One can further allow a company to split into two companies, going from A to (A_1, A_2) , and extend e to the split operation correspondingly. The diagrammatics of split and merge will be similar to the ones developed in the present paper for groups. One can also introduce red lines, describing external changes that modify profits $p(\mathcal{U})$ of $\mathcal{U} \in \mathcal{PS}$. It is not clear whether such diagrammatics may be useful.

(b) For a similar example, Let \mathcal{S} be a set of people, \mathcal{T} a set of tasks (or achievements) that people can accomplish. For a subset $\mathcal{U} \subset \mathcal{S}$ denote by $t(\mathcal{U}) \subset \mathcal{T}$ the set of tasks that the subset \mathcal{U} of people can accomplish together. The one-cochain $t : \mathcal{PS} \rightarrow \mathcal{PT}$ is a function from subsets of people to subsets of tasks.

Consider excess tasks

$$(6.16) \quad e(\mathcal{U}_1, \mathcal{U}_2) := t(\mathcal{U}_1 + \mathcal{U}_2) \setminus (t(\mathcal{U}_1) + t(\mathcal{U}_2)).$$

These are tasks that the union $\mathcal{U}_1 + \mathcal{U}_2 := \mathcal{U}_1 \cup \mathcal{U}_2$ of people can accomplish but that cannot be accomplished individually by \mathcal{U}_1 or \mathcal{U}_2 . Excess tasks is a function

$$e : \mathcal{PS} \times \mathcal{PS} \longrightarrow \mathcal{PT}.$$

Here both \mathcal{PS} and \mathcal{PT} are idempotent commutative monoids of subsets of \mathcal{S} and \mathcal{T} , respectively. Equation (6.16) indicates that $e = dt$, the coboundary of the one-cochain t . One should be careful here, since \mathcal{PT} , the target of maps t and e , is not an abelian group, only a monoid, but with an additional operation \setminus . Defining cohomology structures in this setup might take one into nonabelian homological algebra [Gra13, CC19].

In the above two examples the 2-cocycles are null-homologous. Null-homologous 2-cocycles are less interesting than non-null-homologous ones, and it would make sense to look for more examples similar to the carry cocycle, representing nontrivial cohomology classes.

Remark 6.9. Affine group acting on a bank account. Let us view the amount of money x one has in a bank account as an element of the abelian group $M = \mathbb{Q}$ (for instance, one may have \$100.5 in the account), assuming that the bank allows negative amounts. One may add or subtract some amount (debits and credits), sending x to $x + b$, for $b \in \mathbb{Q}$. The account may also earn interest, scaling x to ax , $a \in \mathbb{Q}^*$ within a unit time (typically, $a - 1$ is a small positive number).

We see that the affine group $\text{Aff}_1(\mathbb{Q})$ acts on the set of possible values $M = \mathbb{Q}$ that money in a bank account can take. The action is not linear but can be made linear by embedding M as an affine line in \mathbb{Q}^2 via the map $x \mapsto (x, 1)$, with the action

$$(6.17) \quad \begin{pmatrix} a & b \\ 0 & 1 \end{pmatrix} \begin{pmatrix} x \\ 1 \end{pmatrix} = \begin{pmatrix} ax + b \\ 1 \end{pmatrix}.$$

Can this toy example be extended to a nontrivial structure relevant to economics or finance? For instance, would it make sense to replace vectors $(x, 1)$ by arbitrary vectors $(x, y) \in \mathbb{Q}^2$ that are acted upon by a subgroup of $\text{GL}(2, \mathbb{Q})$ other than $\text{Aff}_1(\mathbb{Q})$, via the usual matrix action

$$(6.18) \quad \begin{pmatrix} a_{11} & a_{12} \\ a_{21} & a_{22} \end{pmatrix} \begin{pmatrix} x \\ y \end{pmatrix} = \begin{pmatrix} a_{11}x + a_{12}y \\ a_{21}x + a_{22}y \end{pmatrix}?$$

For another relation of the affine group to finance, note that Kelly's original derivation of his famous betting formula [KJ56, Tho11] is based on entropy and information theory, in turn related to $\text{Aff}_1(\mathbb{R})$ as discussed earlier.

REFERENCES

- [AAKM10] Shiri Artstein-Avidan, Hermann König, and Vitali Milman, *The chain rule as a functional equation*, J. Funct. Anal. **259** (2010), no. 11, 2999–3024.
- [Acz79] János D. Aczél, *Derivations and functional equations basic to characterizations of information measures*, C. R. Math. Rep. Acad. Sci. Canada **1** (1978/79), no. 3, 165–168.
- [Arn98] Ludwig Arnold, *Random dynamical systems*, Springer Monographs in Mathematics, Springer-Verlag, Berlin, 1998.
- [Bae22] John Carlos Baez, *Categorical Semantics of Entropy*, Word Press, Azimuth, <https://johncarlosbaez.wordpress.com/2022/04/19/categorical-semantics-of-entropy/> (2022), 1–4.

- [Bae24] John Baez, *What is Entropy?*, arXiv preprint [arXiv:2409.09232](https://arxiv.org/abs/2409.09232) (2024), 1–129.
- [BB15] Pierre Baudot and Daniel Bennequin, *The homological nature of entropy*, *Entropy* **17** (2015), no. 5, 3253–3318.
- [BB20] Maissam Barkeshli and Daniel Bulmash, *Absolute anomalies in $(2+1)$ D symmetry-enriched topological states and exact $(3+1)$ D constructions*, *Phys. Rev. Res.* **2** (2020), 043033.
- [BBFT⁺24] Lakshya Bhardwaj, Lea E. Bottini, Ludovic Fraser-Taliente, Liam Gladden, Dewi S. W. Gould, Arthur Platschorre, and Hannah Tillim, *Lectures on generalized symmetries*, *Phys. Rep.* **1051** (2024), 1–87.
- [BCH⁺23] Maissam Barkeshli, Yu-An Chen, Sheng-Jie Huang, Ryohei Kobayashi, Nathanan Tantivasadakarn, and Guanyu Zhu, *Codimension-2 defects and higher symmetries in $(3+1)$ D topological phases*, *SciPost Phys.* **14** (2023), 065.
- [BE03] Spencer Bloch and Hélène Esnault, *The additive dilogarithm*, *Doc. Math.* (2003), no. Extra Vol., 131–155, Kazuya Kato’s fiftieth birthday.
- [BFL11] John C. Baez, Tobias Fritz, and Tom Leinster, *A characterization of entropy in terms of information loss*, *Entropy* **13** (2011), no. 11, 1945–1957.
- [Bir74] Joan S. Birman, *Braids, links, and mapping class groups*, *Annals of Mathematics Studies*, vol. No. 82, Princeton University Press, Princeton, NJ; University of Tokyo Press, Tokyo, 1974.
- [Bor16] Mikhail Borovoi, *Extending the exact sequence of nonabelian H^1 , using nonabelian H^2 with coefficients in crossed modules*, arXiv preprint [arXiv:1608.07366](https://arxiv.org/abs/1608.07366) (2016), 1–9.
- [Bou09] Gerlof Bouma, *Normalized (Pointwise) Mutual Information in Collocation Extraction*, <https://svn.spraakdata.gu.se/repos/gerlof/pub/www/Docs/npmi-pfd.pdf>, MWE 2008 workshop (2009), 1–11.
- [Bra21] Tai-Danae Bradley, *Entropy as a topological operad derivation*, *Entropy* **23** (2021), no. 9, Paper No. 1195, 11.
- [Bro94] Kenneth S. Brown, *Cohomology of groups*, *Graduate Texts in Mathematics*, vol. 87, Springer-Verlag, New York, 1994, Corrected reprint of the 1982 original.
- [Cal22a] Danny Calegari, *Notes on scissors congruence*, Online lecture notes, University of Chicago, Spring 2022, <https://math.uchicago.edu/~dannyc/notes/scissors.pdf> (2022), 1–35.
- [Cal22b] ———, *Proofs without words*, *Notices Amer. Math. Soc.* **69** (2022), no. 10, 1807–1809.
- [Cat88] Jean-Louis Cathelineau, *Sur l’homologie de SL_2 à coefficients dans l’action adjointe*, *Math. Scand.* **63** (1988), no. 1, 51–86.
- [Cat90] ———, *On the homology of SL_2 , a complement*, *Math. Scand.* **66** (1990), no. 1, 17–20.
- [Cat96] ———, *Remarques sur les différentielles des polylogarithmes uniformes*, *Ann. Inst. Fourier (Grenoble)* **46** (1996), no. 5, 1327–1347.
- [Cat07] ———, *The tangent complex to the Bloch-Suslin complex*, *Bull. Soc. Math. France* **135** (2007), no. 4, 565–597.
- [Cat11] ———, *Infinitesimal dilogarithms, extensions and cohomology*, *J. Algebra* **332** (2011), 87–113.
- [CC09] Alain Connes and Caterina Consani, *Characteristic one, entropy and the absolute point*, arXiv preprint [arXiv:0911.3537](https://arxiv.org/abs/0911.3537) (2009), 1–63.
- [CC19] ———, *Homological algebra in characteristic one*, *High. Struct.* **3** (2019), no. 1, 155–247.
- [CF77] Richard H. Crowell and Ralph H. Fox, *Introduction to knot theory*, *Graduate Texts in Mathematics*, vol. No. 57, Springer-Verlag, New York-Heidelberg, 1977, Reprint of the 1963 original.
- [CFW10] Danny Calegari, Michael H. Freedman, and Kevin Walker, *Positivity of the universal pairing in 3 dimensions*, *J. Amer. Math. Soc.* **23** (2010), no. 1, 107–188.
- [CGPM15] Francesco Costantino, Nathan Geer, and Bertrand Patureau-Mirand, *Some remarks on the unrolled quantum group of $\mathfrak{sl}(2)$* , *J. Pure Appl. Algebra* **219** (2015), no. 8, 3238–3262.
- [CGPM17] ———, *Corrigendum to “Some remarks on the unrolled quantum group of $\mathfrak{sl}(2)$ ”* [*J. Pure Appl. Algebra* **219** (8) (2015) 3238–3262] [[MR3320217](https://arxiv.org/abs/1703.02017)], *J. Pure Appl. Algebra* **221** (2017), no. 3, 749–750.
- [CH90] Kenneth Ward Church and Patrick Hanks, *Word Association Norms, Mutual Information, and Lexicography*, *Computational Linguistics* **16** (1990), no. 1, 22–29.
- [Cor12] David Corfield, *Cohomology in Everyday Life*, *n-Category Café on math, physics and philosophy*, 2012, https://golem.ph.utexas.edu/category/2012/06/cohomology_in_everyday_life.html (version: 2012-06-14).

- [DBR24] Hugh Dance and Benjamin Bloem-Reddy, *Causal Inference with Cocycles*, arXiv preprint [arXiv:2405.13844](https://arxiv.org/abs/2405.13844) (2024), 1–68.
- [DGPV23] Andrew Dudzik, Tamara von Glehn, Razvan Pascanu, and Petar Veličković, *Asynchronous Algorithmic Alignment with Cocycles*, arXiv preprint [arXiv:2306.15632](https://arxiv.org/abs/2306.15632) (2023), 1–17.
- [Dol23] James Dolan, *Carrying Is a 2-Cocycle*, preprint <https://timothychow.net/mathstuff/jdolan.pdf> (2023), 1–9.
- [Dup01] Johan L. Dupont, *Scissors congruences, group homology and characteristic classes*, Nankai Tracts in Mathematics, vol. 1, World Scientific Publishing Co., Inc., River Edge, NJ, 2001.
- [Eba79] Bruce R. Ebanks, *On some functional equations of Jessen, Karpf, and Thorup*, Math. Scand. **44** (1979), no. 2, 231–234.
- [EGNO15] Pavel Etingof, Shlomo Gelaki, Dmitri Nikshych, and Victor Ostrik, *Tensor categories*, Mathematical Surveys and Monographs, vol. 205, American Mathematical Society, Providence, RI, 2015.
- [EVG02] Philippe Elbaz-Vincent and Herbert Gangl, *On poly(ana)logs. I*, Compositio Math. **130** (2002), no. 2, 161–210.
- [Fad56] Dmitry K. Faddeev, *On the concept of entropy of a finite probabilistic scheme*, Uspehi Mat. Nauk (N.S.) **67** (1956), no. 1, 227–231.
- [Fad19] ———, *On the concept of entropy of a finite probabilistic scheme*, English translation of the 1956 article by D. K. Faddeev, <https://arrowtheory.com/pub/notes/025-faddeev-entropy.html> (2019), 1–6.
- [Fan68] Robert M. Fano, *Transmission of Information: A Statistical Theory of Communications*, MIT Press, Cambridge, MA, 1968.
- [FMT24] Daniel S. Freed, Gregory W. Moore, and Constantin Teleman, *Topological symmetry in quantum field theory*, arXiv preprint [arXiv:2209.07471](https://arxiv.org/abs/2209.07471) (2024), 1–77.
- [Gar09] Stavros Garoufalidis, *An extended version of additive K-theory*, J. K-Theory **4** (2009), no. 2, 391–403.
- [Gia17] Noah Giansiracusa, *Occurrences of (co)homology in other disciplines and/or nature*, MathOverflow, 2017, <https://mathoverflow.net/q/60108> (version: 2017-06-10).
- [GIK⁺23a] Paul Gustafson, Mee Seong Im, Remy Kaldawy, Mikhail Khovanov, and Zachary Lihn, *Automata and one-dimensional TQFTs with defects*, Lett. Math. Phys. **113** (2023), no. 93, 1–38.
- [GIK23b] Paul Gustafson, Mee Seong Im, and Mikhail Khovanov, *Boolean TQFTs with accumulating defects, sofic systems, and automata for infinite words*, arXiv preprint [arXiv:2312.17033](https://arxiv.org/abs/2312.17033) (2023), 1–31.
- [GMP04] H. Gopalkrishna Gadiyar, K. M. Sangeeta Maini, and Raghavan Padma, *Cryptography, connections, cocycles and crystals: a p-adic exploration of the discrete logarithm problem*, Progress in cryptology—INDOCRYPT 2004, Lecture Notes in Comput. Sci., vol. 3348, Springer, Berlin, 2004, pp. 305–314.
- [Gor13] Ofir Gorodetsky, *Asymptotics of binomial coefficients and the entropy function*, Mathematics Stack Exchange, 2013, <https://math.stackexchange.com/q/360180> (version: 2013-04-13).
- [Gra13] Marco Grandis, *Homological algebra*, World Scientific Publishing Co. Pte. Ltd., Hackensack, NJ, 2013, In strongly non-abelian settings.
- [Gro13] Misha Gromov, *In a search for a structure, Part 1: On entropy*, European Congress of Mathematics, Eur. Math. Soc., Zürich, 2013, pp. 51–78.
- [Hc56] Aleksandr Y. Hinčin, *On the basic theorems of information theory*, Uspehi Mat. Nauk (N.S.) **11** (1956), no. 1(67), 17–75.
- [IK21] Mee Seong Im and Mikhail Khovanov, *Foams, iterated wreath products, field extensions and Sylvester sums*, arXiv preprint [arXiv:2107.07845](https://arxiv.org/abs/2107.07845) (2021), 1–78, to appear in Theory Appl. Categ.
- [IK22] ———, *Topological theories and automata*, arXiv preprint [arXiv:2202.13398](https://arxiv.org/abs/2202.13398) (2022), 1–70.
- [IK23] ———, *From finite state automata to tangle cobordisms: a TQFT journey from one to four dimensions*, arXiv preprint [arXiv:2309.00708](https://arxiv.org/abs/2309.00708), to appear in Contemporary Mathematics (2023), 1–40.
- [IK24a] ———, *Foam cobordism and the Sah-Arnoux-Fathi invariant*, arXiv preprint [arXiv:2403.06030](https://arxiv.org/abs/2403.06030) (2024), 1–38.
- [IK24b] ———, *One-dimensional topological theories with defects: the linear case*, Contemporary Mathematics **791** (2024), 105–146.

- [IKO23] Mee Seong Im, Mikhail Khovanov, and Victor Ostrik, *Universal construction in monoidal and non-monoidal settings, the Brauer envelope, and pseudocharacters*, arXiv preprint [arXiv:2303.02696](https://arxiv.org/abs/2303.02696) (2023), 1–59.
- [Isa02] Daniel C. Isaksen, *A cohomological viewpoint on elementary school arithmetic*, Amer. Math. Monthly **109** (2002), no. 9, 796–805.
- [IZ22] Mee Seong Im and Paul Zimmer, *One-dimensional topological theories with defects and linear generating functions*, Involve **15** (2022), no. 2, 319–331.
- [Jes68] Borge Jessen, *The algebra of polyhedra and the Dehn-Sydler theorem*, Math. Scand. **22** (1968), 241–256.
- [JKT68] Borge Jessen, Jorgen Karpf, and Anders Thorup, *Some functional equations in groups and rings*, Math. Scand. **22** (1968), 257–265.
- [Kat79] Anatole Katok, *Bernoulli diffeomorphisms on surfaces*, Ann. of Math. (2) **110** (1979), no. 3, 529–547.
- [Kho20] Mikhail Khovanov, *Universal construction of topological theories in two dimensions*, arXiv preprint [arXiv:2007.03361](https://arxiv.org/abs/2007.03361) (2020), 1–56.
- [KJ56] John Larry Kelly Jr., *A New Interpretation of Information Rate*, Bell Sys. Tech. J. **35** (1956), no. 4, 917–926.
- [KL21] Mikhail Khovanov and Robert Laugwitz, *Planar diagrammatics of self-adjoint functors and recognizable tree series*, arXiv preprint [arXiv:2104.01417](https://arxiv.org/abs/2104.01417), to appear in *Pure Appl. Math. Quarterly* (2021), 1–61.
- [Kon02] Maxim Kontsevich, *The $1\frac{1}{2}$ -logarithm. Appendix to: “On poly(ana)logs. I” [Compositio Math **130** (2002), no. 2, 161–210] by P. Elbaz-Vincent and H. Gangl*, Compositio Math. **130** (2002), no. 2, 211–214.
- [Kuc09] Marek Kuczma, *An introduction to the theory of functional equations and inequalities*, second ed., Birkhäuser Verlag, Basel, 2009, Cauchy’s equation and Jensen’s inequality, Edited and with a preface by Attila Gilányi.
- [Lee64] Peter M. Lee, *On the axioms of information theory*, Ann. Math. Statist. **35** (1964), 415–418.
- [Lei21a] Tom Leinster, *Entropy and diversity—the axiomatic approach*, Cambridge University Press, Cambridge, 2021.
- [Lei21b] ———, *Entropy modulo a prime*, Commun. Number Theory Phys. **15** (2021), no. 2, 279–314.
- [Lem97] Mariusz Lemańczyk, *Cohomology groups, multipliers and factors in ergodic theory*, Studia Math. **122** (1997), no. 3, 275–288.
- [LG14] Omer Levy and Yoav Goldberg, *Neural Word Embedding as Implicit Matrix Factorization*, Advances in Neural Information Processing Systems (Z. Ghahramani, M. Welling, C. Cortes, N. Lawrence, and K.Q. Weinberger, eds.), vol. 27, Curran Associates, Inc., 2014, pp. 1–9.
- [MCCD13] Tomas Mikolov, Kai Chen, Greg Corrado, and Jeffrey Dean, *Efficient Estimation of Word Representations in Vector Space*, arXiv preprint [arXiv:1301.3781](https://arxiv.org/abs/1301.3781) (2013), 1–12.
- [Mic10a] Jouko Mickelsson, *From gauge anomalies to gerbes and gerbal actions*, Motives, quantum field theory, and pseudodifferential operators, Clay Math. Proc., vol. 12, Amer. Math. Soc., Providence, RI, 2010, pp. 211–220.
- [Mic10b] ———, *From Gauge Anomalies to Gerbes and Gerbal Representations: Group Cocycles in Quantum Theory*, Acta Polytech. **50** (2010), no. 3, 42–47.
- [Mil17] James S. Milne, *Algebraic groups*, Cambridge Studies in Advanced Mathematics, vol. 170, Cambridge University Press, Cambridge, 2017, The theory of group schemes of finite type over a field.
- [MS06] Gregory W. Moore and Graeme Segal, *D-branes and K-theory in 2D topological field theory*, arXiv preprint [hep-th/0609042](https://arxiv.org/abs/hep-th/0609042) (2006), 1–89.
- [MSC⁺13] Tomas Mikolov, Ilya Sutskever, Kai Chen, Greg S Corrado, and Jeff Dean, *Distributed Representations of Words and Phrases and their Compositionality*, Advances in Neural Information Processing Systems (C.J. Burges, L. Bottou, M. Welling, Z. Ghahramani, and K.Q. Weinberger, eds.), vol. 26, Curran Associates, Inc., 2013, pp. 1–9.
- [MT14] Matilde Marcolli and Ryan Thorngren, *Thermodynamic semirings*, J. Noncommut. Geom. **8** (2014), no. 2, 337–392.
- [MW50] Saunders MacLane and J. H. C. Whitehead, *On the 3-type of a complex*, Proc. Nat. Acad. Sci. U.S.A. **36** (1950), 41–48.

- [Par74] William Parry, *A note on cocycles in ergodic theory*, *Compositio Math.* **28** (1974), 343–350.
- [Par07] Jinhyun Park, *Algebraic cycles and additive dilogarithm*, *Int. Math. Res. Not. IMRN* (2007), no. 18, Art. ID rnm067, 19.
- [Pen93] Roger Penrose, *On the cohomology of impossible figures*, *The visual mind*, Leonardo Book Ser., MIT Press, Cambridge, MA, 1993, pp. 27–29.
- [Rio21] Olivier Rioul, *This is IT: a primer on Shannon’s entropy and information*, *Information theory—Poincaré Seminar 2018*, *Prog. Math. Phys.*, vol. 78, Birkhäuser/Springer, Cham, [2021] ©2021, pp. 49–86.
- [RRV99] Vladimir Retakh, Christophe Reutenauer, and Arkady Vaintrob, *Noncommutative rational functions and Farber’s invariants of boundary links*, *Differential topology, infinite-dimensional Lie algebras, and applications*, *Amer. Math. Soc. Transl. Ser. 2*, vol. 194, Amer. Math. Soc., Providence, RI, 1999, pp. 237–246.
- [SA98] Takakazu Satoh and Kiyomichi Araki, *Fermat quotients and the polynomial time discrete log algorithm for anomalous elliptic curves*, *Comment. Math. Univ. St. Paul.* **47** (1998), no. 1, 81–92.
- [Sah79] Chih-Han Sah, *Hilbert’s third problem: scissors congruence*, *Research Notes in Mathematics*, vol. 33, Pitman (Advanced Publishing Program), Boston, Mass.-London, 1979.
- [San04] Luis Antonio Santaló, *Integral Geometry and Geometric Probability*, *Integral Geometry and Geometric Probability*, Second Edition, Cambridge Mathematical Library, Cambridge University Press, 2004, pp. xi–404.
- [Sch13] Rich Schwartz, *The Dehn-Sydler Theorem Explained*, preprint (2013), 1–23.
- [Sel11] Peter Selinger, *A survey of graphical languages for monoidal categories*, *New structures for physics*, *Lecture Notes in Phys.*, vol. 813, Springer, Heidelberg, 2011, pp. 289–355.
- [Sem98] Igor A. Semaev, *Evaluation of discrete logarithms in a group of p -torsion points of an elliptic curve in characteristic p* , *Math. Comp.* **67** (1998), no. 221, 353–356.
- [Ser02] Jean-Pierre Serre, *Galois cohomology*, English ed., Springer Monographs in Mathematics, Springer-Verlag, Berlin, 2002, Translated from the French by Patrick Ion and revised by the author.
- [Sma99] Nigel Paul Smart, *The discrete logarithm problem on elliptic curves of trace one*, *J. Cryptology* **12** (1999), no. 3, 193–196.
- [Spi23] David I. Spivak, *Polynomial functors and Shannon entropy*, *Proceedings—Fifth International Conference on Applied Category Theory*, *Electron. Proc. Theor. Comput. Sci. (EPTCS)*, vol. 380, EPTCS, [place of publication not identified], 2023, pp. 331–343.
- [Syd65] Jean-Pierre Sydler, *Conditions nécessaires et suffisantes pour l’équivalence des polyèdres de l’espace euclidien à trois dimensions*, *Comment. Math. Helv.* **40** (1965), 43–80.
- [Tab96] Serge Tabachnikov, *Projective connections, group Vey cocycle, and deformation quantization*, *Internat. Math. Res. Notices* (1996), no. 14, 705–722.
- [Tac20] Yuji Tachikawa, *On gauging finite subgroups*, *SciPost Phys.* **8** (2020), no. 1, Paper No. 015, 23.
- [Tem16] Piergiulio Tempesta, *Formal groups and Z -entropies*, *Proc. A.* **472** (2016), no. 2195, 20160143, 17.
- [Tho11] Edward O. Thorp, *The Kelly criterion in blackjack betting, and the stock market*, ch. 9, pp. 789–832, *World Scientific, Finding the Edge: Mathematical Analysis of Casino Games*, *World Scientific Handbook in Financial Economics Series*, 2011, The 10th International Conference on Gambling and Risk Taking, Montreal.
- [TKBB23] Srivatsa Tata, Ryohei Kobayashi, Daniel Bulmash, and Maissam Barkeshli, *Anomalies in $(2+1)$ D fermionic topological phases and $(3+1)$ D path integral state sums for fermionic SPTs*, *Comm. Math. Phys.* **397** (2023), no. 1, 199–336.
- [Tur10] Vladimir Turaev, *Homotopy quantum field theory*, *EMS Tracts in Mathematics*, vol. 10, European Mathematical Society (EMS), Zürich, 2010, Appendix 5 by Michael Müger and Appendices 6 and 7 by Alexis Virelizier.
- [Tve58] Helge Tverberg, *A new derivation of the information function*, *Math. Scand.* **6** (1958), 297–298.
- [Ü21] Sinan Ünver, *A survey of the additive dilogarithm*, *Arithmetic L-functions and differential geometric methods*, *Progr. Math.*, vol. 338, Birkhäuser/Springer, Cham, 2021, pp. 301–324.
- [Uzm22] Alp Uzman, *Intuition of cocycles and their use in dynamical systems*, *Mathematics Stack Exchange*, 2022, <https://math.stackexchange.com/q/4348317> (version: 2022-01-04).
- [Vig19] Juan Pablo Vigneaux, *Topology of statistical systems: a cohomological approach to information theory*, *Theses: Information theory*, Université Sorbonne Paris Cité, 2019.

- [Vig20] ———, *Information structures and their cohomology*, Theory Appl. Categ. **35** (2020), Paper No. 38, 1476–1529.
- [Vig23] ———, *A characterization of generalized multinomial coefficients related to the entropic chain rule*, Aequationes Math. **97** (2023), no. 2, 231–255.
- [Voe04] Vladimir Voevodsky, *A categorical approach to the probability theory*, Institute for Advanced Study, <https://www.math.ias.edu/Voevodsky/files/files-annotated/...Categories/Stage2/stochastic.pdf> (2004), 1–22.
- [Voe08] ———, *Categorical probability*, All-Institute Seminar “Mathematics and its Applications” of the Steklov Mathematical Institute of the Russian Academy of Sciences (2008), 1, School of Mathematics, Institute for Advanced Study, lecture video in Russian, <https://www.mathnet.ru/php/seminars.phtml?presentid=259>.
- [Vol] José Felipe Voloch, *Relating the Smart-Satoh-Araki and Semaev approaches to the discrete logarithm problem on anomalous elliptic curves*, <https://www.math.canterbury.ac.nz/.../disclog2.pdf>, pp. 1–2.
- [Whi49] John Henry Constantine Whitehead, *Combinatorial homotopy. II*, Bull. Amer. Math. Soc. **55** (1949), 453–496.
- [Wik24] Wikipedia contributors, *Pointwise mutual information – Wikipedia, the free encyclopedia*, https://en.wikipedia.org/wiki/Pointwise_mutual_information, 2024, [Online; accessed 8-September-2024].
- [Zor11] Vladimir Zorich, *Mathematical analysis of problems in the natural sciences*, Springer, Heidelberg, 2011, Translated from the 2008 Russian original by Gerald Gould.
- [ZS58] Oscar Zariski and Pierre Samuel, *Commutative algebra, Volume I*, The University Series in Higher Mathematics, D. Van Nostrand Co., Inc., Princeton, NJ, 1958, With the cooperation of I. S. Cohen.

DEPARTMENT OF MATHEMATICS, JOHNS HOPKINS UNIVERSITY, BALTIMORE, MD 21218, USA
 DEPARTMENT OF MATHEMATICS, UNITED STATES NAVAL ACADEMY, ANNAPOLIS, MD 21402, USA
 Email address: meeseong@jhu.edu

DEPARTMENT OF MATHEMATICS, JOHNS HOPKINS UNIVERSITY, BALTIMORE, MD 21218, USA
 DEPARTMENT OF MATHEMATICS, COLUMBIA UNIVERSITY, NEW YORK, NY 10027, USA
 Email address: khovanov@jhu.edu